ION-EXCHANGE RESINS AS HETEROGENEOUS CATALYSTS IN BIODIESEL PRODUCTION FROM TRIOLEIN AND CANOLA OIL

A Thesis Submitted to the College of

Graduate Studies and Research

In Partial Fulfillment of the Requirements

For the Degree of Master of Science

In the Department of Chemical and Biological Engineering

University of Saskatchewan

Saskatoon

By

GREG PATERSON

PERMISSION TO USE

In presenting this thesis in partial fulfilment of the requirements for a postgraduate degree from the University of Saskatchewan, the author agrees that the Libraries of this University may make it freely available for inspection. The author further agrees that permission for copying of this thesis in any manner, in whole or in part, for scholarly purposes may be granted by the professor or professors who supervised my thesis work or, in their absence, by the head of the Department of Chemical and Biological Engineering or the Dean of the College of Engineering. It is understood that any copying or publication or use of this thesis or parts thereof for financial gain shall not be allowed without my written permission. It is also understood that due recognition shall be given to me and to the University of Saskatchewan in any scholarly use which may be made of any material in my thesis.

Requests for permission to copy or to make other use of material in this thesis in whole or part should be addressed to:

Department Head
Chemical and Biological Engineering
University of Saskatchewan
57 Campus Drive
Saskatoon, Saskatchewan
S7N 5A9
Canada

ABSTRACT

Biodiesel is an alternative to petroleum diesel produced from renewable sources. A heterogeneous solid acid catalyst is required to circumvent the issues associated with the continued use of homogeneous catalysts in the production of biodiesel. Ion-exchange resins can be used as catalysts in transesterification. The objective of this research was to identify an ion-exchange resin as an effective heterogeneous catalyst for the production of biodiesel.

Commercial ion-exchange resins from various sources were tested in the transesterification of oils to fatty acid methyl esters (biodiesel). Triolein was used as a model oil feedstock for catalyst screening and statistical optimization of the operating conditions. Amberlyst 15 was the most active ion-exchange resin tested during catalyst screening. Optimized reactor variables were 200˚C, 13 wt% catalyst loading and 1:24 oil to alcohol molar ratio. Conversion of triolein to products at 2 hours was 97 mol%. The acid value of the products was 56 mg KOH/g sample. Water was added to the reactants up to 2 wt% to determine if a hydrolysis reaction was responsible for this increase in acid value and to determine whether water would have a hindering effect on transesterification. Water addition did not have a measurable effect on the reaction products up to 1 wt%. At 2 wt%, conversion to products decreased slightly. Free fatty acid addition up to 15 wt% to simulate low quality feedstock had a negligible impact on conversion to products. From the water and acid value testing it was determined that the catalyst was performing the hydrolysis, esterification and transesterification reactions. In longevity experiments, the catalyst was reused once without an impact on conversion to products. Use of canola oil from green seed as a low cost and low quality feedstock demonstrated similar reaction results compared to results using triolein as feedstock.

The reaction kinetics of Amberlyst 15 in transesterification were studied at temperatures lower than the optimal temperature to minimize the effects of the hydrolysis and esterification

side reactions. Alcohol to oil molar ratio was increased in order to increase conversion to products at the lower temperatures. In the kinetic study, the temperatures examined were 100˚C, 110˚C and 120˚C. Additional reaction parameters were: catalyst loading of 13 wt%, 1:77 oil to alcohol molar ratio, 600 RPM stirring speed and 50 grams of canola oil. This experiment demonstrated a conversion to products of 79 mol% after 72 hours. The rate constants of the three reversible reactions were calculated using a MATLab program to simulate transesterification reaction kinetics. Reaction rate constants for the forward reactions at 120˚C for TG to DG, DG to MG and MG to GL were 0.08, 0.22 and 6.5 L/mol/day, respectively. The activation energy for the rate limiting step (TG to DG) was 120 kJ/mol. Diffusion and internal mass transfer limitations were neglected during the kinetic study due to the results from experiments with a crushed catalyst, the large pore size of Amberlyst 15, the rate of agitation and the high activation energy calculated from experimental results.

.

ACKNOWLEDGMENTS

Thanks to Dr. Ajay Dalai, not only for his support and direction throughout my postgraduate work, but also for encouraging me to pursue my Master of Science degree. I spent my final summer of undergraduate work under the guidance of Dr. Dalai, Dr. Narendra Bakhshi and Kapil Pathak. For this experience I am grateful.

Thanks to Dr. Dalai, Dr. Bakhshi, Dr. Hui Wang and Dr. Jafar Soltan for serving on my advisory committee as well as for their support and encouragement as instructors in completion of my course requirements.

I would like to acknowledge Titipong Issariyakul for his expert guidance throughout my years of research. Also, many thanks to Richard Blondin, Heli Eunike, Dragan Cekic and RLee Prokopishyn for technical assistance and patience. In addition, thanks to Dr. Glyn Kennell, Shannon Dyck, Jon Godwin and Kurt Woytiuk for supporting me and helping me through my work for so many years.

I would like to acknowledge Dr. Amarjeet Bassi of the University of Western Ontario along with Dr. Dalai, who had the foresight to recommend this project to the Natural Science and Engineering Research Council of Canada to provide funding for this project. AUTO21 Network of Centres of Excellence provided additional funding.

Thanks to my sister, Dr. Carolyn Paterson, for her support and advice. Finally, thanks to my parents, Guy and Sharon Paterson for their love, encouragement and assistance.

TABLE OF CONTENTS

PERMISSION TO USE i

ABSTRACT ii

ACKNOWLEDGMENTS iv

TABLE OF CONTENTS v

LIST OF TABLES viii

LIST OF FIGURES ix

LIST OF ABBREVIATIONS x

1. INTRODUCTION 1
   - 1.1. Biodiesel 1
   - 1.2. Limitations of Current Production 1
   - 1.3. Conventional Production Methods 2
   - 1.4. Future Production Methods 3
   - 1.5. Ion-Exchange Resins 3
   - 1.6. Knowledge Gap 4
   - 1.7. Research Objectives 5

2. LITERATURE REVIEW 7
   - 2.1. Feedstock 7
     - 2.1.1 Triolein 7
     - 2.1.2 Canola Oil 7
     - 2.1.3 Greenseed Canola Oil 8
   - 2.2. Transesterification 9
     - 2.2.1 Bronsted Acids and Bases 11
     - 2.2.2 Lewis Acids and Bases 13
   - 2.3. Various Catalysts Used for Biodiesel Production 15
     - 2.3.1 Homogeneous Acid Catalysts 15
     - 2.3.2 Homogeneous Base Catalysts 16
     - 2.3.3 Heterogeneous Acid Catalysts 19
     - 2.3.4 Heterogeneous Base Catalysts 24
   - 2.4. Ion-Exchange Resins 26
   - 2.5. Ion-Exchange Resins in Transesterification 28
   - 2.6. Kinetics of Transesterification 31
   - 2.7. Biodiesel Characteristics 33

3. EXPERIMENTAL METHODS 38
   - 3.1. Materials 38
   - 3.2. Commercial Ion-Exchange Resins 38
   - 3.3. Catalyst Characterization 39

3.3.1 Surface Area, Pore Volume, Pore Diameter 39
3.3.2 Fourier Transform Infrared Spectroscopy 40
3.3.3 Thermogravimetric Analysis 40
3.3.4 Cation Exchange Capacity 40
3.4. Feedstock and Product Analysis 41
3.4.1 High Performance Liquid Chromatography 41
3.4.2 Acid Value 42
3.4.3 Inductively Coupled Plasma Mass Spectrometry 42
3.4.4 Water Content 42
3.4.5 Gas Chromatography 43
3.5. Reaction Procedure 43
3.5.1 Batch Reactions 43
3.5.2 Statistical Design 45
3.5.3 Additional Experiments 46
3.5.4 Catalyst Longevity 46
3.5.5 Kinetic Study 47

4. RESULTS AND DISCUSSION 49
4.1. Catalyst Characterization 49
4.1.1 Surface Area, Pore Volume, Pore Diameter 49
4.1.2 Cation Exchange Capacity 50
4.1.3 Fourier Transform Infrared Spectroscopy 51
4.1.4 Thermogravimetric Analysis 53
4.2. Feedstock Composition 54
4.2.1 High Performance Liquid Chromatography 54
4.2.2 Acid Value 54
4.2.3 Inductively Coupled Plasma Mass Spectrometry 54
4.2.4 Water Content 55
4.3. Reaction Study 55
4.3.1 Catalyst Screening 55
4.3.2 Repeatability Testing 59
4.3.3 Central Composite Design Statistical Optimization 60
4.3.4 Effect of Water Addition 65
4.3.5 Effect of Free Fatty Acid Addition 66
4.3.6 Effect of Greenseed Canola Oil 67
4.4. Product Analysis 68
4.4.1 High Performance Liquid Chromatography 68
4.4.2 Acid Value 69
4.4.3 Inductively Coupled Plasma Mass Spectrometry 69
4.4.4 Water Content 69
4.4.5 Gas Chromatography 70
4.5. Catalyst Longevity 71
4.6. Acid Value and Temperature 72
4.7. Kinetics Study of Transesterification Reaction with Amberlyst 15 73
4.7.1 Kinetic Model Development 73
4.7.2 Transesterification Analysis 74
4.7.3 Reaction Rate Constants 74

4.7.4 Reaction Order 77
4.7.5 Activation Energy 78
4.7.6 Rate Determining Step 78

5. CONCLUSIONS AND RECOMMENDATIONS 81
5.1. Conclusions 81
5.2. Recommendations 82

LIST OF REFERENCES 84

APPENDICES 92
A. Sample Calculations 92
A.1. Error Calculation for Water Content Testing 92
A.2. Calculation of Mole Percentage (mol%) from HPLC Results of Triolein Sample 92
A.3. Error Calculation from Statistical Experiments 93
A.4. Statistical Model Quadratic Equation 94
A.5. Mole Balance 95
A.6. Calculation of Activation Energy 96
B. Rate Law Equation 97
B.1. Transesterification Reaction 97
B.2. Differential Rate Law Equations 97
C. MATLab Program 99
C.1. Input Values for Time Increments and Concentrations (inputvalue.m) 99
C.2. Ordinary Differential Equations Setup (KinODE.m) 99
C.3. Main Program with Initial Guesses for Reaction Rate Constants (main.m) 100
C.4. Graphing Function (plotgraph.m) 101
C.5. Error Calculation Function (err.m) 103
D. Example HPLC Chromatograms 105
D.1. Chromatogram of Triolein Oil 105
D.2. Chromatogram of Canola Oil 106
D.3. Chromatogram of Greenseed Canola Oil 107
D.4. Chromatogram of Experiment at t=0 Minutes at Optimized Conditions 108
D.5. Chromatogram of Experiment at t=120 Minutes at Optimized Conditions 109

LIST OF TABLES

Table 2-1: ASTM standard D6751-2011 for biodiesel fuel blend stock B100 (ASTM, 2011) 34
Table 3-1: Selected ion-exchange resins, functional groups and support components 39
Table 3-2: Controlled variable ranges in CCD statistical design 46
Table 3-3: CCD statistical design experiments 47
Table 4-1: Catalyst characterization summary of surface properties and exchange capacities. 50
Table 4-2: Water content of feedstock and various transesterification reaction products 55
Table 4-3: Temperature testing with Amberlyst 15 and acid value of products after 120 minutes 57
Table 4-4: Statistical design experiments and results 61
Table 4-5: Conversion, acid value and water content of feedstock and various experiments 65
Table 4-6: Fatty acid methyl ester chain length and saturation extent by gas chromatograph 70
Table 4-7: Reaction rate constants for reversible transesterification reactions 75
Table 4-8: Comparison of activation energy in current work and literature values 79
Table A-1: HPLC results of triolein sample and component molecular weights 92
Table A-2: Factors in statistical model to calculate coded factors 94
Table A-3: Feedstock and reactant concentrations in kinetic experiments 95

LIST OF FIGURES

Figure 1-1: Transesterification reaction of triglyceride with methanol 2
Figure 2-1: Triglyceride form of oleic acid, triolein 8
Figure 2-2: Bronsted base-catalyzed mechanism of transesterification (based on Ma, 1999) 12
Figure 2-3: Bronsted acid-catalyzed mechanism of transesterification (based on Demirbas, 2008) 13
Figure 2-4: Lewis acid catalyzed mechanism of transesterification (based on Di Serio, 2008) 14
Figure 2-5: Lewis base catalyzed mechanism of transesterification (based on Helwani, 2009) 15
Figure 2-6: Reaction mechanism for production of methyl esters by acid catalyzed transesterification and esterification (based on Kulkarni, 2006a) 21
Figure 2-7: Structural composition of sulfonic acid styrene-divinylbezene IER (left) and Nafion SAC-13 (right) (based on Dorfner, 1972; López, 2007) 27
Figure 2-8: Transesterification of soybean oil with various catalysts (based on de Rezende, 2008) 29
Figure 2-9: Effect of degree of saturation of fatty acids on cold filter plug point (CFPP, medium grey) and cetane number as well as iodine value (light grey) (Ramos, 2009) 37
Figure 2-10: Fatty acid composition of five oils commonly used for biodiesel production (based on Ramos, 2009) 37
Figure 3-1: Schematic of batch reactor system 45
Figure 4-1: Pyridine adsorption FTIR analysis of tested ion-exchange resins (full spectrum) 52
Figure 4-2: Pyridine adsorption FTIR analysis of three ion-exchange resins (truncated spectrum) 52
Figure 4-3: Thermogravimetric analysis of various ion-exchange resins 53
Figure 4-4: Effect of temperature on transesterification of triolein using Amberlyst 15 56
Figure 4-5: Catalyst screening using transesterification of triolein using ion-exchange resins 58
Figure 4-6: Repeatability of transesterification of triolein using Amberlyst 15 60
Figure 4-7: Transesterification of triolein using optimized reactor conditions 64
Figure 4-8: Numerical model of transesterification yield of triolein using Amberlyst 15 64
Figure 4-9: Effect of water and free fatty acid addition on transesterification of triolein 67

Figure 4-10: Transesterification of greenseed canola oil using optimized reactor conditions 68
Figure 4-11: Amberlyst 15 longevity in successive transesterification of triolein 72
Figure 4-12: Transesterification of canola oil at various temperatures over Amberlyst 15 73
Figure 4-13: Plotgraph function from MATLab model temperature 120˚C 76
Figure 4-14: Pseudo-second order reaction kinetics for triglyceride consumption over Amberlyst 15 77
Figure 4-15: Arrhenius plot of tri- di- and monoglyceride consumption during transesterification 79

LIST OF ABBREVIATIONS

A	Pre-exponential factor
Å	Angstrom
ACS	American Chemical Society
AOCS	American Oil Chemists' Society
AS	Surface area
ASTM	American Society for Testing and Materials
BET	Brunauer, Emmett and Teller
˚C	Degrees Celsius
CCD	Central composite design
CEC	Cation exchange capacity
CFPP	Cold filter plug point
CIE	Compression ignition engine
cm	Centimeter
CSTR	Continuous stirred tank reactor
DCM	Dichloromethane
DG	Diglyceride
dP	Pore diameter
DTA	Differential thermal analysis
DVB	Divinylbenzene
E	Activation energy
FAME	Fatty acid methyl esters (biodiesel)
FID	Flame ionization detector
FTIR	Fourier transform infrared spectrometry
g	Grams
GC	Gas chromatograph
GL	Glycerol
HHV	Higher heating value
HPLC	High performance liquid chromatography
ICP-MS	Inductively coupled plasma mass spectrometry
IER	Ion-exchange resin
k	Rate constant or number of factors
K_a	Chemical equilibrium constant
kJ	Kilojoules
LH	Langmuir-Hinshelwood
m	Meter
M	Molarity, motor
max	Maximum
m_{eq}	Milliequivalents
ME	Methyl esters
MeOH	Methanol
MG	Monoglyceride

min	Minutes or minimum
mL	Millilitres
mm	Millimeter
mol	Mole
mol%	Mole percent
MPa	Megapascals
mg	Milligrams
N	Normality or number of experiments
N_C	Number of replicated experiments
NFPA	National Fire Protection Association
P	Pressure
PFR	Plug flow reactor
P-H	Pseudo-homogeneous
ppm	Parts per million
R	Universal gas constant
RI	Refractive index
RPM	Rotations per minute
SAC	Solid acid catalyst
SBA-15	Santa Barbara amorphous #15
SBC	Solid base catalyst
t	Time
T	Temperature
TFEt-P2PVE	Tetrafluroroethylene perfluoro-2-(fluorosulfonylethoxy)propyl vinyl ether
TG	Triglyceride
TGA	Thermogravimetric analysis
THF	Tetrahydrofuran
TLC	Thin layer chromatography
TPA	12-tunstophosphoric acid
TPD	Temperature programmed desorption
vol%	Volume percent
vP	Pore volume
wt%	Weight percent
µL	Microlitres
µm	Micrometer

1. INTRODUCTION

1.1. Biodiesel

Biodiesel is a renewable and non-toxic alternative to petroleum diesel and is derived from biological sources such as oils and fats. Biodiesel makes use of renewable organic feedstocks and does not add sequestered carbon to the atmosphere (Peterson, 1998). Biodiesel is composed of fatty acid methyl esters (FAME) of varying chain length and saturation. Petroleum diesel is composed of saturated hydrocarbons and aromatic hydrocarbons. As a fuel, biodiesel has very similar physical properties to petroleum diesel with a few notable exceptions: biodiesel exhibits higher viscosity, higher lubricity and biodiesel does not contain sulfur or aromatic hydrocarbons. The advantages of using biodiesel are numerous: it is portable as a liquid fuel, it is readily available from oil feedstocks, it is renewable and it is energy dense (Ma, 1999). Biodiesel is produced from triglycerides through a process called transesterification. The chemical reaction is acid (or base) catalyzed as demonstrated in Figure 1-1. The reaction occurs in a stepwise fashion. In each reversible step, a methyl ester ($R_{1\text{-}3}COOCH_3$) molecule is produced from the glyceride reactant. Current annual petroleum diesel usage in Canada is 40 billion litres per year and the Canadian government has mandated to replace up to 800 million litres per year with biodiesel in 2012 (Banks, 2008). There is an urgent requirement in Canada for an expansion of biodiesel production.

1.2. Limitations of Current Production

Biodiesel can replace some petroleum diesel currently in use. However it should be produced from low cost and non-edible feedstocks. The use of conventional oil crops in biodiesel production causes an unfavourable competition between fuel production and food sources; as

such, producing biodiesel from non-edible oils is important. Food crops also lack the capability to supply a significant amount of fuel to supply society's energy needs. Roughly 80% of the cost of palm oil derived biodiesel is due to the high cost of the feedstock (Chisti, 2007). Biodiesel feedstock for the expansion of production in Canada must be sourced from low cost, non-edible oils and fats. Current biodiesel production methods also require large scale improvements.

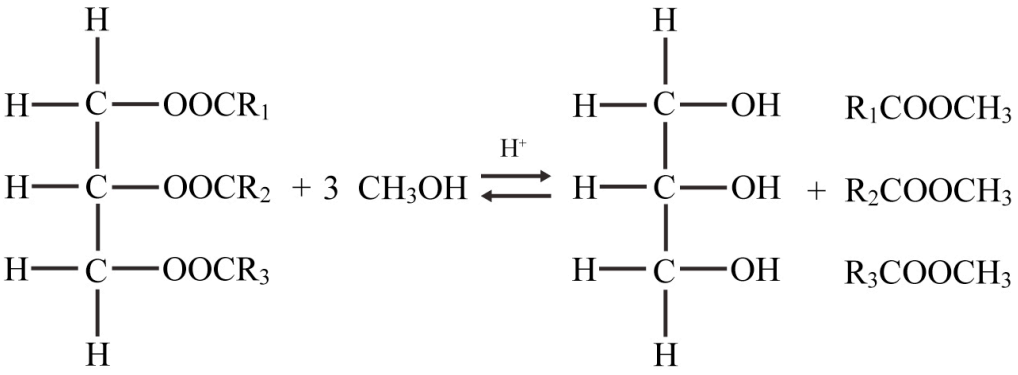

Figure 1-1: Transesterification reaction of triglyceride with methanol

1.3. Conventional Production Methods

The cost of processing biodiesel is another factor in the economics of biodiesel production. Homogeneous acid and/or base catalysts for biodiesel production have a high production cost, use significant amounts of water, present corrosion problems and yield toxic byproducts (e.g. sodium hydroxide, sulfuric acid, hydrochloric acid) depending on the catalyst(s) used. The use of these aqueous acids or bases requires product neutralization and washing steps. The acids or bases are soluble in the product mixture. Additional acids or bases are added to the products to neutralize the catalyst. The salts and water formed from the interaction of acids and bases during neutralization are removed by water washing stages. Additional water removal steps (e.g. distillation or adsorption) can also be used to further purify the biodiesel product. These processing steps result in a quantity of hazardous liquid waste, which requires proper disposal. In addition, basic catalysts have the undesirable side reaction saponification. Hydrolysis of the ester

produces free fatty acids that are saponified with bases to produce salts and consume the catalyst. There are numerous issues associated with traditional biodiesel production methods. Processing costs could be reduced by simplifying process streams and with the elimination or reduction of waste streams (Di Serio, 2008).

1.4. Future Production Methods

The use of solid acid catalysts (SAC) can remove the need for washing that is required in homogeneous catalysts (Demirbas, 2008; D'Cruz, 2007). Solid acid catalysts offer many advantages over homogeneous catalysts. SAC are less corrosive than homogeneous catalysts and allow for simple filtration separation from liquid products. The use of SAC can reduce contamination in the final product and catalysts can typically be reused. Solid acid catalysts can also eliminate the need for aqueous washing for removal of the homogeneous catalysts. There is a significant amount of research being conducted on the applications of solid acid catalysis in transesterification (Melero, 2009b).

1.5. Ion-Exchange Resins

Many solid catalysts are available for study as discussed in section 2.3. Of the available catalysts, ion-exchange resins (IER) have been selected for examination in transesterification for biodiesel production. An IER is a polymer or copolymer support containing a bonded functional group with the ability to exchange ions. IER have been selected for the following reasons: IER are physically strong, they are not readily oxidized or hydrolyzed and are resistant to high temperatures. Some Nafion brand resins are resistant up to 200˚C, this is the upper thermal limit of the applicability of resins as catalysts. Resins can be used in any type of reactor, any medium (due to their insolubility) and are used in a wide variety of reactions in industrial processes

(Dorfner, 1972). The reusability of resins may be their best attribute. A catalyst that does not degrade and is reusable is the most cost-effective. Ion-exchange resins demonstrate potential as catalysts in organic reactions and are subject to examination in various subject areas.

The most common substrate of IER is a copolymer of styrene and divinylbenzene (DVB). A functional group is added to the resin structure to make a resin polymer chemically active. There are many options for acids and bases, both strong and weak; the most common functional group is sulfonic acid (SO_3H). Sulfonic acid groups are cation-exchanging functional groups. Sulfonic acid groups on resins do not undergo chemical degradation during use (Dorfner, 1972). In general, cation-exchanging resins are more stable than anionic resins and stability is relative to the amount of cross-linking; the greater the divinylbenzene content, the more stable the resin becomes (Dorfner, 1972). The resins of interest are cross-linked by primary chemical bonds and as such can withstand "numerous ion-exchange cycles without significant losses due to solubility" (Abrams, 1967). The activity, durability, chemical stability and degradation resistance make IER composed of polymerized divinylbenzene with cationic sulfonic acid groups potential catalysts for transesterification of oils. The co-polymerization of styrene and divinylbenzene is well documented. Commercial resins typically vary between 4 to 30 wt%, the most common resins are composed of 8 wt% divinylbenzene (Abrams and Benezra, 1967).

1.6. Knowledge Gap

Published works pertaining to heterogeneous catalysis in transesterification have yet to achieve two important milestones, a reaction rate comparable to that of homogeneous catalysts and the production of biodiesel to satisfy ASTM standards. Furthermore, the reviewed literature is lacking in the thorough examination of IER in transesterification. Omissions in the study of IER in transesterification include:

- Transesterification with IER at temperatures above the boiling point of methanol;
- Statistical optimization of transesterification reaction conditions using IER;
- Use of greenseed canola oil in conjunction with IER;
- Development of a kinetic model at temperatures above the boiling point of methanol.

After reviewing all relevant publications on biodiesel production, solid acid catalysis and ion exchange resins, there are several knowledge gaps open to examination. A small variety of oils have been used as feedstock for biodiesel production using IER as catalysts. There have been no statistical optimization studies on the reactor conditions while using IER above the boiling point of methanol. No research papers have been found using IER in a process capable of achieving the conversions required for commercial production without excessive alcohol molar ratios or catalyst leaching. Only one published work exceeded the boiling point of methanol (65˚C) while using IER.

1.7. Research Objectives

The biodiesel industry requires a heterogeneous catalyst that is capable of reaction rates comparable to those of homogeneous catalysts and that can produce high quality biodiesel. The objective of this research project was to identify and optimize an IER as a solid acid catalyst for converting oils to fatty acid methyl esters through transesterification for biodiesel production. The intent of this work was to adapt reactor conditions to achieve reaction rates comparable to homogeneous catalysts using IER and producing biodiesel consisting of fatty acid methyl esters (FAME). By examining temperatures above the boiling point of methanol and statistically optimizing reactor conditions using triolein, canola oil and greenseed canola oil as feedstocks, the knowledge gaps outlined in section 1.6 will be addressed.

The sub-objectives of this work were to:

- Screen a variety of commercial IER as solid acid catalysts in transesterification of triolein and canola oil;
- Optimize reaction conditions using triolein with the most highly active catalyst using statistical optimization and perform reusability tests;
- Characterize catalysts to gain insight into catalytic performance;
- Examine transesterification at temperatures up to the critical point of methanol, 240˚C;
- Gain understanding of the transesterification process by using a variety of feedstocks, analyzing FAME products and reaction kinetics;
- Develop a mathematical kinetic model derived from the rate law to fit experimental data to determine kinetic parameters of transesterification.

2. LITERATURE REVIEW

2.1. Feedstock

Oils and fats derived from both plants and animals are feedstock for biodiesel production. They are lipid materials, namely triglycerides (TG), diglycerides (DG) and monoglycerides (MG). Oils consist of a glycerol molecular backbone bonded to a number of hydrocarbon chain carboxylic groups. The hydrocarbon chains can be of any length with any number of double bonds. An example of a triglyceride is oleic acid, seen in Figure 2-1. Each hydrocarbon chain consists of 18 carbon molecules and one double bond. The naming convention for oleic acid is C18:1; C for carbon, 18 for the number of carbon molecules and 1 for the number of double bonds. Oils can be used directly as a substitute for diesel fuel; however, the high viscosity of oils causes injection problems and prevents proper atomization in compression ignition engines (CIE). The purpose of the transesterification is to reduce the viscosity of the feedstock oil (Demirbas, 2008).

2.1.1 Triolein

Triolein or trioleoyl glycerol is used as a model feedstock in numerous publications examining transesterification (Iso, 2001; Ebiura, 2005; Hanh, 2009). Triolein is a triglyceride with oleic acid carboxylic groups. As will be illustrated in section 2.7, oleic acid and its 18 carbon chain and monounsaturated bond can be converted into a methyl ester with desirable fuel properties. Figure 2-1 illustrates the structure of triolein.

2.1.2 Canola Oil

Of the 205 million litres of biodiesel currently produced annually in Canada, 29 million litres are produced exclusively from canola oil. An additional 135 million litres is produced from

multiple feedstocks which include canola oil (CFRA, 2011). The carbon life cycle analysis has been reported and demonstrates the advantages of canola derived biodiesel over petroleum diesel in terms of net carbon released (Peterson, 1998). Both homogeneous catalysts (Issariyakul, 2006) and heterogeneous catalysts (Jothiramalingam, 2009) have been examined utilizing canola oil as a feedstock for biodiesel production. The dominant component in canola oil is the triglyceride form of oleic acid (C18:1), triolein.

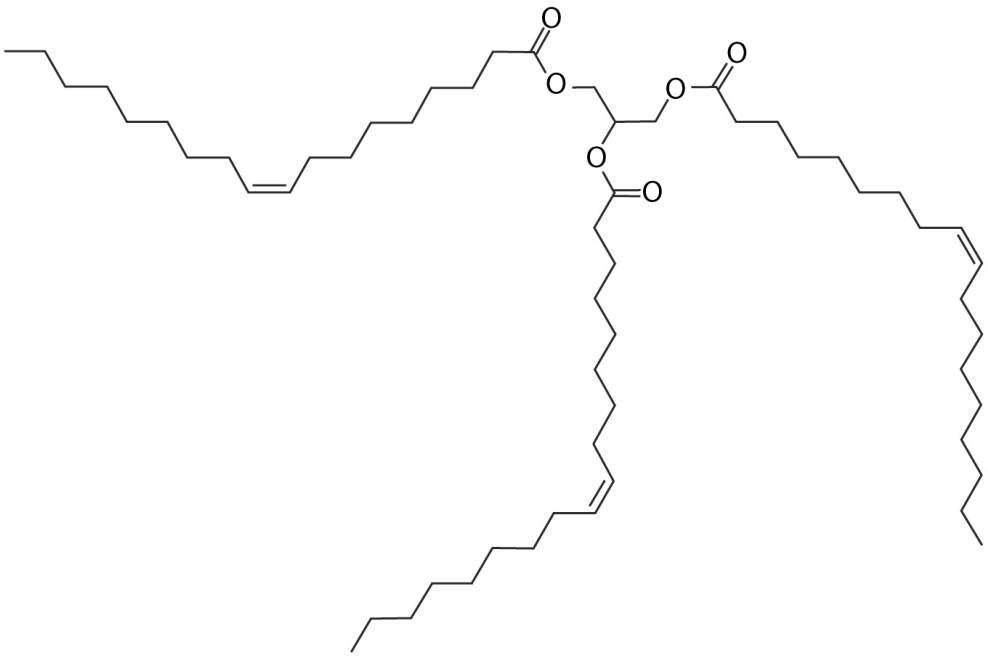

Figure 2-1: Triglyceride form of oleic acid, triolein

2.1.3 Greenseed Canola Oil

Greenseed canola oil is produced as a result of extracting oil from canola seed containing chlorophyll. Canola seed contains chlorophyll when the seed is unable to properly mature. Greenseed canola oil is low quality due to its chlorophyll content. Chlorophyll is often retained due to exposure to sub-lethal frosts (0 to 5˚C) during seed maturation (Kulkarni, 2006b). Number 1 canola is high purity canola oil containing less than 25 ppm chlorophyll. Number 2 canola oil

is a lower grade and contains between 26 - 45 ppm. Number 3 canola oil contains between 46 - 100 ppm chlorophyll (Issariyakul, 2010). Both number 2 and 3 grades are considered greenseed canola oil. As chlorophyll content increases the price of each type of canola oil decreases (Issariyakul, 2010). Additionally, greenseed canola oil can be used to produce biodiesel to meet ASTM standards (Kulkarni, 2006b).

2.2. Transesterification

Transesterification is an organic chemical reaction involving the exchange of an ester group between two molecules. A high molecular weight ester is reacted with a low molecular weight alcohol to produce an ester with a lower molecular weight (Gelbard, 2005). Catalysts with acidic or basic functional groups are often used to increase conversion to products and lower activation energy. In biodiesel production, a vegetable oil or animal fat reacts with methanol to produce esters and glycerol. Transesterification of triglycerides to fatty acid methyl esters (FAME) involves a three step reversible reaction. The net reaction is illustrated in Figure 1-1, the stepwise reactions are demonstrated in equations 2-1, 2-2 and 2-3. Reaction components are: triglyceride (TG), diglyceride (DG), monoglyceride (MG), methyl ester (ME), methanol (MeOH), glycerol (GL) and the catalyst is listed as a Bronsted acid (i.e. a proton donor). Methanol and glycerol must be separated from the reaction products. Methanol is removed by distillation and can be recycled into the process. Glycerol can be separated by gravity filtration and washing with water. The reaction proceeds in the presence of both acidic and basic catalysts such as potassium hydroxide (KOH), sodium hydroxide (NaOH) and sulfuric acid (H_2SO_4). Reaction mechanisms for homogeneous reactions are discussed in section 2.3.1. Alternatively, heterogeneous catalysts such as metal oxides, carbonates, zeolites, heteropoly acids, functionalized zirconia or silica, ion-exchange resins, hydrotalcites or alkaline salts can also be

used (Demirbas, 2008; Helwani, 2009). Many different alcohols can be used in transesterification such as methanol, ethanol, propanol, or butanol (Ma, 1999). The stoichiometric molar ratio required in this reaction of oil to alcohol is 1:3. Since the transesterification reaction is reversible, excess alcohol is used to shift the reaction to the products by LeChatelier's principle, where an excess of a reactant will shift chemical equilibrium to favour products.

$$TG + MeOH \overset{H^+}{\rightleftharpoons} DG + ME \quad (2\text{-}1)$$

$$DG + MeOH \overset{H^+}{\rightleftharpoons} MG + ME \quad (2\text{-}2)$$

$$MG + MeOH \overset{H^+}{\rightleftharpoons} GL + ME \quad (2\text{-}3)$$

In the transesterification reaction, a triglyceride molecule reacts with methanol in the presence of an acid or base to produce a diglyceride and a methyl ester molecule. Similar reactions occur with lower glyceride molecules (diglyceride and monoglyceride). The net reaction as illustrated in Figure 1-1 is the decomposition of a triglyceride molecule with three methanol molecules to glycerol and three methyl ester molecules. There are numerous variables that have an effect on transesterification, including the feedstock properties (chain length, saturation, purity), alcohol type and molar ratio relative to feedstock, catalyst used (acid or alkaline; homogeneous or heterogeneous), catalyst loading, reaction temperature, etc. (Demirbas, 2008). Current priorities in research conducted on biodiesel production are to determine an adequate oil source, determining an appropriate oil to alcohol molar ratio and evaluating solid acid, solid base and lipase immobilized enzyme catalysts (Jothiramalingam, 2009).

The purpose of a catalyst in transesterification is to induce an electrophilic attack. In the case of acid catalysis, the carbonyl carbon of the glyceride gains a positive charge from the catalyst leading to electrophilic attack by the electrons of the oxygen atoms in the alcohol. In the

case of basic catalysts, the alcohol is deprotonated first, allowing for electrophilic attack of the carbonyl carbon of the glyceride. Acid and bases are subdivided into Bronsted type and Lewis type; all are capable of catalyzing the transesterification reaction. Bronsted acids are more active in the esterification reaction, while Lewis acids are more active in the transesterification reaction (Di Serio, 2008). Bronsted and Lewis acids can be used in the synthesis of biodiesel from low quality feedstocks since they both catalyze the esterification and transesterification reactions (Di Serio, 2008).

2.2.1 Bronsted Acids and Bases

Bronsted acids and bases are chemical species with an available proton (H^+) in acids or proton acceptor (OH^-) in bases (Di Serio, 2008). Examples of Bronsted acids and bases are: sulfuric acid (H_2SO_4), sodium hydroxide (NaOH) and potassium hydroxide (KOH) (Balat, 2008). In transesterification, Bronsted acids catalyze the reaction by protonating the carbonyl group that allows for nucleophilic attack by the alcohol reactant (Di Serio, 2008). Bronsted bases, when combined with alcohol, form an alkoxide anion. The alkoxide anion subsequently attacks the carbonyl carbon atom in the triglyceride molecule. The Bronsted alkaline metal hydroxides (eg. potassium hydroxide or sodium hydroxide) are cheaper alternatives compared to Lewis alkaline metal alkoxides (eg. sodium methoxide) The alkaline metal hydroxide catalysts are less active as catalysts and require loadings of 1 or 2 mol% compared to 0.5 mol% loadings using alkaline metal alkoxides (Helwani, 2009).

The mechanism for the Bronsted base-catalyzed reaction begins with the deprotonation of the alcohol. The alcohol anion attacks the carbonyl carbon atom of the triglyceride to form a tetrahedral intermediate. This tetrahedral intermediate reacts with another alcohol molecule to regenerate the alcohol anion. In the final step, the tetrahedral intermediate is rearranged to form a

diglyceride molecule and an ester (Ma, 1999). This mechanism is illustrated in Figure 2-2. The alkali-catalyzed reaction is much faster than the acid-catalyzed reaction because of the difference in reaction mechanisms.

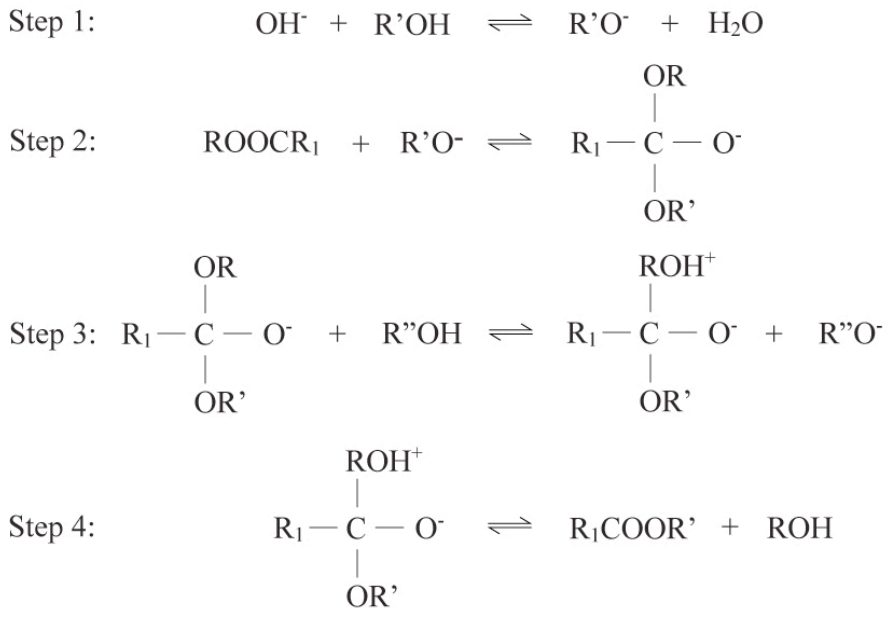

Figure 2-2: Bronsted base-catalyzed mechanism of transesterification (based on Ma, 1999)

The mechanism of Bronsted acid-catalyzed transesterification is described by Demirbas (2008) and is illustrated in Figure 2-3. The first step is the protonation (donated from the acid catalyst) of the triglyceride. R_1 is the ester chain, R' is the glycerol backbone and R" is the methyl group of the alcohol. The alcohol attacks the carbonyl carbon to produce a tetrahedral intermediate cation (step 2). Next, the glycerol chain (R'OH) is released. Finally, the ester is produced when the proton is regenerated. Acid catalysis is a slower mechanism due to the first step the protonation of the triglyceride. In basic catalysis, a proton is removed from the alcohol, which has less stearic hindrance allowing for a faster rate limiting first step.

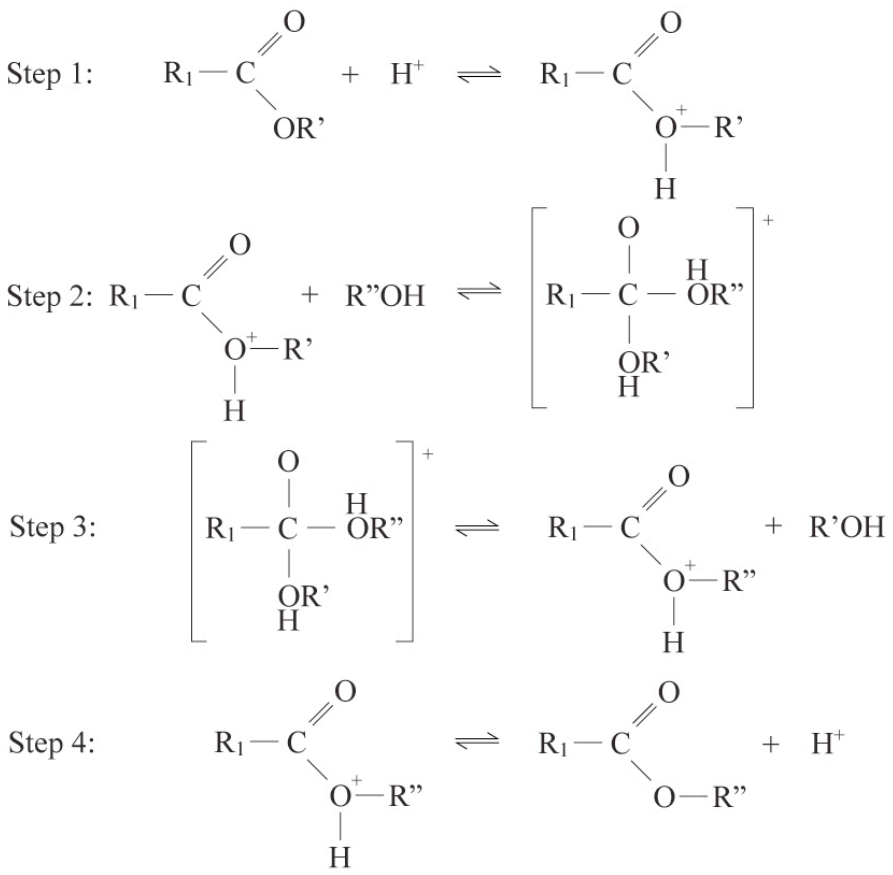

Figure 2-3: Bronsted acid-catalyzed mechanism of transesterification (based on Demirbas, 2008)

2.2.2 Lewis Acids and Bases

Lewis acids and bases are chemical species that are electron pair acceptors (acids) or electron pair donors (bases). Examples of Lewis acids are aluminum chloride ($AlCl_3$) and lead acetate ($Pb(OOCH_3)_2$). Examples of Lewis bases are sodium methoxide ($NaOCH_3$) and ammonia (NH_3). The mechanism is illustrated in Figure 2-4. In transesterification, a Lewis acid first forms a complex with the carbonyl group. The alcohol attacks the carbonyl nucleus and an ester is formed and released. The release of the ester is dependent on the strength of the Lewis acid. A strong acid will not allow desorption of the product species. Strong Lewis acids are less active as catalysts (Di Serio, 2008).

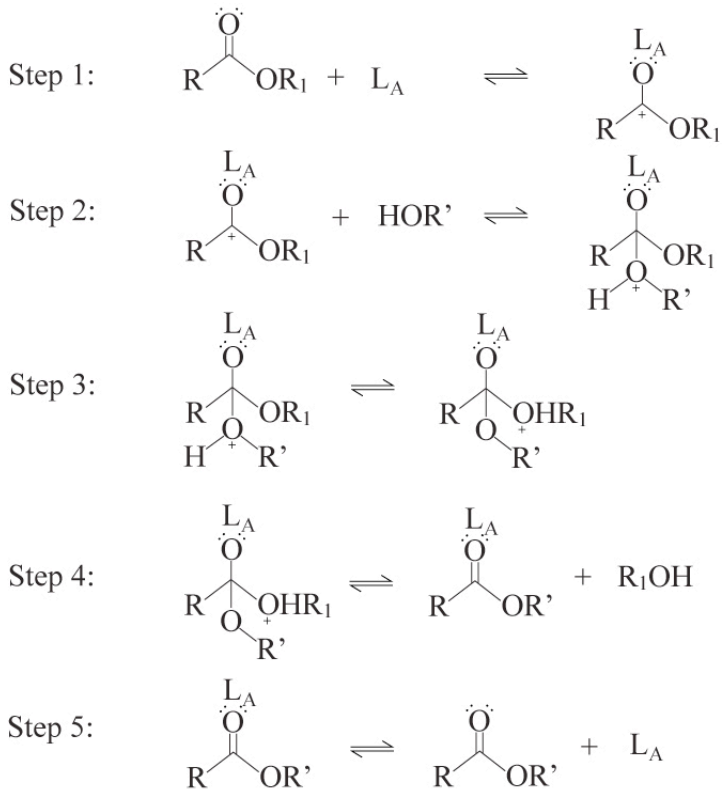

Figure 2-4: Lewis acid catalyzed mechanism of transesterification (based on Di Serio, 2008)

Lewis bases rely on the formation of the alkoxide anion, similar to the mechanism with Bronsted bases. The catalyst removes the proton from the alcohol allowing for electrophilic attack of the carbonyl carbon of the glyceride. A second alcohol molecule donates a proton to the tetrahedral intermediate, allowing removal of the tetrahedral alcohol of the carbonyl group, forming an ester. This mechanism is illustrated in Figure 2-5. Alkaline metal alkoxides (eg. sodium methoxide) are among the most active homogeneous Lewis acid catalysts (Balat, 2008). They provide yields above 98 wt% in 30 minutes at a catalyst loading of 0.5 mol% with an oil to methanol ratio of 1:6 (Helwani, 2009).

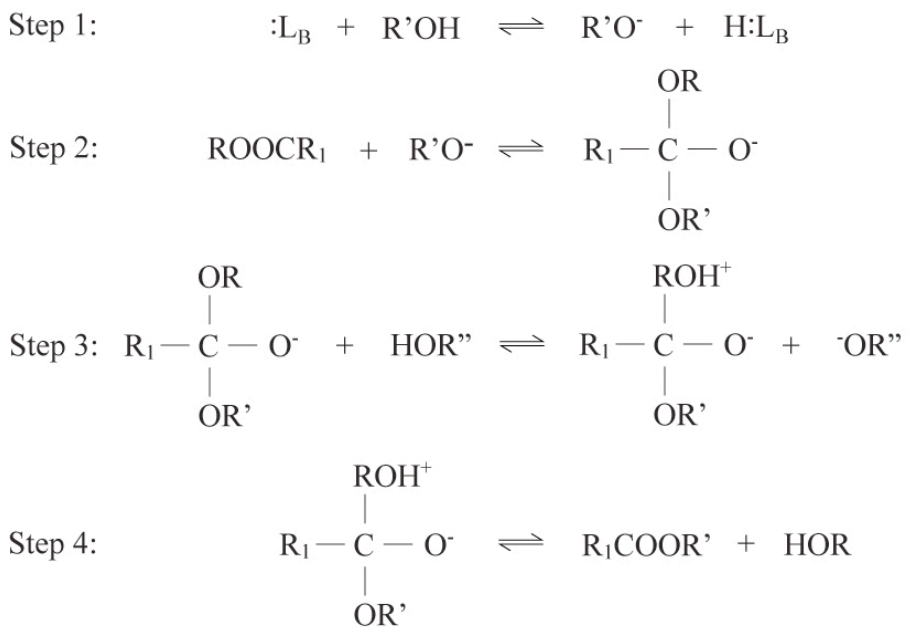

Figure 2-5: Lewis base catalyzed mechanism of transesterification (based on Helwani, 2009)

2.3. Various Catalysts Used for Biodiesel Production

2.3.1 Homogeneous Acid Catalysts

Commercial biodiesel is typically produced using non-reusable homogeneous catalysts resulting in corrosion of equipment, additional processing steps and wastewater disposal problems (Melero, 2009b). Homogeneous acidic catalysts such as sulfuric acid, sulfonic acid, phosphoric acid or hydrochloric acid are commonly applied in transesterification. Acidic catalysts are insensitive to free fatty acid content of low quality feedstock and are less sensitive to water content (Helwani, 2009). Acid catalyzed reactions require higher oil to methanol ratios (1:30 compared to 1:9) to achieve conversions similar to basic catalysts (Freedman, 1984). The rates of reaction of acidic catalysts in transesterification are slower than with basic catalysts, so the time required for the reaction to proceed to completion is longer (3 h to 48 h) (Freedman, 1984).

Lewis acid catalysts were examined in esterification and transesterification of soybean oil and added palmitic acid as a model free fatty acid (Hou, 2007). Acetates of lead, cadmium and zinc were examined [$Pb(OOCCH_3)$, $Cd(OOCCH_3)$ and $Zn(OOCCH_3)$]. Autoclave reaction conditions were 180˚C, 1:30 oil to methanol molar ratio, 2 wt% catalyst loading, 2 MPa, for 30 minutes. Reported content of FAME in reaction products was 83.4 wt%, with an acid value of 11.2 mg KOH/g sample. While the catalysts were active in both esterification and transesterification reactions, the respective yields of both reactions do not satisfy ASTM standards. The Lewis catalyzed reactions are reportedly slow due to mass-transfer limitations between the hydrophobic oil phase and the methanol phase (Hou, 2007). Homogeneous acid catalysts are not ideal for biodiesel production due to the slow reaction rates requiring lengthy reaction times. The ability of homogeneous acid catalysts to simultaneously catalyze esterification and transesterification, as well as their demonstrated tolerance to water content, are desirable qualities.

2.3.2 Homogeneous Base Catalysts

Basic catalysts are more common in industry because they have a higher reaction rate compared to acid catalysts (Helwani, 2009). However, basic catalysts require anhydrous conditions and the feedstock must have low levels of free fatty acids (FFA) to prevent saponification (Lotero, 2005). This side reaction occurs when an ester is hydrolyzed to a salt and the catalyst is consumed. Saponification lowers ester yield, reduces the ease of separation of the ester and glycerol product layers and causes difficulty during product washing (Ma, 1999). Some work suggests that a two-stage process can be employed (Issariyakul, 2007). Homogeneous acid pretreatment followed by homogeneous base catalysis aids in the processing of low-quality feedstock, however the problems associated with homogeneous catalysts remain an issue.

Homogeneous catalysts can't be reused, they present corrosion issues with equipment and the products require neutralization and washing with water to remove caustic substances. Removal of the catalyst from product streams is a technical challenge and adds cost to the process (Helwani, 2009). In addition feedstock oils and methanol must be anhydrous when using homogeneous base catalysts to avoid saponification, which causes difficulties in the separation of products.

Use of potassium hydroxide (KOH) as a catalyst for transesterification of green seed oils has been reported (Issariyakul, 2010). To treat the feedstock, montmorillonite K10 was used as an adsorbant clay to remove 99.5% of all pigments (i.e. chlorophyll A, chlorophyll B, pheophytin A and pheophytin B) from the oil. Reaction conditions were 60˚C, 1:6 oil to alcohol molar ratio, 1 wt% catalyst loading, 600 RPM stirring speed and a reaction time of 90 minutes. Various mixtures of canola oil and treated and untreated greenseed canola oil were used as feedstock. Methanol, ethanol and a mixture of both alcohols were used in controlled experiments. The reported composition of esters produced with a mixture of treated greenseed canola oil and canola oil with methanol was 96.8 wt% (Issariyakul, 2010). Use of ethanol decreased ester production compared to experiments with methanol. No difference was reported between reactions with treated and untreated greenseed canola oil. Therefore, it was concluded that pigments found in greenseed canola oil do not have a measurable impact on the transesterification reaction. The pigments were found to have a negative impact on the oxidative stability of products. Biodiesel produced from crude greenseed canola oil had an induction time of 0.5 hours, versus an induction time of 0.7 hours in the treated greenseed oil (Issariyakul, 2010). The minimum induction time for ASTM standard biodiesel is three hours (ASTM, 2011). The authors also state that the high degree (30%) of polyunsaturated fatty acids present in

greenseed canola oil also had an adverse effect on the oxidative stability reported (Issariyakul, 2010).

Dmytryshyn (2004) examined canola oil, greenseed canola oil and waste fryer grease in transesterification with potassium hydroxide in a two-stage process. Identical reaction conditions were used in both steps: 25˚C, 1:6 methanol molar ratio, 0.5 wt% catalyst loading, stirring for 20 minutes. The reaction product glycerol was separated by gravity filtration between stages. After both stages, products were washed with water in order to remove the catalyst and some of the remaining methanol. A Rota-Evaporator was applied to evaporate remaining methanol. Silica gel and sodium sulfate were added to the FAME products to remove any traces of water. The highest yield of esters (FAME) produced using canola oil was reported to be 87 wt% relative to the theoretical yield. Greenseed canola oil and waste fryer grease conversions were 75 wt% and 51 wt%, respectively. Fuel characteristics were examined and compared between FAME produced from different feedstocks. Density, viscosity, cloud point, iodine value, lubricity and acid value were among the characteristics examined. Canola oil was reported to be the best choice for an alternative or additive to diesel fuel (Dmytryshyn, 2004).

Transesterification of algal oil (derived from *Cynara cardunculus* L.) using homogeneous base catalysts has been reported (Encinar, 1999). Reaction variables examined were type of catalyst (NaOH, KOH, $NaOCH_3$), methanol concentration (5-21 wt%), catalyst loading (0.1-1 wt%) and temperature (25-60˚C). Reported yield of esters was 94 wt% at the optimized conditions: 60˚C, 18 wt% methanol loading (1:5 molar ratio), 1 wt% catalyst loading, using sodium methoxide. The biodiesel produced was characterized by density, viscosity, higher heating value (HHV), cloud point, pour point, flash point, etc. FAME standards were met with

the authors noting that the cloud point and pour point were slightly higher than in diesel fuel which may result in cold-start issues in compression ignition engines (Encinar, 1999).

Homogeneous bases are the most commonly used catalysts for biodiesel production. However, homogeneous catalysts are not reusable, they are associated with corrosion issues of processing equipment, require hazardous waste disposal and require additional washing stages for purification. Homogeneous basic catalysts are not tolerant to water or free fatty acids typically present in low-quality feedstocks. Due to the issues involved in the continued use of homogeneous catalysts, there is a need for the development of a suitable heterogeneous catalyst for use in the biodiesel production industry (Melero, 2009b).

2.3.3 Heterogeneous Acid Catalysts

Heterogeneous catalysts have the potential to replace homogeneous catalysts and circumvent some of the problems associated with conventional production methods. Solid acid catalysts (SAC) have been reported to simultaneously catalyze the esterification and transesterification reactions (Zabeti, 2009). Both Bronsted and Lewis acid sites are capable of catalyzing the esterification reaction (Melero, 2009b). Of the materials reviewed by Melero (2009b), sulfated materials had the highest catalytic activity, but they are subject to poisoning effects. Other heterogeneous catalysts such as sulfonated solids, metal oxides and supported heteropolyacids have been examined in transesterification. Many of the catalysts were unable to achieve conversions to FAME approaching ASTM standards. Several of the catalysts that were highly active were subject to sulfate leaching and deactivation in successive reactions. Supported heteropolyacids, zirconia titania and zirconia alumina were the most active and stable catalysts. Organically functionalized solid acid catalysts have demonstrated high catalytic activities in both esterification and transesterification. Additional work is required to increase stability and

longevity of these catalysts (Melero, 2009b). Helwani (2009) presents a review of various types of heterogeneous catalysts for biodiesel production, focusing on solid base catalysts. Examples of solid acid catalysts reviewed are zeolites, heteropoly acids, functionalized zirconia and silica, tungsten oxides, ion-exchange resins and sulfonated saccharides. Due to the low activity of SAC at conventional temperatures used in biodiesel production they are largely dismissed in this review (Helwani, 2009). Solid acid catalysts, including zeolites, heteropoly acids, tungsten oxides, sulfated zirconia and tin oxides, have been reviewed previously (Jothiramalingam, 2009). Jothiramalingam (2009) concludes that 'An ideal ... solid acid catalyst should possess interconnected large porous texture with moderate to high concentration of acid sites and a hydrophobic surface'. A hydrophobic surface is essential to promote preferential adsorption of oily hydrophobic species on the catalyst surface and to avoid possible deactivation of catalytic sites by the strong adsorption of polar byproducts such as water and glycerol. (Jothiramalingam, 2009).

The role of solid (Lewis) acidic catalysts in the transesterification reaction is illustrated in Figure 2-6. The reaction takes place via the single site Eley-Rideal mechanism. This mechanism describes the adsorption of one species on the catalyst surface, followed by the reaction when the second species reacts with the surface-bonded species (as illustrated in Figure 2-6). In the case of transesterification this involves nucleophilic attack of the surface-bonded carboxylic acid group reacting with the alcohol (Di Serio, 2008). The electron rich carbonyl oxygen of a triglyceride is attracted to an acidic or basic functional group. The oxygen atom of methanol forms a transition state with the carbon atom of the triglyceride carbonyl group. Electron transfer from the Lewis bonded oxygen atom allows the removal of the glycerol chain (diglyceride) replacing an ester group with a hydroxide group. The methyl ester leaves the Lewis acid site. This reaction is a

three-step reversible reaction: triglyceride to diglyceride to monoglyceride to glycerol (Kulkarni, 2006a). The Lewis acid 12-tungstophosphoric acid (TPA), supported on hydrous zirconia, silica, alumina and activated carbon, were evaluated in simultaneous esterification and transesterification of low quality canola oil. TPA supported on hydrous zirconia was selected as the most highly active catalyst. At a temperature of 200˚C, 1:9 oil to alcohol molar ratio, 3 wt% catalyst loading was reported to have an ester yield of 90 wt%. The catalyst was reused with no loss of activity in longevity testing (Kulkarni, 2006a).

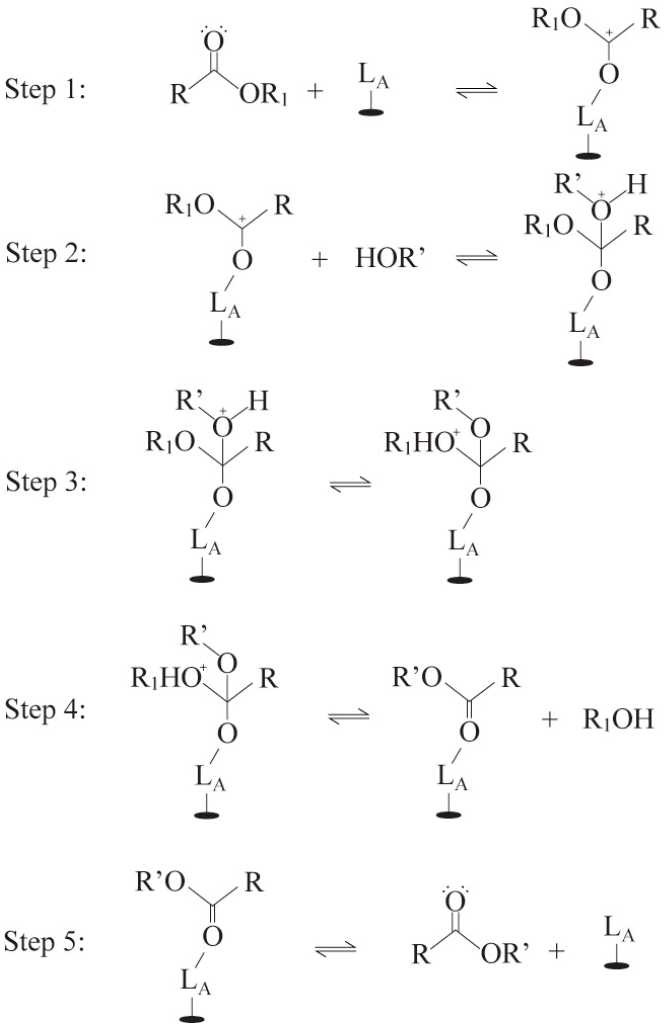

Figure 2-6: Reaction mechanism for production of methyl esters by acid catalyzed transesterification and esterification (based on Kulkarni, 2006a)

Singh (2008) examined numerous metal oxides as solid Lewis acid catalysts for transesterification of soybean oil. Catalysts examined were magnesium oxide (MgO), calcium oxide (CaO), lead oxide (PbO), lead dioxide (PbO_2), lead tetraoxide (Pb_2O_4), titanium trioxide (Ti_2O_3) and zinc oxide (ZnO). Each catalyst was characterized using the BET method (Brunauer, 1938) and acid site strength and type. Several temperatures were examined: 75˚C, 150˚C and 225˚C. Catalyst loading was 2 wt%, using an oil to methanol ratio of 1:77. A yield of 89% was reported with PbO and PbO_2 after two hours. A significant quantity of metal leaching was detected in both the glycerol and biodiesel products (eg. 13,000 ppm lead detected in biodiesel) (Singh, 2008).

Jacobson (2008) studied various heterogeneous acidic catalysts including: molybdenum-zirconia, tungsten-oxide-zirconia, zinc stearate on silica and 12-tungstophosphoric acid on zirconia. Waste cooking oil containing 15 wt% FFA was used as feedstock. Reaction conditions were 200˚C, 1:18 oil to alcohol ratio and 3 wt% catalyst loading. Simultaneous esterification and transesterification were carried out in batch reactions over 10 hours. Zinc stearate was the most active catalyst, achieving an ester yield of 98 wt%. Acid value was decreased from 30 mg KOH/g sample to 2 mg KOH/g sample during the reaction. A longevity study was conducted to determine if the catalyst was reusable. The used catalyst was separated via filtration, washed with hexane to remove non-polar compounds and then with methanol to remove polar compounds. The catalyst was dried at 80˚C overnight. Five successive reactions were carried out with no detectable decrease in catalytic activity (Jacobson, 2008).

Hara (2009) presents an overview of solid acid catalysts for biodiesel production. Solid acid catalysts (SAC) are capable of producing biodiesel from low-quality feedstocks. The capability of SAC to simultaneously catalyze esterification and transesterification is a desirable

catalyst property. Amberlyst 15, sulfated zirconia, Nafion NR50, tungstated zirconia and supported phosphoric acid are all reported to catalyze esterification of free fatty acids. Tungstated zirconia-alumina and sulfated tin oxide are reported to be highly active at 200˚C in transesterification and esterification, respectively (Hara, 2009). Metal oxides (Lewis acids, eg. TiO_2/ZrO_2, Al_2O_3/ZrO_2 and ZnO) were also reviewed as catalysts for esterification and transesterification. Low activities were noted, unless temperatures above 170˚C were used. A novel catalyst examined was an amorphous carbon structured like graphene with sulphonic acid (SO_3H) functional groups. The catalyst was reported to be highly active and stable in both esterification of FFA and transesterification of triglycerides. Triolein was converted to methyl oleate at 130˚C, 15 wt% catalyst loading, 1:43 oil to methanol molar ratio, 0.7 MPa. A yield of 96 wt% was reported at 5 hours (Hara, 2009). In a follow-up publication, a similar catalyst at nearly identical conditions achieved a yield of methyl oleate of 99 wt%, with minimal loss of activity in successive reuses (Hara, 2010).

Melero (2009a) examined a sulfonic acid supported on a mesostructured silica support, SBA-15 (Santa Barbara Amorphous #15). A central composite design was used to optimize reaction conditions. A linear model was found to be inadequate to describe the reaction. A quadratic model was developed and it was found that all three variables (temperature, alcohol molar ratio and catalyst loading) were statistically significant. Interaction effects were significant between temperature-catalyst loading, temperature-alcohol molar ratio and catalyst loading-alcohol molar ratio. Alcohol molar ratio was reported to have the highest impact on product composition. Reaction conditions for the highest FAME composition in the product mixture was 195˚C, 1:10 oil to alcohol molar ratio and 9 wt% catalyst loading. FAME composition in the products was reported to be 99.8 wt%. The equation from the statistical model is presented as

equation 2-4. In the predictive model equation, X represents conversion to FAME, T is temperature, C is catalyst loading and A is alcohol molar ratio (Melero, 2009a):

$$X = 87.4 + 5.1T + 7.2C - 18.8A - 5.9T^2 - 0.6T \times C - 6.3T \times A - 3.9C^2 + 3.5C \times A - 5.9A^2 \quad (2\text{-}4)$$

The variables are presented in coded factors varying from +1 to -1 for the highest and lowest values for each variable. In the case of this predictive equation variable ranges for temperature are 195˚C (+1) to 165˚C (-1), catalyst loading 9 wt% (+1) to 3 wt% (-1) and methanol molar ratio 50:1 (+1) to 10:1 (-1). When the coded factors are used for any value of the variables within the model limits, this equation provides an accurate approximation of the yield of biodiesel produced by this reaction. The numerical value is indicative of the relative weights of the effect that each variable and interaction effects, have on the yield of FAME.

2.3.4 Heterogeneous Base Catalysts

Solid basic catalysts have faster reaction times when compared to solid acid catalysts. Catalyst efficiency is reported to depend on physical surface properties such as surface area, pore size, pore volume and active site concentration (Zabeti, 2009). Most heterogeneous base catalysts were tested at the boiling point of methanol (Helwani, 2009; Zabeti, 2009; Ebuira, 2008). The mechanism of heterogeneous Bronsted basic catalysis in transesterification is similar to that of homogeneous Bronsted basic catalysis, relying on the formation of the alkoxide cation (CH_3O^-) bonded to the catalyst surface (Zabeti, 2009). Solid base catalysts and enzymatic lipases including alkali metal, alkali earth metals, hydrotalcites and transition metals on various supports, hydrotalcites and alkali oxides, have been examined (Jothiramalingam, 2009; Peterson, 1984; Helwani, 2009).

Many catalysts achieved reported conversions above 90%. An example is calcium methoxide ($Ca(OCH_3)_2$); using a temperature of 65˚C, oil:alcohol molar ratio of 1:24 and a catalyst loading of 2 wt%, a conversion of 98% was reported (Zabeti, 2009). A conversion of 99% has been reported using calcium oxide on calcium carbonate (Helwani, 2009). Temperature was 65˚C and reaction time was 2 hours. Alcohol molar ratio and catalyst loading were not reported. Helwani (2009) concluded that solid base catalysts are of higher commercial interest, but notes that more research into solid acid catalysis is required. Modified dolomites (hydrotalcites) achieved a reported biodiesel yield of 99.9% (Jothiramalingam, 2009). Lipase catalysts reported yields up to 94% and are stated to be a promising candidate for future research in biodiesel production (Jothiramalingam, 2009). Ebuira (2008) examined alumina loaded with alkali metals in solid base catalysis of triolein in transesterification. Metal salts such as potassium carbonate (K_2CO_3), lithium nitrate ($LiNO_3$) and sodium nitrate ($NaNO_3$) were doped on alumina (Al_2O_3). Reaction conditions were as follows: temperature of 60˚C, 1:24 oil to methanol ratio, 5 wt% catalyst loading and tetrahydrofuran (THF) as a co-solvent over a reaction time of one hour. Potassium carbonate was found to be the most highly active catalyst. The highest reported yield of methyl oleate (FAME) was 94 mol% (Ebuira, 2008). A high molar ratio of alcohol to oil, high level of catalyst loading and high temperatures and pressures are required when using heterogeneous catalysts for transesterification (Zabeti, 2009). The use of solid basic catalysis for biodiesel production has been widely examined, with a lack of research into solid acid catalysts (Jothiramalingam, 2009).

In a study on the production of biodiesel from canola oil using heterogeneous basic catalysts, a statistical method was used to optimize process conditions (D'Cruz, 2007). Various alkali metal doped and alkali earth metal oxides were tested as catalysts. Of the catalysts tested

potassium carbonate (K_2CO_3) doped on alumina (Al_2O_3) was selected for optimization experiments. A 3-factor, 2-level central composite design (CCD) was used to optimize reactor temperature, catalyst loading and alcohol to oil molar ratio. Six centre points were used in a total of 20 experiments. Temperature was varied between 40˚C and 60˚C, catalyst loading from 2 to 4 wt% and oil to methanol molar ratio from 1:6 to 1:12. The response surface methodology produced a second-order polynomial to describe the final production weight percentage of methyl esters. The model produced was significant due to an F-value of less than 0.0001. All three factors were significant based on their probability F-values. The R-squared value of the model was 0.99. Optimum ester yield was 96.3 wt% after 2 hours at 60˚C, 3.16 wt% K_2CO_3/Al_2O_3 and 1:11.48 oil to methanol molar ratio. Some leaching of potassium was detected (D'Cruz, 2007).

2.4. Ion-Exchange Resins

The property of certain materials to exchange ions was first discovered over 155 years ago. Commercial ion-exchange resins (IER) have been in production for more than 60 years (Dorfner, 1972). There are hundreds of commercial varieties based on many different insoluble matrices, including acrylics, amines and phenols. The functional groups of resins are typically acids or bases, with either strong or weak strengths. Ion-exchange resins catalyze reactions by providing acidic or basic functional groups for chemical reactions. The efficacy of an acid-catalyzed reaction is dependent on both Bronsted and Lewis acid sites of ion-exchange resins (Gelbard, 2005). In the case of sulfonic acid (SO_3H) as a functional group, a hydrogen ion (H^+) is available for ionic reactions. The most common substrate is a copolymer of styrene and divinylbenzene (DVB), illustrated in Figure 2-7. The percentage of DVB is the variable that determines the amount of cross-linking in the copolymer matrix. Increased amounts of cross-linking can be

unfavorable as it lowers the ion-exchange capacity of the resin (Shibasaki, 2007). Conversely, higher cross-linking increases the physical strength and porosity of a resin, the latter of which can increase the catalytic activity in transesterification (de Rezende, 2008).

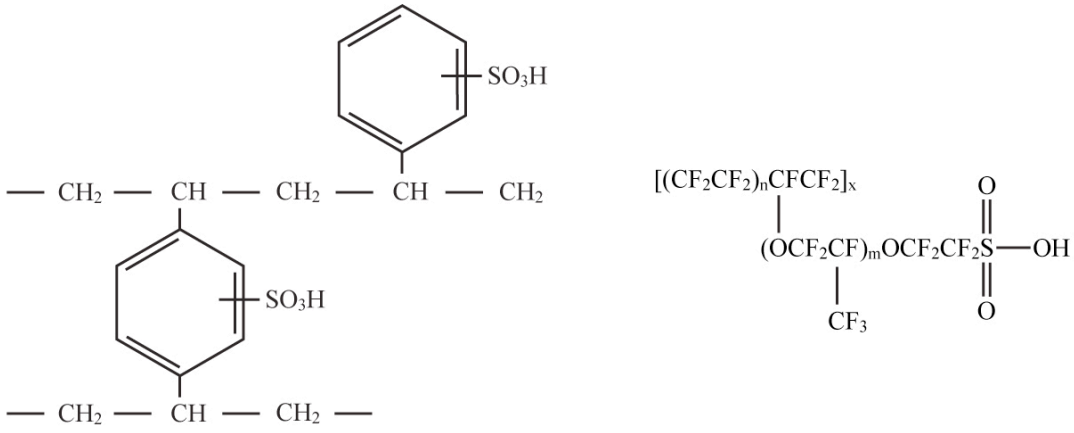

Figure 2-7: Structural composition of sulfonic acid styrene-divinylbezene IER (left) and Nafion SAC-13 (right) (based on Dorfner, 1972; López, 2007)

Sharma (1995) discussed the useful potential of ion-exchanging resins as catalysts. Resins can be used in any type of reactor, with any solution (due to their insolubility) and are used in a wide variety of reactions in industrial processes such as dimerization, esterification, hydration and transalkylation (Sharma, 1995). All ion-exchange resins are stable in water at 120˚C (Dorfer, 1972) and some are stable up to 200˚C (Sigma-Aldrich, 2012). An article by Harmer and Sun (2001) from DuPont studied a variety of commercially available resins. Some of the many organic reactions using ion-exchange resins as catalysts are acylation, alkylation, esterification, isomerization, oligomerization and nitration (Harmer, 2001). Gelbard (2005) expanded on the organic reactions catalyzed by ion-exchange resins. Among the types of reactions examined in depth were acylation, alkylation (of alkenes, aliphatics and phenol), aldolization, ketolization, isomerization, oligometization, carbonylation, esterification, transesterification, hydrolysis,

etherification, hydrogenation, oxidation and epoxidation (Gelbard, 2005). Ion-exchange resins are widely used in organic reactions.

2.5. Ion-Exchange Resins in Transesterification

Lotero (2005) reported that an ideal catalyst for the production of biodiesel would be a solid acid catalyst with an interconnected system of large pores, moderate to strong acid sites and a hydrophobic surface. Ion-exchange resins fit the description of an ideal biodiesel catalyst presented above. IER have been examined to some degree in transesterification. The majority of published works examining IER in transesterification used cationic resins, the acid-functionalized version of IER. Dos Reis (2005) examined the use of various commercial cationic resins in the transesterification of various vegetable oils native to Brazil. The Amberlyst brand of resins provided by Rohm & Haas were the subjects of the study. Catalyst properties as well as composition of the oils were compared. The ion-exchange resins used were Amberlyst 15, 31, 35 and 36. The results showed conversion up to 75% when oil to alcohol ratios were as high as 1:300 over a six hour reaction time (dos Reis, 2005).

Transesterification of soybean and babaçu coconut oils was conducted using commercial resins as well as resins prepared in-house consisting of polymers of styrene and divinylbenzene (de Rezende, 2008). Methyl ester yields of 99% and 97% were obtained using babaçu oil and soybean, respectively under the following reaction conditions: 1:150 oil to alcohol ratio, 65˚C, 50 wt% resin loading. The resins prepared by this group were polymers of styrene and divinylbenzene, similar to most commercial resins. The content of divinylbenzene ranged from 20% to 100%. The catalyst listed as ‘30a’ proved to be the most efficient (de Rezende, 2008). Results were compared with those performed experimentally with a standard homogeneous acid catalyst, as well as various commercial resins. Figure 2-8 shows the results of the experiments

with sulfuric acid, Amberlyst 15, Amberlyst 35 and the optimum catalyst '30a'. The optimum results were achieved at 99% conversion of babaçu oil and 97% conversion of soybean oil with no degradation of the catalyst. These high conversions are due to the activity of the catalyst, an extreme excess of alcohol and lengthy reaction times. The most highly active catalyst in the paper had one of the lowest cation-exchange capacities (de Rezende, 2008). Previously published work concluded that a lower degree of cross-linking was favourable to a higher reaction rate and that a higher degree of cross-linking would restrict the access of sulfonic groups to the aromatic rings during sulfonation (Shibasaki-Kitakawa, 2005). Contrary to previous findings suggesting that the catalytic activity is dependent on the cation-exchange capacity, the resin was reported to be highly active due to its macroporosity, high surface area (442 m^2/g) and high degree of cross-linking (de Rezende, 2008). The activity of a solid acid catalyst and strength of acidic sites have not been directly correlated (Helwani, 2009).

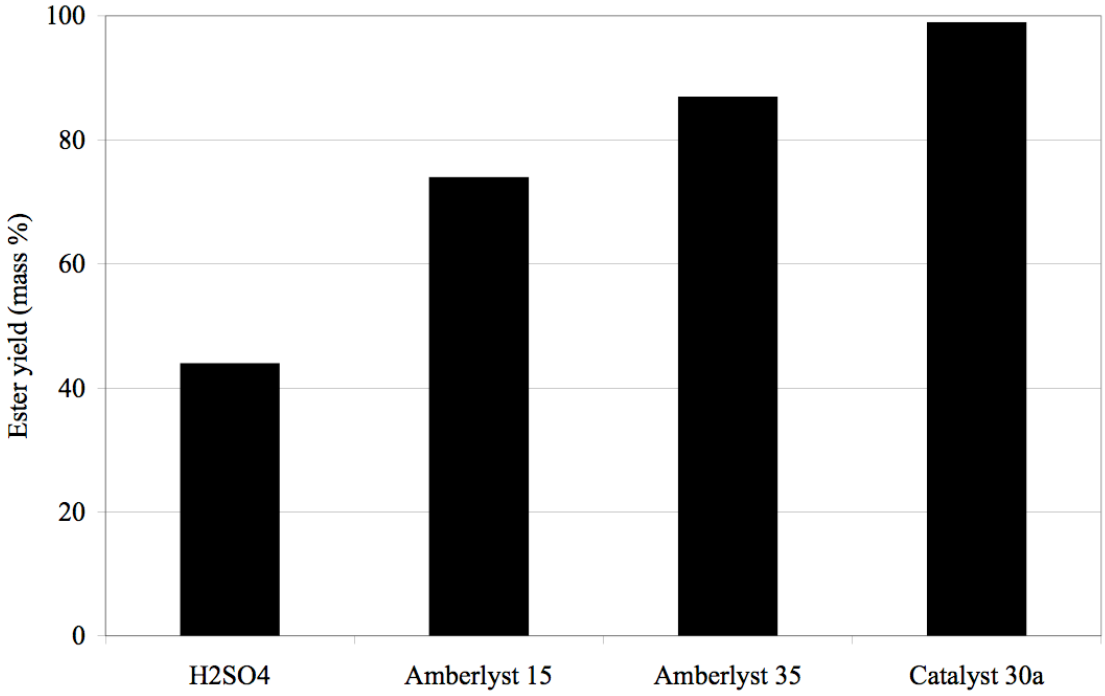

Figure 2-8: Transesterification of soybean oil with various catalysts (based on de Rezende, 2008)
Conditions: 65˚C, 1:100 oil:methanol, catalyst loading 50 wt%, soybean oil, 8 hours

Anionic resins are base-functionalized and have been examined in a number of publications. Peterson (1984) examined an anion exchange resin, Dowex 2-X8 in hydroxide form, in transesterification of canola oil. The resin was tested at 200˚C (6.9 MPa) and at 91˚C (0.93 MPa). Qualitative results were compared to homogeneous catalysis using sodium methoxide using thin layer chromatography (TLC). Yield of methyl esters was not reported. The experiment at 91˚C yielded trace amounts of FAME, the 200˚C experiment yielded twice the qualitative FAME production compared to sodium methoxide (Peterson, 1984). Anion-exchange resins have also been used as heterogeneous catalysts in transesterification of triolein (Shibasaki-Kitakawa, 2005). It has been shown that the base catalyzed transesterification reaction is faster compared to acid catalyzed reactions (due to the mechanism discussed below and in sections 2.2.2 and 2.3.3). A conversion to products of 85% was reported using an anionic resin (Diaion PA306s). This catalyst was reusable, however three regeneration steps were required: 1) washing with 5 vol% citric acid in ethanol, 2) regeneration with 1M sodium hydroxide and water wash, 3) swelling in ethanol (Shibasaki-Kitakawa, 2005).

The mechanism of transesterification using ion-exchange resins has been proposed as similar to a previously published mechanism for homogeneous catalysts (Shibasaki-Kitakawa, 2005). The mechanism for cation-exchange resins ($I(H^+)$) in the transesterification of a triglyceride (TG) with an alcohol (A) to a methyl ester (ME) and a diglyceride (DG) is listed in equations 2-5, 2-6 and 2-7. The first step of the mechanism is the adsorption of the triglyceride to the ion-exchange resin functional group. A similar mechanism would progressively convert diglycerides to monoglycerides followed by monoglycerides to glycerol, producing methyl esters and consuming an alcohol at each reversible step.

$$TG + I\left(H^+\right) \rightleftharpoons TG \cdot I\left(H^+\right) \tag{2-5}$$

$$TG \cdot I\left(H^+\right) + A \rightleftharpoons TG \cdot I\left(H^+\right) \cdot A \quad (2\text{-}6)$$

$$TG \cdot I\left(H^+\right) \cdot A \rightleftharpoons I\left(H^+\right) + ME + DG \quad (2\text{-}7)$$

Similarly, the mechanism for transesterification using anion-exchange resins ($I(OH^-)$) is also proposed in equations 2-8 through 2-11:

$$A + I\left(OH^-\right) \rightleftharpoons A^- + I\left(OH^-\right) \cdot H^+ \quad (2\text{-}8)$$

$$A^- + TG \rightleftharpoons A \cdot TG^- \quad (2\text{-}9)$$

$$A \cdot TG^- \rightleftharpoons ME + DG^- \quad (2\text{-}10)$$

$$DG^- + I\left(OH^-\right) \cdot H^+ \rightleftharpoons DG + I\left(OH^-\right) \quad (2\text{-}11)$$

The first step in the mechanism is the adsorption of the alcohol on the anion-exchange resin. The strength of adsorption of the alcohol on the resin is much higher than that of the triglyceride, this is why anion-exchange resins demonstrate higher catalytic activities compared to cation-exchange resins (Shibasaki-Kitakawa, 2005).

2.6. Kinetics of Transesterification

Kinetics of the transesterification reaction have been examined in several publications. Darnoko (2000) used palm oil and sodium hydroxide as a catalyst. Experimental conditions were a 1:6 oil:methanol molar ratio, catalyst loading of 1 wt% potassium hydroxide and temperatures ranging from 50˚C to 65˚C. Reaction rate constants for the forward reactions were reported in the range of 0.018 to 0.191 $(wt\%\cdot min)^{-1}$. Activation energies is the energy required for a given reaction to occur. In a three step reaction of transesterification, the reaction with the highest activation energy is the rate determining step. Activation energy for the forward reactions were 61.5, 59.4 and 26.8 kJ/mol for the tri-, di- and monoglyceride reactions. The triglyceride to

diglyceride step was reported to be the rate limiting step of the three reversible reactions (Darnoko, 2000).

The kinetics of transesterification of soybean oil with methanol over sodium hydroxide at temperatures between 30˚C to 70 ˚C has been examined using the rate law. A statistical and mathematical software package called MLAB was used for kinetic modeling. The effect of Reynolds number in the stirred reactor and temperature were studied. Alcohol to oil molar ratio, catalyst loading and reaction time were constants. Activation energy for the triglyceride, diglyceride and monoglyceride decomposition reactions were 56.9 kJ/mol, 78.6 kJ/mol and 21.7 kJ/mol, respectively (Noureddini, 1997). The activation energy was reported to be 78.6 kJ/mol is reported for the diglyceride decomposition reaction. Since this value is the highest of the reported quantities, it is denoted as the rate limiting step.

The influence of temperature (40˚C to 57˚C), alcohol molar ratio and catalyst loading on the kinetics of transesterification of methyl acetate were examined over Amberlyst 15 with *n*-butanol (Bozek-Winkler, 2006). This work examined two kinetic models: Langmuir-Hinshelwood (LH) and pseudo-homogeneous (P-H), both models yielded similar results. The LH model assumes a surface reaction where two reacting species are adsorbed on a surface where they react and are desorbed, whereas the P-H model assumes a homogeneous catalyst confined within the catalyst particle. The P-H model is applicable when mass-transfer is negligible and one component is highly polar. To validate and compare models, chemical equilibrium constants were calculated using the models and compared to experimental values. The chemical equilibrium constants K_a reported were 0.982 and 0.976 for the LH model and P-H model, respectively. The chemical equilibrium constant from kinetic testing was reported to be 0.980, very close to the results from both models. This suggests that both the Lanmuir-Hinshelwood

and pseudo-homogeneous models are good approximations of the mechanism of reaction (Bozek-Winkler, 2006).

The kinetics of transesterification of methyl esters to synthetic lubricants has been simulated in MATLab (Hamid, 2010). The overall reaction under examination was a three step reversible reaction of trimethylpropane with methyl esters to produce triesters and methanol using sodium methoxide as a catalyst. Ordinary differential equations were produced from the rate law based on each component's concentration and weight fraction. Initial values for rate constants were input and concentrations were solved using the ODE45 solver and the Runge-Kutta method. Rate constants and component concentrations were examined at five temperatures between 70˚C and 110˚C. Activation energy values for each reaction were determined. The rate determining step for the forward reactions was the first step of trimethylpropane to monoester, with an activation energy of 119 kJ/mol (Hamid, 2010).

Kinetic studies involving organic reactions similar to and including transesterification using both homogeneous and heterogeneous catalysts have been published. Published works demonstrate that the rate law model and the Langmuir-Hinshelwood and pseudo-homogeneous models can each accurately represent experimental data. Activation energies varied for the reactions considering the multiple reaction mechanisms and types of catalysts. In the work reviewed, activation energy varied from 20 kJ/mol to 120 kJ/mol. Various software packages have been used to validate the multiple competing reaction models.

2.7. Biodiesel Characteristics

The American Society for Testing and Materials (ASTM) provided the testing methods and physical standards for biodiesel in North America (ASTM, 2011). The most recent publication lists 19 fuel characteristics that must be measured to ensure commercial biodiesel fuels meet the

standards. ASTM standards for biodiesel (D6751) are listed in Table 2-1. Flash point is the temperature at which combustion can occur and is set at a minimum of 93˚C so that biodiesel can be considered a non-hazardous material under the National Fire Protection Association (NFPA) codes in the United States. Alcohol content is a measure of the remaining unreacted alcohol in the fuel, this directly impacts the flash point property. Additional alcohol lowers the flash point of biodiesel, as methanol has a flash point of 11˚C. Viscosity has a lower limit of 1.9 mm^2/s to minimize injection pump power losses and injector leakage. The viscosity maximum of 6.0 mm^2/s is important in combustion systems considering engine size, design and injector system characteristics. Sulfur affects engine wear, buildups in the engine and emissions control. Biodiesel is typically sulfur free (ASTM, 2011). Sulfated ash, calcium/magnesium and sodium/potassium limits indirectly control the quantity of soaps present in biodiesel fuels, which is often a result of base catalysts combined with low quality feedstocks.

Table 2-1: ASTM standard D6751-2011 for biodiesel fuel blend stock B100 (ASTM, 2011)

Property	Limit grade S15	Units
Flash point	93 min	˚C
Methanol content	0.2 max	mass %
Water and sediment	0.050 max	vol %
Kinematic viscosity, 40˚C	1.9-6.0	mm^2/s
Sulfur	0.0015	mass %
Cetane number	47 min	-
Cloud point	Report	˚C
Acid number	0.50 max	mg KOH/g
Free glycerin	0.020 max	mass %
Total glycerin	0.240 max	mass %
Sulfated ash	0.020 max	mass %
Copper strip corrosion	No 3. max	-
Carbon residue	0.050 max	mass %
Cold soak filterability	360 max	seconds
Phosphorus content	0.001 max	mass%
Distillation temperature	360 max	˚C
Calcium & magnesium	5 max	ppm
Sodium & potassium	5 max	ppm
Oxidation stability	3 min	hours

Free glycerin is a measure of the glycerol byproduct remaining in the biodiesel after the separation stages. Glycerol can cause injector deposits, clog fuel systems and settle to the bottom of fuel storage tanks. Glycerol contaminants that remain in biodiesel are known to produce formaldehyde and acetaldehyde upon combustion (Helwani, 2009). Total glycerin measures the unreacted oil (triglycerides, diglycerides and monoglycerides) and includes the glycerol remaining in the fuel. Cloud point defines the temperature at which solid crystals begin to form as the fuel is cooled to its melting point. Cloud point is of concern in regions with cold winter temperatures. A value for cloud point is not prescribed by the ASTM standard, but the cloud point of a fuel must be reported by the manufacturer. Acid number or acid value is a measure of the quantity of free fatty acids (FFA) and acidic functional groups present in biodiesel. FFA content increases fuel deposits and increases corrosion (ASTM, 2011). Copper strip corrosion measures acid and sulfur compounds that can corrode copper and brass components in fuel systems. Carbon residue is an approximation of the tendency of a fuel to leave engine deposits. It is measured by distilling a sample and weighing the remaining solids. Phosphorus content has an adverse effect on catalytic converters, but is typically 1 ppm in biodiesel fuel well below the 10 ppm (0.001 mass %) limit. The boiling point of C16 to C18 FAME components of biodiesel is typically in the range of 330˚C to 357˚C. The distillation temperature limit is to ensure high boiling point contaminants are not present in biodiesel fuels. Oxidation stability is concerned with the degradation of FAME into acids or polymers. These products can cause fuel clogging and engine deposits. Fuel additives can improve the oxidation stability of biodiesel (ASTM, 2011).

The composition of the oils or fats used to produce biodiesel has a measurable impact on fuel properties. Both the degree of saturation and chain length of fatty acids have an effect on the

properties of the fuel produced (Ramos, 2009). For instance, minimizing the amount of double bonds (unsaturation) increases the cetane number and decreases iodine number. These are favorable changes to a diesel fuel. An ideal biodiesel is produced from an oil that is high in monounsaturation; polyunsaturated and saturated fatty acids have negative impacts on fuel characteristics. Conversely, a higher saturation degree leads to higher oxidation stability; this influences the stability of the long-term storage of the biodiesel fuel (Ramos, 2009). The composition of saturated FAME in green seed canola oil is responsible for the oxidation stability issues (Issariyakul, 2010). Figure 2-9 relates degree of saturation to three important biodiesel properties. From the figure, low degree of saturation and high monounsaturation satisfy cold filter plug point (CFPP, or cold soak filterability), which is a measure of the ability of the fuel to flow at low temperatures. In addition, high saturation and low polyunsaturation satisfy cetane number and iodine value (Ramos, 2009). Cetane number is a measure of ignition quality of a fuel and combustion properties of a fuel; a high number (>47) means a high quality fuel with good compression ignition properties (ASTM, 2011). Iodine value measures the saturation extent, which is a reflection of the stability of FAME molecules. A desirable composition of oil is to have monounsaturated and saturated fatty acids for a high cetane number, low iodine number and low cold filter plug point. Ramos (2009) studied the production of biodiesel using almond, olive, corn, rapeseed and sunflower oils with high oleic acid content. The composition of these oils includes mainly monounsaturated fatty acids (Ramos, 2009). Figure 2-10 shows the fatty acid and saturates content of these oils. Oleic acid is the primary component in the oils and is an ideal fatty acid for biodiesel feedstock. Sharma (2008) reported that a higher composition of saturated fatty acids in biodiesel increases oxidation stability, while lowering cloud and pour points. Increasing composition of unsaturated fatty acids enhances cloud and pour point properties,

while lowering oxidation stability. A feedstock must be selected with a balanced ratio of saturated and unsaturated fatty acids.

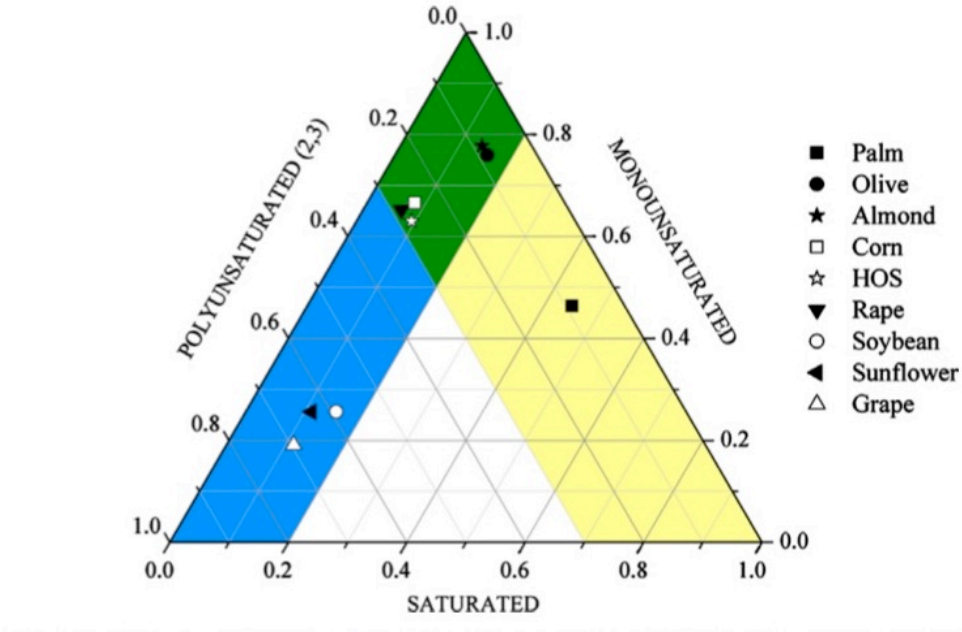

Figure 2-9: Effect of degree of saturation of fatty acids on cold filter plug point (CFPP, medium grey) and cetane number as well as iodine value (light grey) (Ramos, 2009)

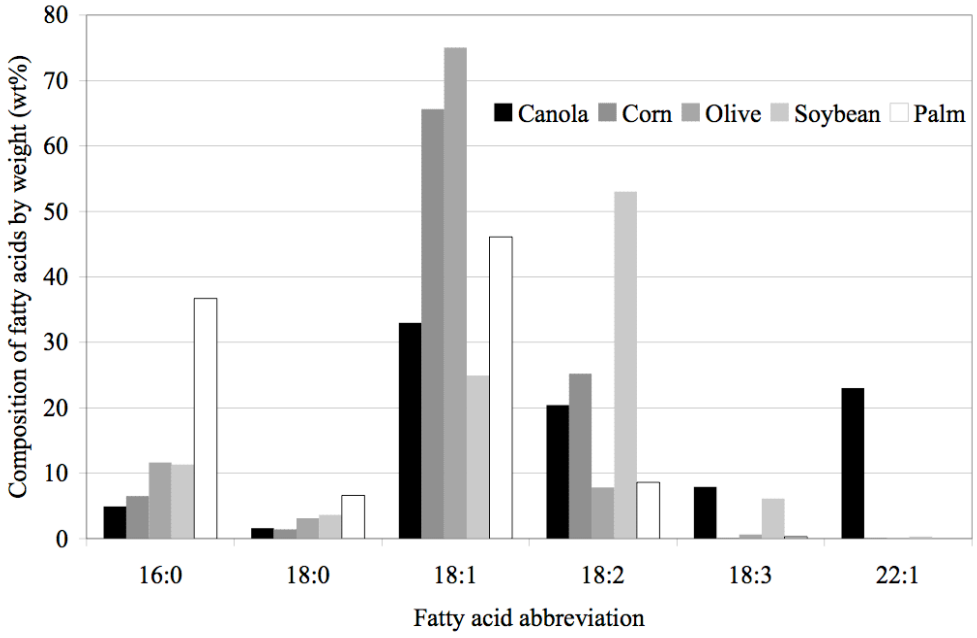

Figure 2-10: Fatty acid composition of five oils commonly used for biodiesel production (based on Ramos, 2009)

3. EXPERIMENTAL METHODS

3.1. Materials

Triolein (technical grade, 65%), dicholoromethane (DCM), pheholphthalein and potassium bromide (KBr) were purchased from Sigma-Alrich Corporation, St. Louis, USA. American Chemical Society (ACS) grade methanol, tetrahydrofuran (THF) and sodium hydroxide (NaOH) were acquired from EMD Chemicals Inc., Darmstadt, Germany. Ethanol was purchased from Commercial Alcohol Inc., Brampton, Canada. Liquid nitrogen, nitrogen (N_2), hydrogen (H_2) and air (N_2, O_2) were ordered from Praxair Inc., Danbury, USA. Stearic acid (99%) was acquired from BDH Chemical Ltd., Toronto, Canada. Canola oil was purchased from Loblaws Inc., Brampton, Canada. Number 3 (94 ppm) greenseed canola oil was acquired from Milligan Bio-Tech Inc., Foam Lake, Canada. Nitric acid (HNO_3) and hydrochloric acid (HCl) were from Fisher Scientific Company, New Jersey, USA. Whatman #1 coarse filter paper used for catalyst filtration was purchased from VWR International, USA. All materials were used as received.

3.2. Commercial Ion-Exchange Resins

A variety of commercial ion-exchange resins were tested in batch reactions. The resins selected for trials included Amberlyst 15, which is seen most often in the literature in cation exchange processes (Coutinho, 2006; Harmer, 2001; Yu, 2004). Two other resins tested were Amberlite IR-120 (H) and Amberlite IRA 200 (Na). These resins were selected based on their highly acidic sulfonic functional groups and cation exchange capacities. Amberlite IRA 400 (Cl) was selected as an anion exchange resin as it is highly basic due to a quaternary ammonium functional group. The supports for four of these resins were based on a co-polymer of styrene and divinylbenzene. Nafion SAC-13 was also tested, as examined in previous work (López,

2005). This cation exchange resin is a copolymer of tetrafluoroethylene (TFEt) and perfluoro-2-(fluorosulfonylethoxy)-propyl vinyl ether (P2PVE) supported on a silica structure (Sigma-Aldrich, 2012). The structure of Nafion SAC-13 is illustrated in Figure 2-7. The functional group of Nafion SAC-13 is sulfonic acid. Amberlite IR-120H and Nafion SAC-13 were acquired from Sigma-Alrich Corporation, St. Louis, USA. Amberlyst 15 (H, wet), Amberlite 200 (Na) and Amberlite 400 (Cl) ion-exchange resins were purchased from Alfa Aesar Company, Ward Hill, USA. These commercially available ion-exchange resins have been used as catalysts in identical reaction conditions. Table 3-1 lists the catalysts, supports and functional groups subjected to screening experiments. The ammonium functional group listed in the table is a quaternary ammonium group (NH^+OH^-), a basic Bronsted functional group. The mechanism of reaction is similar to other basic catalysts, where an alkoxide anion is formed on the nitrogen cation, replacing the hydroxide group as demonstrated in Figure 2-2 (Di Serio, 2008).

Table 3-1: Selected ion-exchange resins, functional groups and support components

Catalyst Name	Manufacturer	Functional group	Support structure
Amberlyst 15	Rohm & Haas	Sulfonic acid	Styrene-divinylbenzene
Amberlite IR-120	Rohm & Haas	Sulfonic acid	Styrene-divinylbenzene
Amberlite 200	Rohm & Haas	Sulfonic acid	Styrene-divinylbenzene
Amberlite 400	Rohm & Haas	Ammonium	Styrene-divinylbenzene
Nafion SAC-13	DuPont	Sulfonic acid	TFEt-P2PVE*

*TFEt-P2PVE, tetrafluroroethylene perfluoro-2-(fluorosulfonylethoxy)propyl vinyl ether

3.3. Catalyst Characterization

3.3.1 Surface Area, Pore Volume, Pore Diameter

Surface area, pore volume and pore diameter were measured using the Brunauer, Emmett and Teller (B.E.T.) method (Brunauer, 1938) using a Micrometrics ASAP 2000 adsorption apparatus at 78 K with liquid nitrogen. Prior to analysis, catalyst samples were weighed and

evacuated under a vacuum of 50 Pa to remove moisture from the porous structure. An automated process measured adsorption of nitrogen to the catalyst surface.

3.3.2 Fourier Transform Infrared Spectroscopy

Fourier transform infrared (FTIR) spectroscopy with pyridine adsorption examines chemical structure and functional groups of the catalyst. FTIR was performed using a Perkin Elmer Spectrum GX-A system. The spectrum was recorded from 400 - 4000 cm^{-1} after 32 scans using a resolution of 8 cm^{-1}. A background scan was performed to subtract signal noise. Catalyst pellets were crushed using a mortar and pestle, a few milligrams were thoroughly mixed in to 200 mg of potassium bromide (99% A.C.S. reagent from Sigma-Aldrich). The mixture was loaded into a Pike Technologies 13 mm die and compressed into a thin translucent circular disk under 55 MPa of pressure in the die. The disk was loaded into the FTIR sample plate and analyzed.

3.3.3 Thermogravimetric Analysis

Thermogravimetric analysis (TGA) was performed using a Perkin Elmer Pyris Diamond Thermogravimetric/Differential Thermal Analyzer (TG/DTA). A microgram quantity of sample was placed on the weighing arm and sealed. The TGA process measures the change in sample weight as temperature changes. Flow rate of air was 10 mL/min and heating was from 22˚C to 500˚C at 10˚C/min with holding for 15 minutes.

3.3.4 Cation Exchange Capacity

Cation exchange capacity (CEC) is a measure of the quantity of functional groups of cationic resins. It is the equivalent of temperature programmed desorption (TPD) used to characterize other heterogeneous catalysts. Titration is used to quantitatively determine the

quantity of ions that can be taken up by an ion-exchange resin (Dorfner, 1972). Five grams of an ion-exchange resin was converted to the hydrogen form by washing with 1 litre of nitric acid (HNO_3), followed by rinsing with de-ionized water. One gram of the rinsed resin was accurately measured and placed in a 250 mL flask, the rest of the resin was placed in a 110˚C oven for drying for 8 hours. Standardized 0.1 N sodium hydroxide (NaOH) was added to the flask and salt was added to 5 wt% of the NaOH solution and left for 14 hours. Back-titration was performed on the resin solution with 50 mL aliquots of 0.05 N hydrochloric acid (HCl) and phenolphthalein as an indicator. The unit of measurement for CEC is milliequivalents per gram of dry resin (m_{eq}/g), where an equivalent is the quantity of a substance that will react with one mole of hydrogen.

3.4. Feedstock and Product Analysis

3.4.1 High Performance Liquid Chromatography

Feedstock oil (triolein, canola and greenseed canola oil) and reaction products were characterized by high performance liquid chromatography (HPLC) to measure the composition of triglycerides, diglycerides, monoglycerides and ester content. An Agilent 1100 HPLC was used, equipped with a refractive index (RI) detector. Two 300 mm x 7.8 mm phenogel columns connected in series were used with tetrahydrofuran (THF, HPLC grade) as the mobile phase. Detector temperature was maintained at 35˚C. Solvent pumping rate was 1 mL/min. Injection volume was 5 μL. Samples were diluted to 5 vol% in THF. Retention time is a factor of a molecule's size: large compounds evolve first. Smaller compounds penetrate the stationary phase to a greater extent than do large molecules. HPLC is used to measure the completion of reaction in terms of conversion to products. HPLC measures in terms of weight percent (wt%), which is converted to mol%. An example calculation is in Appendix A.2. Therefore, conversion to products is the mole percentage of products produced in the reaction. Reaction completion is

reported as conversion to products as the mole fraction of chemical species produced during the reaction.

3.4.2 Acid Value

Acid value is a quantitative measurement to determine the number of acidic functional groups present in biodiesel; measurement is in terms of the quantity of potassium hydroxide required to neutralize a quantity of sample (Sharma, 2008). Content of free fatty acids in reactants and products was measured as acid value using the American Oil Chemists' Society (AOCS) standard method Ca 5a-40 (AOCS, 1997). Ethanol (95 vol%) was neutralized using 0.25 N standardized NaOH with phenolphthalein as an indicator. Five grams of sample were weighed into 75 mL of neutral ethanol. End point of titration was determined when a pink colour remained in solution for 30 seconds. Acid value was calculated from equation 3-1.

$$Acid\ value = \frac{vol\ KOH\ x\ 0.25N\ KOH\ x\ 56.1}{sample\ mass} \tag{3-1}$$

3.4.3 Inductively Coupled Plasma Mass Spectrometry

Inductively coupled plasma mass spectrometry (ICP-MS) using a Perkin Elmer ELAN 5000 was used to determine the sulfur content of the feedstock and products. This method is used to determine if leaching of catalyst's sulfur-based functional groups was taking place. ICP-MS measures the quantity of the element sulfur in parts per million (ppm). A continuous flow system was employed with a channel electron multiplier as the detector.

3.4.4 Water Content

Water content was analyzed using a Mettler Toledo DL32 Karl Fischer Coulometer. The coulometer used Aquastar brand CombiCoulomat fritless Karl Fischer reagent for coulometric water determination, composed of methanol and bromoform. To calibrate the coulometer, a one

wt% water standard from Aquastar supplied by EMD Chemicals was used. Titration is used to measure water content in weight percent (wt%).

3.4.5 Gas Chromatography

An Agilent 7890A Gas Chromatograph System (GC) using a flame ionization detector (FID) was used to analyze the fatty acid methyl ester chain lengths and saturation extent. The column was a J&W 122-2362 DB23 60m x 250µm x 0.25 µm. Split mode of a split-splitless inlet injector was used with a ratio of 100:1 and injection volume was 1 µL. The FID column was maintained at 260˚C, at a hydrogen flow of 40 mL/min and an air flow of 400 mL/min. The temperature program was held at 140˚C for 5 minutes and ramped at 4˚C/min to 240˚C. Final hold time was 10 minutes. Since this detection method only measures fatty acid methyl esters (FAME), feedstock oil must first be converted to their FAME derivatives by a standard transesterification method using potassium hydroxide. This procedure measures the mass percentage (mass%) of components calibrated using various standards.

3.5. Reaction Procedure

3.5.1 Batch Reactions

Reactants were weighed using a 1500 ± 0.01g ARA520 scale from Ohaus Corporation; the catalyst was weighed using a 220 ± 0.0001g Mettler Toledo AB204-S scale. One hundred grams of oil was added first, followed by catalyst beads at a specific loading relative to oil, then methanol at a specific molar ratio relative to oil. The reactor was sealed, pressurized with nitrogen and stirred as it was heated to the temperature set-point. As the reactor heats up to the set-point, time zero (t=0) is selected as the moment when the set-point is reached. Heating the reactor to the set-point required approximately 20 minutes, depending on the temperature set

point. From an outlet valve, samples of approximately 1 mL were taken at set intervals. Reaction conditions for testing of Amberlyst 15 were: 3 wt% catalyst loading, 1:9 oil to alcohol ratio, 600 rotations per minute (RPM) stirring velocity and a nitrogen pressure of 4 MPa at various temperatures between 120˚C and 200˚C. Each of the catalysts was tested at 200˚C, using conditions used in previous work (Jacobson, 2008). Stirring rate was 600 rotations per minute (RPM) based on previous work (Kulkarni, 2006a). Nitrogen atmosphere pressure was maintained above 4 MPa to ensure methanol remained in a liquid state. After heating the final pressure was between 8 and 10 MPa, depending on the quantity of methanol present. As shown in Figure 1-1, methanol is the second reactant in transesterification; it is typically used in excess of the 1:3 oil to alcohol stoichiometric molar ratio. Experiments vary from a 1:3 to 1:24 oil to alcohol molar ratio.

Amberlyst 15 was pre-screened for catalytic activity at various temperatures. The current reactor system is a stainless steel, 300 mL, continuously stirred jacketed reactor from Parr Instrument Company, Moline, USA. A reactor schematic is shown in Figure 3-1. The unit labeled ‘M’ is the stirring motor, and ‘P’ is the pressure gauge. Samples are taken through a sample outlet at regular intervals during batch reactions. The solid catalyst was separated by gravity filtration. A separatory funnel removed glycerol. The final ester products as well as feedstock were both tested using high-performance liquid chromatography (HPLC) to determine the quantity of triglycerides converted to products. The biodiesel that is produced must meet national standards. In North America, the standards of the American Society for Testing and Materials (ASTM) are generally accepted. These fuel standards specify 19 physical characteristics of the fuel to ensure consistency. Table 2-1 lists the standards outlined in the ASTM standards for B100 biodiesel (ASTM, 2011). The two most important characteristics

measured in this work were conversion to products and acid value. If adequate conversion to products is measured and acid value is low enough, the remainder of the fuel characteristics can be measured.

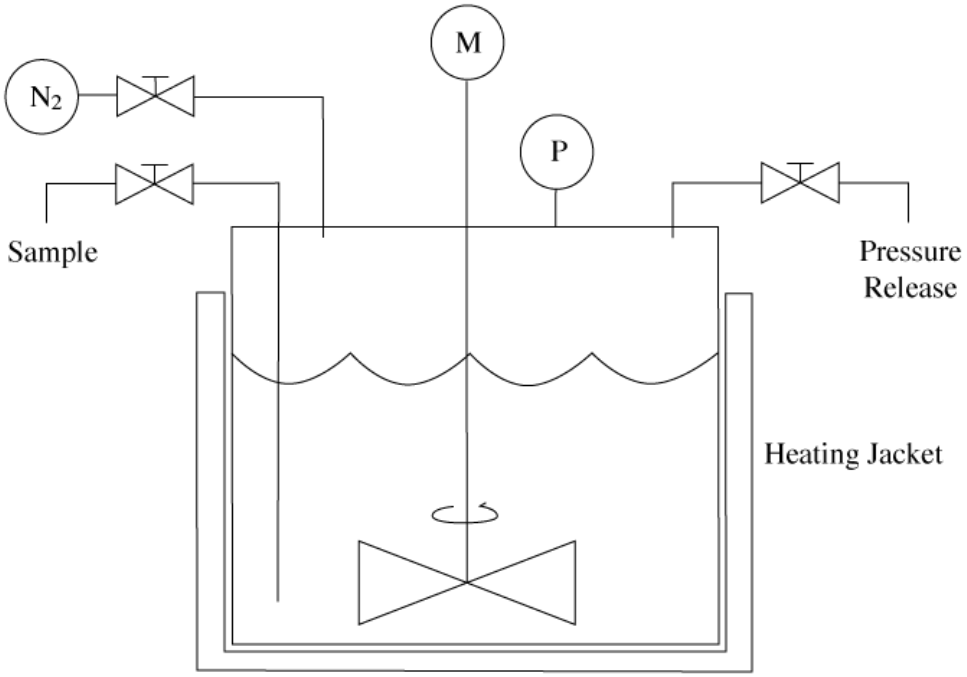

Figure 3-1: Schematic of batch reactor system

3.5.2 Statistical Design

Three experimental variables were examined in statistical optimization: temperature, catalyst loading and oil to alcohol molar ratio. Table 3-2 represents the proposed ranges of each of these controlled variables. As mentioned in section 2.4, there is an upper temperature limit to the application of IER, whereas the experiments were limited to 220˚C. Statistical design methods have been applied.

Central composite statistical design (CCD) was applied according to the following formula:

$$N = 2^k + 2(k) + N_C \tag{3-2}$$

Where N is the number of experiments, k is the number of factors and N_C is the number of replicated experiments. Applying three factors (temperature, catalyst loading and oil to alcohol ratio) and six replicated experiments yielded 20 experiments. The statistical design in Table 3-3 was produced using Design Expert 6.0, a statistical modeling software package.

Table 3-2: Controlled variable ranges in CCD statistical design

Property	Low test value	High test value
Temperature (˚C)	160	220
Catalyst loading (wt%)	1	20
Oil to alcohol ratio	1 to 9	1 to 24

3.5.3 Additional Experiments

Optimized experiments were repeated to ensure results were identical in repeatable trials. To determine if the hydrolysis of methyl esters was taking place and if there was an inhibitory effect, water was added to the reactant mixture. Water was added in the following increments: 0.1, 0.5, 1 and 2 wt% relative to oil, based on previous work where the addition of as little as 0.1 wt% of water reduced ester yields using acidic catalysts (Canakci, 1999). Similarly, stearic acid was added to the feedstock as a free fatty acid to determine if the catalyst could simultaneously perform the esterification reaction. Stearic acid was added at 5, 10 and 15 wt% relative to oil. Number 3 greenseed canola oil was used in several experiments as a low quality feedstock at the optimized reaction conditions.

3.5.4 Catalyst Longevity

Following a batch reaction, the catalyst was sieved using gravity filtration and Whatman #1 coarse filter paper. The catalyst was rinsed with methanol and reused in a subsequent reaction under identical conditions. This process was repeated multiple times to determine the longevity of the catalyst in successive reactions.

Table 3-3: CCD statistical design experiments

Experiment	Temperature (˚C)	Catalyst loading (wt%)	Alcohol Molar Ratio
1	160	1.0	24.0
2	190	26.5	16.5
3	190	10.5	16.5
4	220	1.0	9.0
5	160	1.0	9.0
6	190	10.5	16.5
7	160	20.0	9.0
8	190	10.5	16.5
9	140	10.5	16.5
10	190	10.5	16.5
11	190	10.5	29.1
12	240	10.5	16.5
13	190	10.5	3.9
14	220	20.0	9.0
15	220	20.0	24.0
16	190	10.5	16.5
17	160	20.0	24.0
18	190	0.0	16.5
19	220	1.0	24.0
20	190	10.5	16.5

3.5.5 Kinetic Study

A kinetic study was undertaken using canola oil as a feedstock. Canola oil was selected because of its high purity and low acid value. For kinetic studies, a lower temperature was necessary to avoid the hydrolysis side reaction. Three temperatures were examined: 100˚C, 110˚C and 120˚C. Molar excess of alcohol was raised to 1:77 to promote a high methyl ester yield in the transesterification reaction. Samples were taken every 24 hours over the 72 hour reaction time, yield of methyl esters was measured by HPLC. Results were iterated in MATLab and fit to the transesterification model developed using the rate law based on equations 2-1, 2-2 and 2-3. Differential rate law equations are expressed in Appendix B.2. Least squares non-linear regression was used with the Runge-Kutta method to solve for the reaction constants maximizing Pearson correlation coefficients. The MATLab program is compiled in Appendix C. To

determine the order of the overall transesterification reaction at the specified reaction conditions used in the kinetics study, several figures must be developed. From the rate law, zero-order reactions are a straight line when concentration is plotted as a function of time. First order reactions occur when the natural logarithm of concentration is a linear function of time. Second order reactions plot a straight line when the inverse of the reaction rate constant is plotted versus time. The activation energy was calculated from kinetics experiments using an Arrhenius plot and equation 3-3:

$$k = Ae^{\frac{-E}{RT}} \tag{3-3}$$

The variable k is the rate constant of a chemical reaction, A is the pre-exponential factor based on collision theory, E is the activation energy, R is the universal gas constant and T is the temperature in degrees Kelvin.

4. RESULTS AND DISCUSSION

Experimental methods are discussed in section 3. Ion-exchange resins selected in section 3.2 were characterized using a variety of methods. Chemical properties and composition of feedstock oil and reaction products were examined as outlined in section 3.3. Reaction procedures for initial batch reactions, catalyst screening, statistical optimization, longevity experiments and the kinetic study are discussed in section 3.5. Results from experiments are discussed in the following sections.

4.1. Catalyst Characterization

4.1.1 Surface Area, Pore Volume, Pore Diameter

Physical properties are measured to determine the effect that the various parameters have on catalysis. The five ion exchange resins under examination were characterized by the methods listed in section 3.2. Some of these results are summarized in Table 4-1. Amberlyst 15 had very similar physical properties (surface area, pore diameter and pore volume) when compared to the physical properties of Amberlite 200. Both catalysts had surface areas of approximately 45 m^2/g, pore diameters greater than 200 Angstroms (Å) and pore volumes of approximately 0.25 cm^3/g. Each of the measured physical properties of Amberlite 120 is an order of magnitude lower in value when compared to those of Amberlyst 15 and Amberlite 200. Amberlite 120 had a surface area of 4 m^2/g, pore diameter of 12 Å and an average pore volume of 1.30×10^{-3} cm^3/g. Amberlite 400 had a similar surface area to that of Amberlite 120, while the pore diameter and volume are approximately twice that of Amberlite 120. Nafion SAC-13 had the highest surface area of the tested commercial ion-exchange resins, 233 m^2/g. Pore diameter of Nafion SAC-13 was measured to be 143 Å and the largest pore volume of the tested IER at 0.83 cm^3/g. The

physical properties of the catalysts tested were measured to determine their impact on the catalytic activity in transesterification. The effect that physical properties of the catalysts have on catalytic activity is discussed in section 4.3.1.

Table 4-1: Catalyst characterization summary of surface properties and exchange capacities.

Catalyst	AS (m^2/g)	dP (Å)	υP (cm^3/g)	C.E.C. (m_{eq}/g)
Amberlyst 15	43	231	0.25	4.4
Amberlite IR-120	4	12	1.30×10^{-3}	1.0
Amberlite 200	45	204	0.23	4.5
Amberlite 400	5	22	2.71×10^{-3}	1.9*
Nafion SAC-13	233	143	0.83	≤11

AS, surface area; dP, pore diameter; Å, Angstrom (10^{-10} m); υP, pore volume; C.E.C., cation exchange capacity; m_{eq}, milliequivalents; *(Sigma-Aldrich, 2012)

4.1.2 Cation Exchange Capacity

Cation exchange capacity (CEC) is a measure of the overall acidity of a cationic exchange resin, comparable to temperature programmed desorption (TPD). Amberlite 120 had the lowest measured CEC, 1.0 m_{eq}/g, as listed in Table 4-1. In addition to the similar surface properties, Amberlyst 15 and Amberlite 200 share very similar CEC at 4.4 and 4.5 m_{eq}/g, respectively. Nafion SAC-13 has more than twice the exchange capacity of Amberlyst 15 at 11 m_{eq}/g. The anion exchange capacity of Amberlite 400 is 1.9 m_{eq}/g (Sigma-Aldrich.com, 2012). Similar to the physical properties measured in section 4.1.1, Amberlyst 15 and Amberlite 200 have similar cation exchange capacities while Amberlite 120 has a significantly lower cation exchange capacity. The influence of cation exchange capacity on catalytic activity is discussed in section 4.3.1.

4.1.3 Fourier Transform Infrared Spectroscopy

Fourier transform infrared spectroscopy (FTIR) is used to determine the chemical properties based on the spectral emission and absorbance of infrared light at specific wavenumbers. The FTIR spectra of these catalysts demonstrate similarities between Amberlyst 15 and Amberlite 120. The similarities in FTIR wave number spectra are apparent in Figure 4-1. Peaks observed at 580 cm^{-1}, 1600 cm^{-1} and 2920 cm^{-1} are the aromatic ring stretching of the polystyrene supports of Amberlyst 15, Amberlite 120, Amberlite 200 and Amberlite 400 (Silverstein, 2005). The peaks at 1030 cm^{-1} for Amberlyst 15, Amberlite 120 and Amberlite 200 are from sulfur-oxygen double bonds. Lewis acidic sites are denoted on Amberlyst 15, Amberlite 120 and Amberlite 200 at 1440 cm^{-1} and 1600 cm^{-1}(Yazici, 2010). These peaks are denoted in Figure 4-2. Also visible in Figure 4-2, Amberlite 200 demonstrates a sharp peak at wavenumber 1645 cm^{-1} associated with strong Bronsted acid sites (Yazici, 2010). Lewis and Bronsted acids are defined in sections 2.2.1 and 2.2.2. Lewis acid peaks are denoted in Figure 4-2 with an 'L', the Bronsted peak of Amberlite 200 with a 'B'. The Lewis acid peaks of Amberlite 200 have large amplitudes indicating strong acidic sites. Amberlite 200 differs from both Amberlyst 15 and Amberlite 120 in peak intensity for Lewis acid sites; it also contains a unique Bronsted acid peak. As stated in section 2.2.2, catalysts with strong Lewis acid sites are less active as catalysts due to the decrease in desorption of reacted species from the site of reaction (Di Serio, 2008). The Amberlite 400 functional group (ammonium, NH_4^+) contains nitrogen-carbon bonds that can be observed in a peak at 1480 cm^{-1}. In Figure 4-1, SAC-13 has a Lewis acid peak at 1628 cm^{-1} and a Bronsted site at 1695 cm^{-1}. The functional group of Nafion SAC-13 is sulfonic acid, which is not observed at 1000 cm^{-1} in this instance since carbon-fluorine and sulfur-oxygen double bonds all absorb at wavenumbers between 1000-1250 cm^{-1} (Silverstein, 2005). As seen in Figure 4-1, there is no transmittance for Nafion SAC-13 at these wavenumbers. The influence of the

results of FTIR analysis on the catalytic activity of the tested ion exchange resins is discussed in section 4.3.1.

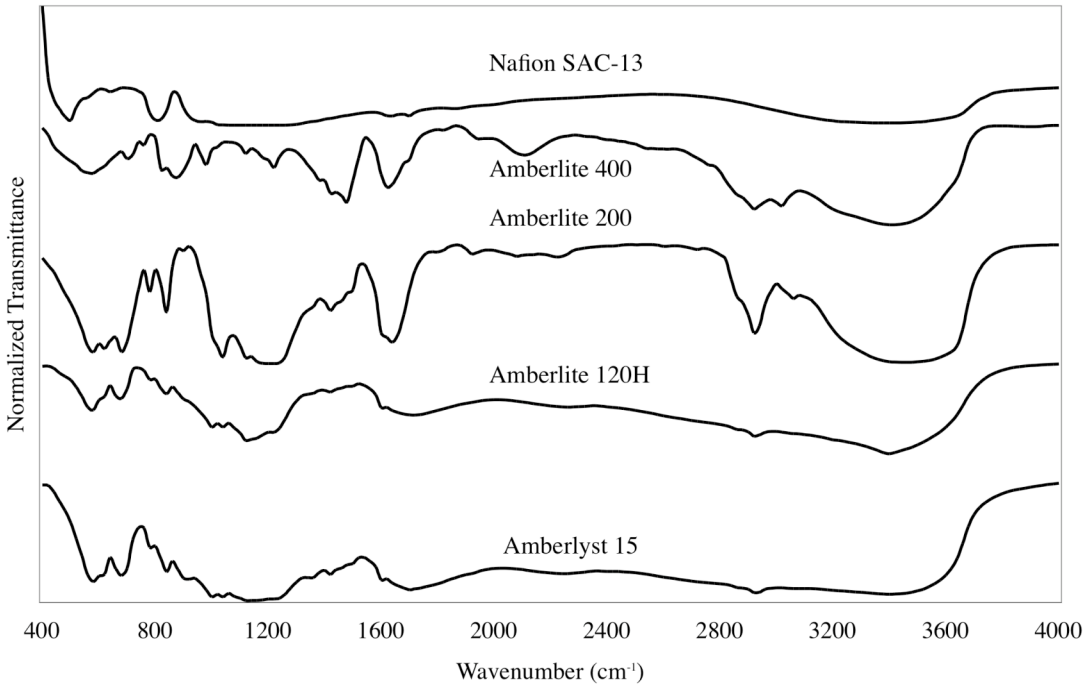

Figure 4-1: Pyridine adsorption FTIR analysis of tested ion-exchange resins (full spectrum)

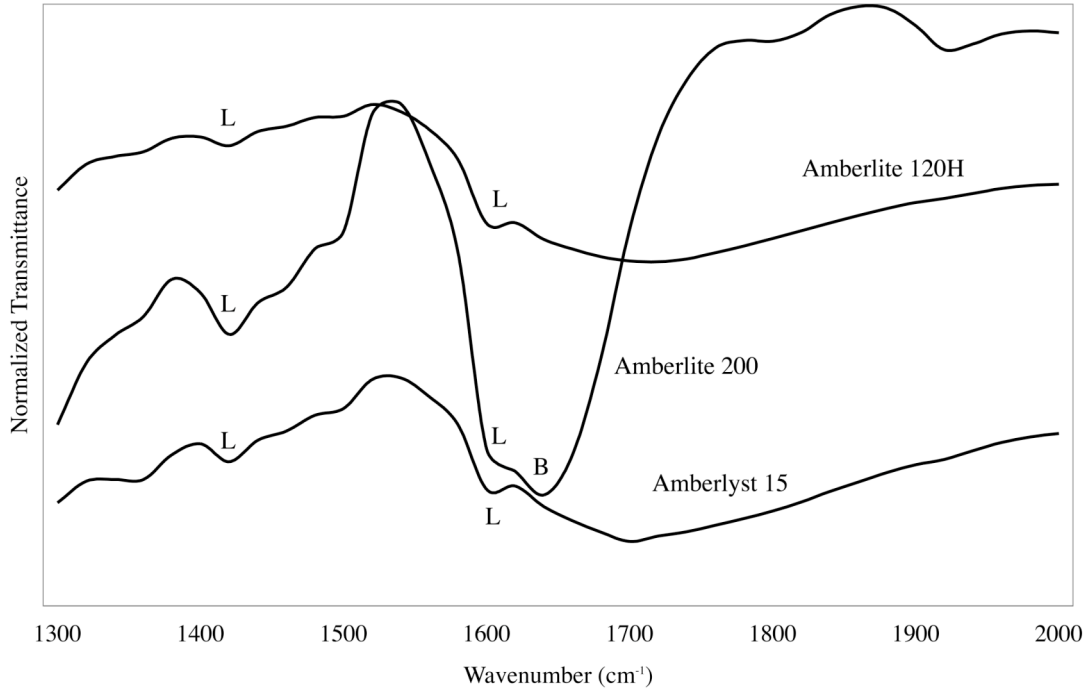

Figure 4-2: Pyridine adsorption FTIR analysis of three ion-exchange resins (truncated spectrum)

4.1.4 Thermogravimetric Analysis

Manufacturer temperature limits on the IER vary from 120˚C up to 200˚C (Dorfner, 1972; Sigma-Aldrich.com, 2012). Thermogravimetric analysis (TGA) is applied to the tested IER to determine the thermal stability of each resin at the temperatures examined in catalyst screening and optimization. TGA results of each of the catalysts are illustrated in Figure 4-3. It can be ascertained from the thermogravimetric analysis (TGA) that the ion-exchange resins under study lose a small percentage of their total mass up to 200˚C. The loss of mass up to 200˚C is between 4 - 10 mass% for each catalyst tested. Nafion SAC-13, Amberlite 200 and Amberlite 120 are close to 4% loss in mass. Amberlite 400 and Amberlyst 15 lose roughly 10% of their mass up to 200˚C. This analysis demonstrated the thermal stability of the catalysts at the temperatures used in optimization experiments.

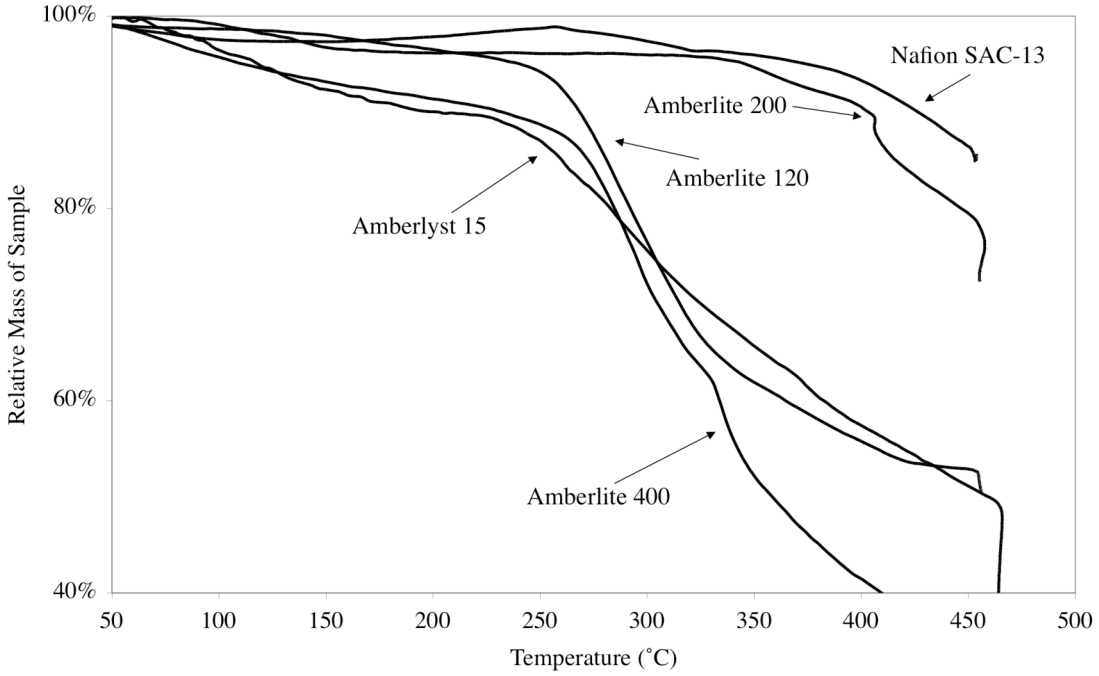

Figure 4-3: Thermogravimetric analysis of various ion-exchange resins
Conditions: 15 mL/min air, 10˚C/min, 1 sample / 20 sec, smoothed 20 points

4.2. Feedstock Composition

4.2.1 High Performance Liquid Chromatography

Technical grade triolein was measured to contain: 64 mol% triglycerides, 27 mol% diglycerides, 9 mol% monoglycerides as calculated from HPLC measurements. The di- and monoglyceride content is higher than that typically found in fresh vegetable oils, i.e. canola oil consisted of 92 mol% triglycerides and 8 mol% diglycerides. Greenseed canola oil consisted of 89 mol% triglycerides and 11 mol% diglycerides. Appendix D contains representative examples of HPLC chromatograms. Three distinct peaks are visible in Appendix D.1 for triolein. Triglycerides evolve first at 16.1 minutes due to the large size of the TG molecule. Diglycerides are the second compound detected at 16.8 minutes followed by monoglycerides at 18.0 minutes. Appendix D.2 is canola oil, where one large peak for triglycerides dominates the plot with trace quantities of diglycerides. Appendix D.3 is greenseed canola oil. More diglycerides are visible compared to canola oil. Additionally, the reaction product peak is visible which is due to the free fatty acid content of greenseed canola oil.

4.2.2 Acid Value

The acid value of triolein was measured to be 2.5 mg KOH/g sample using the procedure described in section 3.4.2. The acid value of greenseed canola oil was 8.2 mg KOH/g sample. Canola oil as purchased contained no detectable free fatty acids and therefore has an acid value of zero.

4.2.3 Inductively Coupled Plasma Mass Spectrometry

As in section 3.4.3, ICP-MS analysis for sulfur content indicated a concentration of 21 parts per million (ppm) in triolein. This test is to determine if leaching of sulfuric acid groups is taking place during reactions and was tested only with triolein.

4.2.4 Water Content

Water content was measured as outlined in section 3.4.4. Water content of triolein was measured to be 0.01 wt%. Canola oil water content was 0.02 wt% and greenseed canola oil had a slightly higher water content measured to be 0.05 wt%. Experimental error was calculated from a standard of known water content. A sample calculation is in Appendix A.1. Table 4-2 lists the water content of feedstock used in reactions. All three feedstock oils had very low water content.

Table 4-2: Water content of feedstock and various transesterification reaction products

Feedstock	Water content (wt%)
Triolein	0.01
Canola oil	0.02
Greenseed oil	0.05

4.3. Reaction Study

4.3.1 Catalyst Screening

Amberlyst 15 was pre-screened to determine reaction conditions for catalyst screening. Reaction conditions for catalyst screening are listed in Figure 4-4 and are based on previous work (Jacobson, 2008). As illustrated in Figure 4-4, the apparent reaction rate and conversion to products of transesterification increase with temperature. At 120˚C, conversion to products was 33 mol%. Both the final conversion to products and reaction rate increase with increasing temperatures. A significant increase in conversion was observed as reaction temperature was increased from 140˚C to 160˚C, final conversion increased from 50 mol% to 85 mol%. An increase to 180˚C increased the conversion to products by 1 mol%. A conversion of 93 mol% after 120 minutes is reported when temperature was increased further to 200˚C. Acid value of reaction products at end of the reaction time increases with each increase of temperature. Table 4-3 tabulates conversion for the five temperatures tested as well as acid values of products at

each temperature. The acid value numbers of the reaction products are far higher than ASTM standards allow (0.5 mg KOH/g); see Table 2-1 for tabulated ASTM standards. This increase in acid value indicates that hydrolysis of esters is taking place as a side reaction. Hydrolysis is the reverse of the esterification reaction, where a hydrogen atom leaving a free fatty acid replaces the methyl group of the ester. Leaching of sulfonic acid groups was eliminated as a factor in the increase in acid value of the products by two methods. Washing with distilled water would separate aqueous-soluble sulfonic acid groups; this step had no effect on the acid value. Additionally, inductively coupled plasma mass spectrometry (ICP-MS) was used to measure sulfur content of reaction feedstock (triolein) and respective products. These tests did not indicate an increase in sulfur content (leaching of acidic functional groups). See sections 4.2.3 and 4.4.3 for ICP-MS results of feedstock and products.

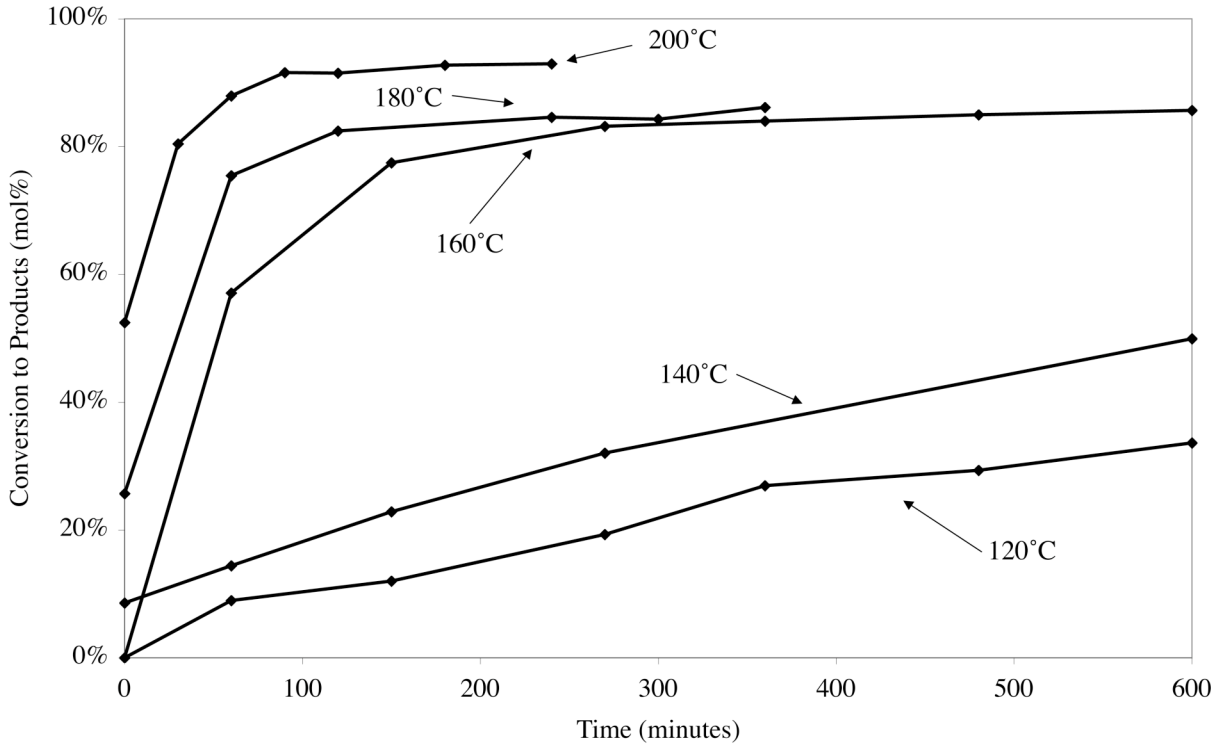

Figure 4-4: Effect of temperature on transesterification of triolein using Amberlyst 15
Conditions: 1:9 oil:methanol, 3 wt% loading, 600 RPM, 4MPa, 100g triolein

Table 4-3: Temperature testing with Amberlyst 15 and acid value of products after 120 minutes

Temperature (˚C)	Conversion to products (mol%)	Acid value (mg KOH/g)
200	98.1	50
180	82.4	23
160	77.5	13
140	22.9	10
120	12.0	3

Four additional ion-exchange resins were tested at 200˚C at the reaction conditions listed in Figure 4-5. The figure illustrates the conversion to products from triolein using different IER as catalysts. Amberlyst 15 and Amberlyst IR-120 achieved conversions of 85 mol% and 93 mol% respectively. Nafion SAC-13 conversion to products was 75 mol% after 4 hours. From the figure, the Nafion reaction had not yet approached pseudo-equilibrium and may achieve higher conversion to products over a longer reaction at these conditions. Amberlyst 200 and Amberlyst 400 were less active as catalysts, both achieving conversions to products of 50 mol%. The conversion to products with Amberlyst 15 as the catalyst was the highest and therefore the most active catalyst and was selected for optimization experiments.

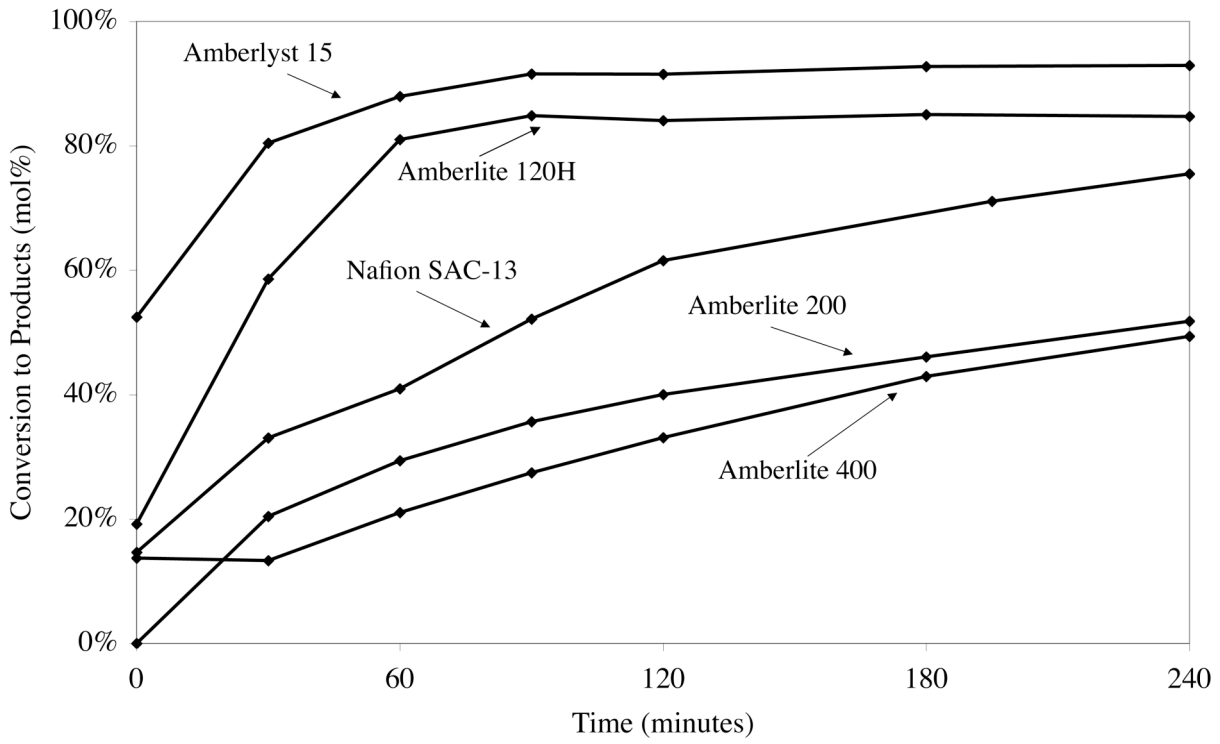

Figure 4-5: Catalyst screening using transesterification of triolein using ion-exchange resins
Conditions: 1:9 oil:methanol, 600 RPM, 4MPa, catalyst loading 3 wt% of oil

Comparison of the data presented in Figure 4-1 and Figure 4-5 indicates the similarity in FTIR spectra and catalytic activity of Amberlyst 15 and Amberlite 120 and the respective differences in surface properties (Table 4-1) suggests that surface properties are not the only determining factor for catalytic activity. Amberlyst 15 and Amberlite 120 have very different surface properties and cation exchange capacities, as discussed in sections 4.1.1 and 4.1.2. This confirms that catalytic activity and strength of acidic sites are not directly correlated (Helwani, 2009; de Rezende, 2008). Examination of the Lewis and Bronsted acidity from FTIR of Amberlyst 15, Amberlite 120 and Amberlite 200 in Figure 4-2 and contrasting with the activities in Figure 4-5, demonstrates why physically similar IER have such different activities. The weak Lewis acid functional groups of Amberlyst 15 and Amberlite 120 (the weak peaks at 1440 cm^{-1} and 1600 cm^{-1} in Figure 4-2) are highly active in the transesterification reaction. This also

explains the moderate catalytic activity of Nafion SAC-13. The strongly acidic Lewis functional group (at 1600 cm^{-1}) of Amberlite 200 is detrimental to the reaction as discussed in sections 2.2.2 and 4.1.3. As discussed in sections 4.1.1 and 4.1.2, the physical properties of Amberlite 120 are very different from Amberlyst 15 despite their similar activities in catalyzing the transesterification reaction. Conversely, Amberlyst 15 and Amberlite 200 have very similar physical characteristics (surface properties and concentration of acid sites) and have very different activities when tested in transesterification. The physical properties measured using the B.E.T. method in section 4.1.1 and cation exchange capacity in section 4.1.2 have a minor influence on the catalytic activity of the tested IER catalysts. Weakly acidic Lewis sites are the predominant factor influencing catalytic activity in these experiments.

4.3.2 Repeatability Testing

Identical experiments were carried out to ensure repeatability. Reaction conditions were re-tested to confirm results and to ensure experimental as well as measurement errors were not responsible for initial results. Figure 4-6 demonstrates the repeatability of the results in experiments using Amberlyst 15. After 60 minutes, the results of the two identical trials are repeatable. Since the initial results were repeatable, the optimization experiments were carried out using Amberlyst 15 and triolein.

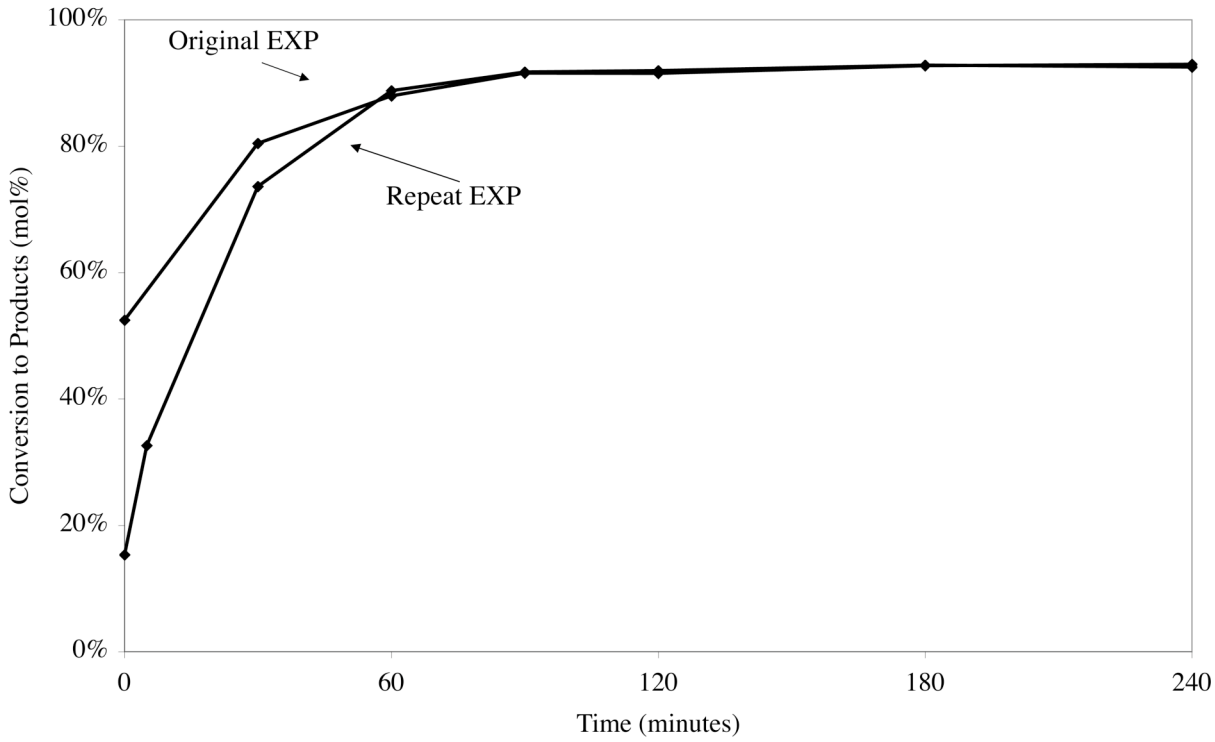

Figure 4-6: Repeatability of transesterification of triolein using Amberlyst 15
Conditions: 200˚C, 1:9 oil:methanol, 600 RPM, 4MPa, catalyst loading 3 wt% of oil

4.3.3 Central Composite Design Statistical Optimization

Statistical optimization of reaction conditions was carried out as outlined in section 3.5.2. Error bars in all cases have been calculated from replicate experiments from the statistically designed experiments. The 95% confidence interval varies with reaction rate, at the lowest rate confidence is highest due to reduced experimental error. The confidence interval was calculated to be 6% at 30 minutes when the reaction rate was high, to 0.3% at 120 minutes. Sample calculations are in Appendix A.3. Experimental results for conversion to products are tabulated in Table 4-4. The highest conversion achieved in the randomized trials was at a temperature of 220˚C, 20 wt% catalyst loading and 1:24 oil:methanol ratio. This achieved a conversion to products of 99.4 mol%. The results were input into Design Expert 6.0 software for analysis and

model development. The F-value of the polynomial model was found to be 0.01 meaning the model is significant ($F < 0.05$), with an R^2 value of 0.81.

Table 4-4: Statistical design experiments and results

Experiment	Temperature (˚C)	Catalyst loading (wt%)	Alcohol:oil molar ratio	Conversion (mol%)
1	160	1.0	24.0	70.5
2	190	26.5	16.5	63.0
3	190	10.5	16.5	89.6
4	220	1.0	9.0	97.1
5	160	1.0	9.0	54.1
6	190	10.5	16.5	93.5
7	160	20.0	9.0	21.1
8	190	10.5	16.5	91.0
9	140	10.5	16.5	16.7
10	190	10.5	16.5	93.7
11	190	10.5	29.1	98.3
12	240	10.5	16.5	98.7
13	190	10.5	3.9	94.7
14	220	20.0	9.0	98.7
15	220	20.0	24.0	99.4
16	190	10.5	16.5	95.6
17	160	20.0	24.0	92.6
18	190	0.0	16.5	37.7
19	220	1.0	24.0	98.6
20	190	10.5	16.5	93.0

The polynomial using significant terms is listed in Equation 4-1. The variable X is conversion to products (mol %), T is temperature (˚C), A is oil to alcohol molar ratio and C is catalyst loading (wt%). Each variable is in terms of coded factors, varying from -1 to +1. These coded factors are based on the variable ranges for the statistical design listed in Table 3-2. The low value (-1) is the lowest value of initial conditions and the high value (+1) is the highest value from initial conditions. From this, the coded factor of zero for each controlled variable is the median value, where the six replicated experiments were conducted. The coded factors create even magnitudes across the three variables. Therefore, the magnitude of the numerical

coefficients can be compared. The numerical model developed is the following polynomial, used to predict conversion to products:

$$X = 89 + 21.5T + 3.6C + 7.1A - 8.7T^2 - 11.5C^2 + 5.1A^2 - 10.7T \times A \qquad (4\text{-}1)$$

This model is applicable at the conditions listed in Table 3-2 and is limited by the fixed reaction conditions (feedstock, stirring speed, pressure, type of reactor, etc.). Comparing the magnitudes of each component of this equation illustrates the relative effect each variable had on the final conversion to products. Interaction effects between controlled variables can also be compared. The constant value of 89 represents the conversion to products when all the variables are equal to zero, which occurs at the median value of each variable. It is clear from the model that temperature has the most significant impact on the final conversion to products. The coefficient for the temperature variable is 21.5, which is greater than that of alcohol molar ratio (7.1), which is greater than that of catalyst loading (3.6). The quadratic terms have less of an impact on the conversion variable compared to the linear terms, since the variables are less than or equal to one, squaring the terms reduces the magnitude of their effect. A similar minimizing effect occurs during the interaction of variables in the final term of equation 4-1. Only the interaction of temperature and alcohol molar ratio was significant. The sign of each coefficient is indicative of the effect that each variable has on the conversion to products. For example, the temperature coefficient is a positive value, which means that from the median value of zero to the maximum coded factor 1, this coefficient increases the final result. The interaction coefficients sign can vary depending on the magnitude of the variables. For example, the temperature and alcohol molar ratio coefficient is -10.7. In the case where both the temperature and alcohol molar ratio coded variables are greater than the respective median values, there is a negative effect on the final conversion to products. However, if one of the coded variables is less

than the mean, the effect is positive. By converting variables into coded factors and entering them into equation 4-1, the final conversion to products is estimated within the specified reaction conditions. A sample calculation is in Appendix A.4.

From the numerical optimization, the optimized reactor conditions were selected to be 200˚C, 13 wt% catalyst loading, 1 to 24 oil to alcohol molar ratio, 4 MPa nitrogen atmosphere, stirring speed 600 RPM using 100 grams of oil. The predicted conversion to methyl esters from the model at the selected conditions was 98.1%, while the experimental value at the same conditions was 97.0%. Figure 4-7 demonstrates the high conversion of the optimized experiment. As demonstrated in the figure, this experiment was reliably repeated. The experimental variable values were selected from the model. Within the experimental bounds, the maxima for each of the controlled variables were at the selected values. The numerical model as illustrated in Figure 4-8, is found to be a hyperbolic paraboloid. This shape is due to local maxima in the oil to alcohol axis and local minima on the loading axis. The maxima and minima are visible in Figure 4-8. The maxima and minima are present at each value in both dimensions (alcohol to oil ratio axis and catalyst loading axis). Experimental results demonstrate the same effect. In experiments where the only variable is alcohol to oil molar ratio, the minima is observable. Similarly, the maxima of the catalyst loading axis are also verified by experiment. The local maximum on the catalyst loading axis may be due to loading effects of excess catalyst. The minima could be due to the formation of methyl sulfonates on the sulfonic acid groups of the catalyst via esterification (Melero, 2009b).

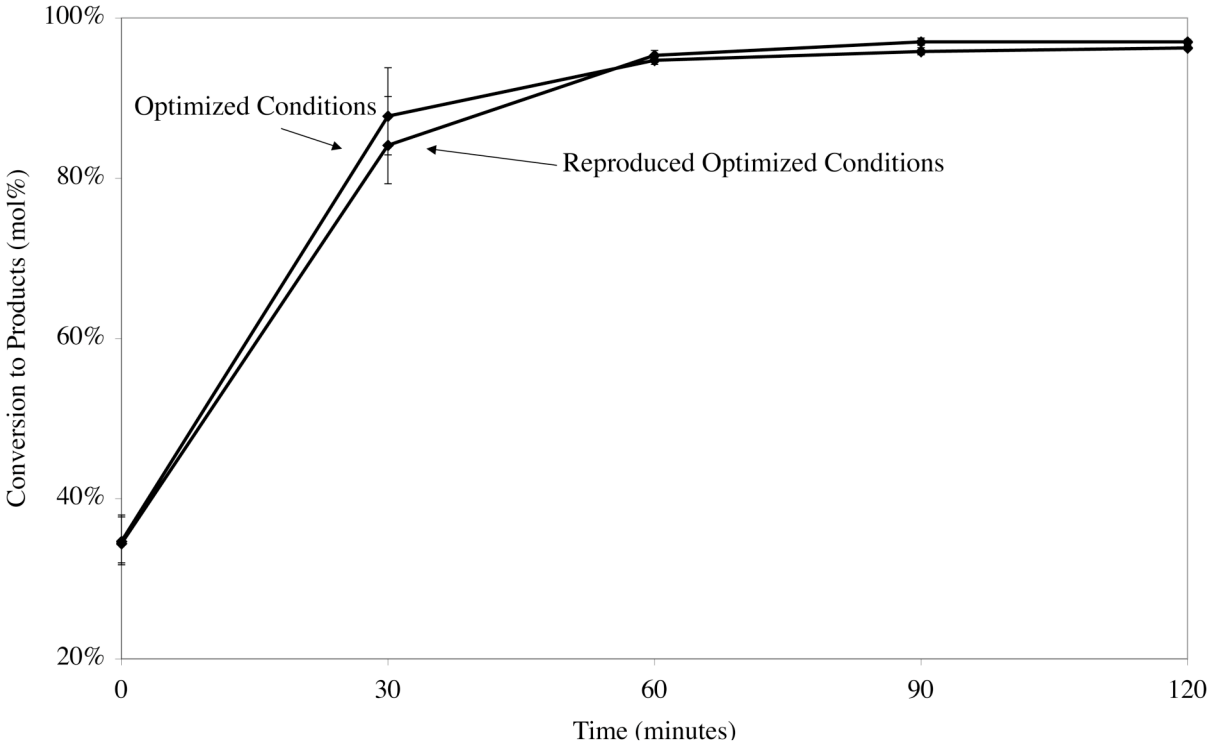

Figure 4-7: Transesterification of triolein using optimized reactor conditions
Conditions: 200˚C, 1:24 oil:methanol, 13 wt% loading, 600 RPM, 4 MPa,100g oil

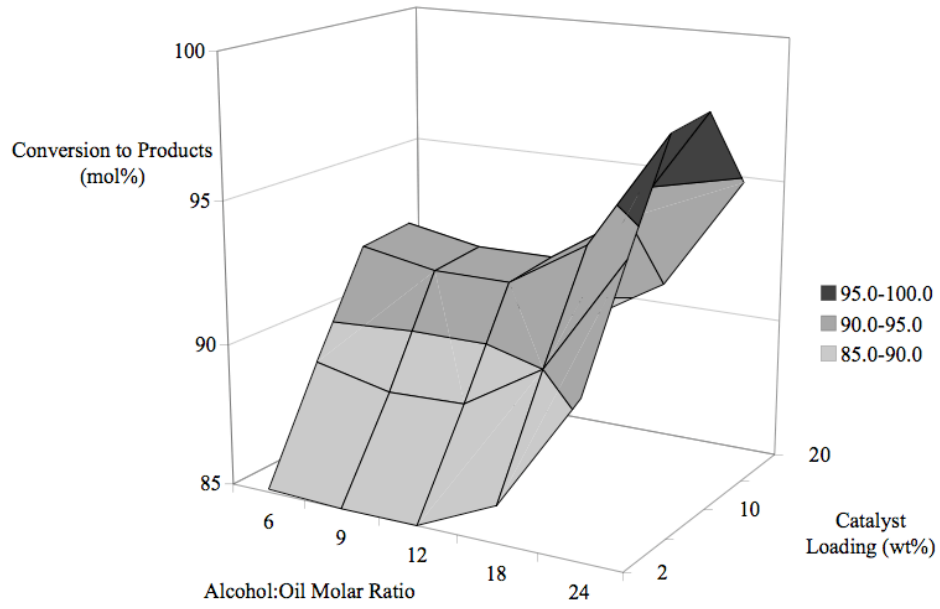

Figure 4-8: Numerical model of transesterification yield of triolein using Amberlyst 15
Conditions: 200˚C, 4 MPa, 600 RPM, 2 hours

4.3.4 Effect of Water Addition

Results from water addition testing are illustrated in Figure 4-9. Water content of 0.1 wt% relative to oil up to 1 wt% did not greatly impact the reaction products as measured by HPLC or in acid value. At 2 wt% loading of water, a 2 mol% decrease in conversion to products is apparent. The water content of the products for each of the water addition reactions (0.1, 0.5, 1 and 2 wt%) is listed in Table 4-5. Comparatively, the water content of the optimized reaction conditions without water addition had a water content of 0.69 wt%. All reaction products have water content between 0.62 and 0.72 wt%, independent of the quantity of water or free fatty acids (FFA) added to the reactants mixture. This suggests that water is being produced as well as being consumed in different side reactions during batch experiments. The identical values for water content listed below suggest that pseudo-equilibrium of water production is achieved near 0.7 wt% at the optimized reaction conditions.

Table 4-5: Conversion, acid value and water content of feedstock and various experiments

Feedstock or experiment	Conversion to products (mol%)	Acid value (mg KOH/g)	Water content (wt %)
Triolein	N/A	2.5	0.01
Canola oil	N/A	0	0.02
Greenseed oil	N/A	8.2	0.05
Optimized conditions	96.8	55.0	0.69
0.1 wt% water products	95.8	57.8	0.67
0.5 wt% water products	95.2	55.5	0.72
1 wt% water products	96.3	58.5	0.71
2 wt% water products	92.6	56.1	0.72
5 wt% FFA products	96.7	55.9	0.66
10 wt% FFA products	97.1	48.1	0.62
15 wt% FFA products	97.5	53.3	0.60

From the water content data listed in Table 4-5, it can be concluded that hydrolysis of methyl esters to free fatty acids as a side reaction is taking place. When added in excess, water is being consumed. In addition, water is being produced from the esterification reaction as illustrated in Figure 2-6. There is no clear trend to indicate that water addition has a significant effect on the products of transesterification. Table 4-5 lists conversion to products and respective acid values. The addition of water did not have a significant impact on the results of the transesterification reaction. Previous work has demonstrated that water addition can have an inhibitive effect on the transesterification reaction at concentrations as low as 0.1 wt% (Canakci, 2001). Amberlyst 15 is not inhibited by water content during transesterification.

4.3.5 Effect of Free Fatty Acid Addition

Stearic acid was added to the feedstock as a free fatty acid (FFA) to simulate the use of low quality feedstocks such as waste cooking oil. When stearic acid was added to the feedstock up to 15 wt%, no significant effect was detected on ester content and acid value, see Figure 4-9. Marginal increases in conversion to products are detected with each 5 wt% increase in FFA content of the feedstock. Table 4-5 lists conversion to products and respective acid values. The acid value of products was still 53 mg KOH/g sample. There is no clear trend to indicate that free fatty acid addition has a significant effect on the products of transesterification. Conversely, previously published research into the addition of free fatty acids has significantly reduced final conversion to products when 15 wt% palmitic acid was added to the triolein feedstock (Canakci, 1999). This further demonstrates that the catalyst can simultaneously catalyze esterification (including the reverse reaction, hydrolysis) and transesterification.

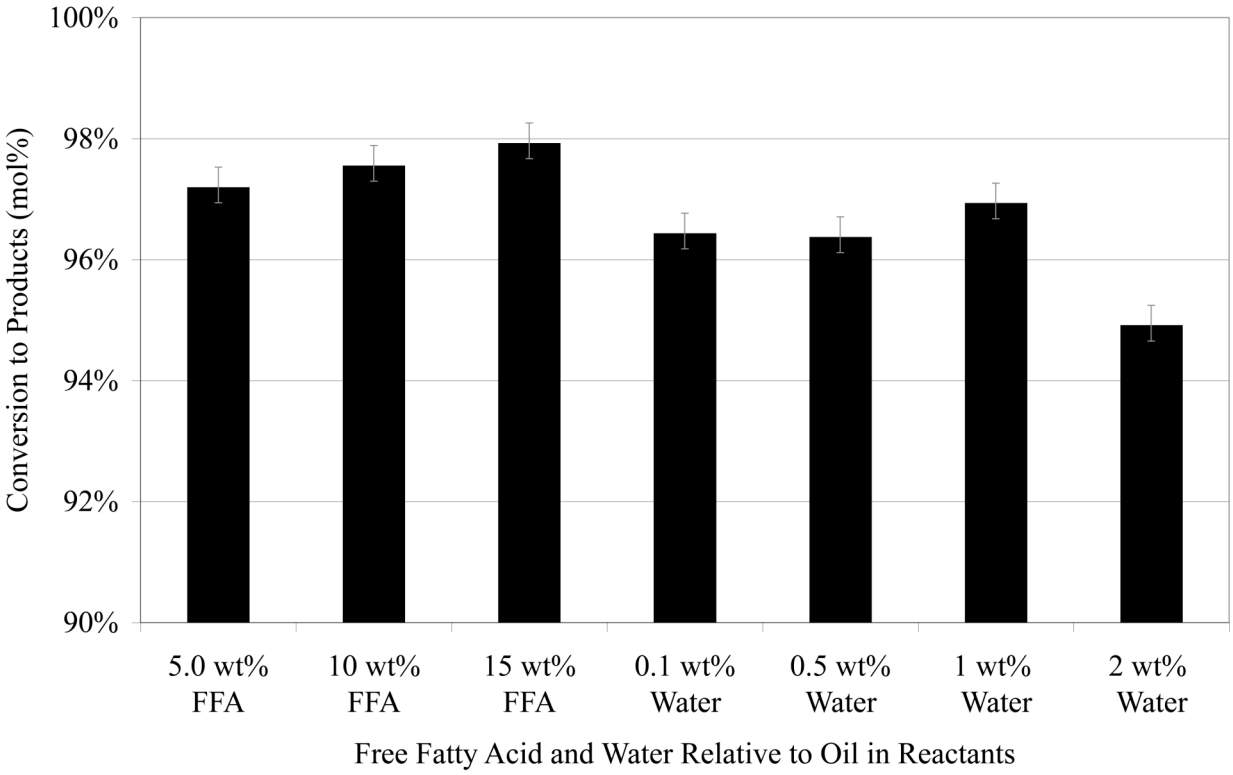

Figure 4-9: Effect of water and free fatty acid addition on transesterification of triolein
Conditions: 200˚C, 1:24 oil:methanol, 13 wt% loading, 600 RPM, 4 MPa,100g oil

4.3.6 Effect of Greenseed Canola Oil

To test the effects of using low-quality feedstocks, greenseed canola oil was substituted for triolein at the optimized reaction conditions. Greenseed canola oil is considered to be a low quality feedstock due to the chlorophyll content (Issariyakul, 2010) and due to FFA content. The acid value of greenseed canola oil was 8.2 mg KOH/g sample. Reaction results are presented in Figure 4-10. Final conversion to products for this experiment was 97.5 mol%. Comparing the data in Figure 4-7 and Figure 4-10 the results with triolein and greenseed canola oil agree to within 1% error at 60 minutes. Therefore, the use of greenseed canola oil as a low quality feedstock did not significantly affect catalyst activity. Solid acid catalysts (SAC) that are not sensitive to alternative feedstocks is beneficial for commercial development, given that 80% of the cost of biodiesel production is due to the cost of feedstock oils (Chisti, 2007).

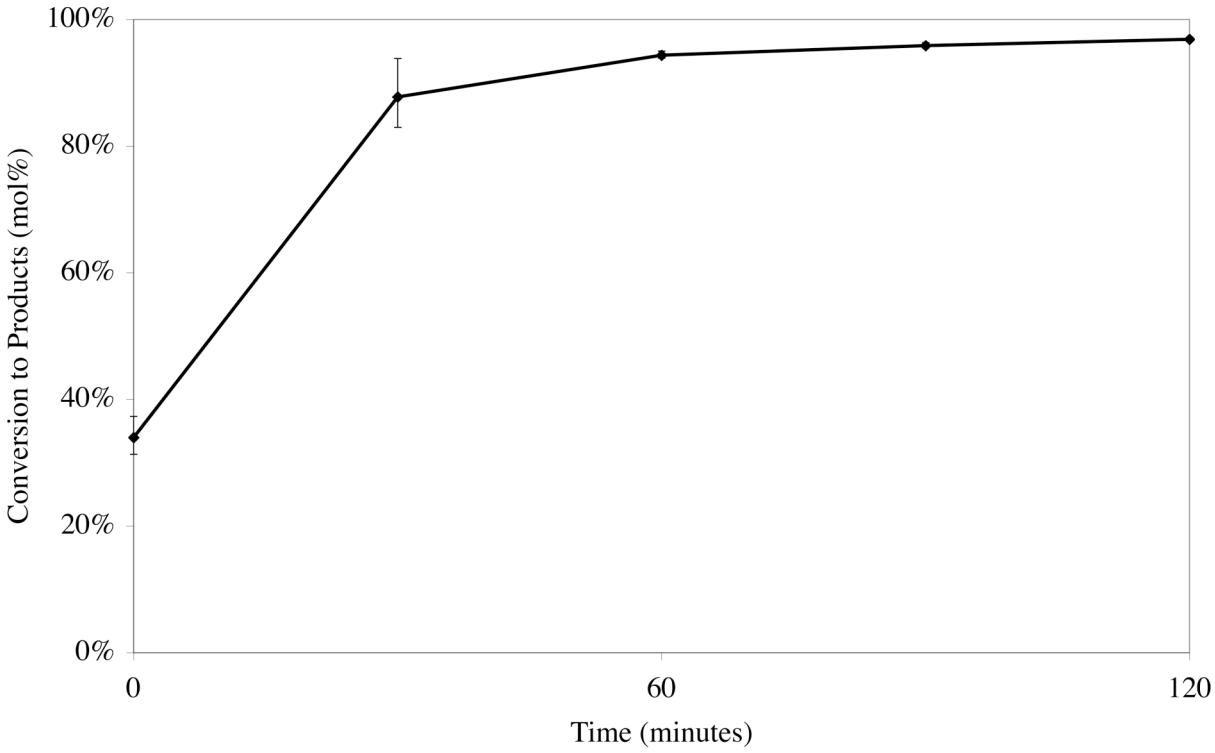

Figure 4-10: Transesterification of greenseed canola oil using optimized reactor conditions
Conditions: 200˚C, 1:24 oil:methanol, 13 wt% loading, 600 RPM, 4 MPa,100g oil

4.4. Product Analysis

4.4.1 High Performance Liquid Chromatography

Appendix D presents representative HPLC chromatograms of reaction products from the optimized conditions discussed in section 4.3.3. Appendix D.4 is the sample taken at time zero (t=0) when the reactor reaches the set-point temperature. Four peaks are visible, triglycerides, diglycerides, monoglycerides and products. The ester peak is visible since some transesterification takes place as the reactor reaches the temperature set point. Appendix D.5 is the sample taken at the final time, at 120 minutes (t=120). Triglyceride and diglyceride components are not detected in this example due to the high conversion achieved at optimized reaction conditions. Since monoglyceride and ester peaks are unified, they are separated at 18.2

minutes (based on HPLC chromatograms with separate monoglyceride and ester peaks) prior to integration. HPLC results show conversion to products as demonstrated in Figure 4-7.

4.4.2 Acid Value

The measured acid value of products was higher than that of the reactants. The acid value of products from the reaction at 200˚C was typically titrated to be 50 mg KOH/g sample. The acid value of the products from the optimized reaction conditions in Figure 4-7 was 55 mg KOH/g sample. Table 4-3 and Table 4-5 illustrate acid values of reactants and products in various feedstocks and experiments. Examination of the product acid value suggests hydrolysis of the ester products is taking place as discussed in section 4.3.1. The high acid values of the reaction products are above the limit of ASTM standards.

4.4.3 Inductively Coupled Plasma Mass Spectrometry

ICP-MS was employed to test for leaching of catalyst sulfur functional groups. Sulfur content was measured in triolein and the products from the optimized reaction. Triolein was found to contain 21 ppm (parts per million), while the products contain 12 ppm. It can be concluded that sulfur leaching is negligible, given the sulfonic functional group of Amberlyst 15. The decrease in sulfur content can be attributed to the glycerol layer containing a portion of the sulfur present in the feedstock. Therefore, the presence of sulfonic acid due to catalyst leaching is not contributing to the acid value of the products.

4.4.4 Water Content

Water is produced during esterification as illustrated in Figure 2-6. Triolein has less than 0.01 wt% water and when the catalyst is dried prior to the reaction the water content of the products was unaffected. The water content of the products is consistently 0.7 wt% meaning that water is being produced in a side reaction as discussed in section 4.3.1.

Table 4-5 lists water content for reaction products. The increase of water content is clear when results from feedstocks and reaction products are compared. The ASTM standard for water content (and sediment, see Table 2-1) is a maximum value of 0.06 wt%. Subsequently, the water content of the products at optimized conditions exceeds ASTM standards. An additional processing step to remove water from the product could be used such as: distillation, centrifugation, gravity separation, or adsorption by a hydroscopic substance.

4.4.5 Gas Chromatography

The methyl ester form of oleic acid is the primary component of the FAME mixture in the products. Results from gas chromatography examining the chain length and saturation composition are summarized in Table 4-6. The methyl esters produced from triolein consist of 85 mass% unsaturated and monounsaturated fatty acids. FAME chain length and saturation extent effect characteristics concerning various ASTM standards as discussed in section 2.7. Figure 2-10 illustrated the chain length and saturation of various oil sources including canola oil. Given the similarity in composition of triolein to canola oil, the FAME produced from triolein will have similar chemical properties compared to FAME produced from canola oil.

Table 4-6: Fatty acid methyl ester chain length and saturation extent by gas chromatograph

Amount (mg/mL)	Percent (mass %)	Name	Group
0.76	1.8%	Myristic	14:0
0.20	0.5%	Myristoleic	14:1
0.07	0.2%	Pentadecanoic	15:0
1.60	3.8%	Palmitic	16:0
1.68	4.1%	Palmitoleic	16:1
0.08	0.2%	Heptadecanoic	17:0
0.56	1.4%	Stearic	18:0
28.8	69.3%	Oleic	18:1
1.23	3.0%	Elaidic	18:1
3.34	8.1%	Linoleic	18:2
0.84	2.0%	Linolenic	18:3
0.02	0.0%	Arachidic	20:0
0.22	0.5%	cis-11-Eicosenoic	20:1

4.5. Catalyst Longevity

Successive reactions reused Amberlyst 15 to test catalyst longevity and activity at the optimized reaction conditions. As shown in Figure 4-11, there is a negligible decrease in the conversion of triolein to products after the second use, measured to be 0.2 mol%. Subsequent reuses of the catalyst show significant decrease in catalytic activity. Following the third use of Amberlyst 15 achieved a final conversion of 80 mol%, while the fourth successive use demonstrated 54 mol%. Therefore, from the longevity study, Amberlyst 15 can be reused once under the current reaction conditions, while maintaining high conversion to products. Previous work examining transesterification of triacetin reported a reduction of 40% from the original conversion after 5 successive uses of Amberlyst 15 at 60˚C for two hours (López, 2005). It was reported that 92% of the original sulfur remained in the catalyst structure, suggesting that the decrease in activity may be due to intermediate species or products adsorbed on the catalyst surface. Further work could be undertaken to determine if the catalyst could be regenerated and reused in subsequent reactions. Catalyst longevity is important in heterogeneous catalysis as mentioned in section 1.5.

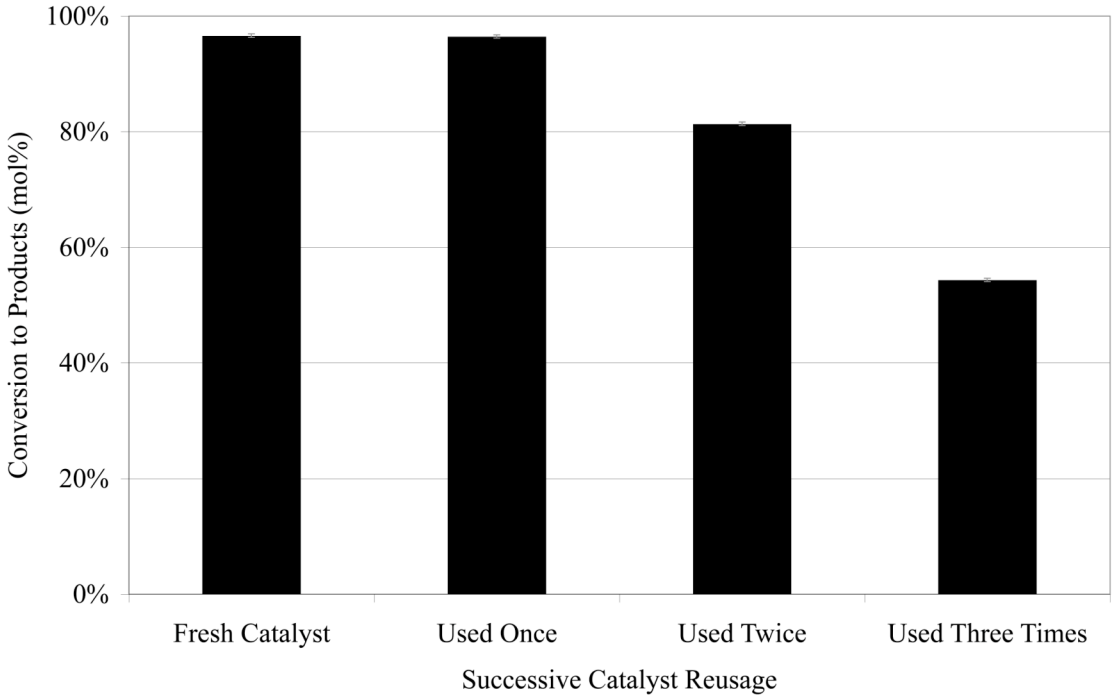

Figure 4-11: Amberlyst 15 longevity in successive transesterification of triolein
Conditions: 200˚C, 1:24 oil:methanol, 13 wt% loading, 600 RPM, 4 MPa,100g oil

4.6. Acid Value and Temperature

Due to the hydrolysis side reaction occurring at the optimized reaction conditions, the MATLab model developed for transesterification was not applicable to the optimized reaction. The model was developed for the three successive reversible reactions of transesterification, additional esterification and hydrolysis reactions invalidate the model. Subsequently, a lower temperature, higher alcohol molar excess and longer reaction duration were selected to avoid the side reactions. Temperature was maintained at or below the Amberlyst 15 recommended temperature limit of 120˚C. Oil quantity was decreased to 50 grams per reaction. Oil to alcohol molar ratio was raised to 1:77, to the maximum capacity of the reaction vessel. After 24 hours, at the new reaction conditions the conversion to products was 45 mol%. At 72 hours, conversion increased to 80 mol%. Experimental results are illustrated in Figure 4-12. The acid value of

products at three days was 2 mg KOH/g sample. This is significantly lower than optimized experiments, while still above ASTM standards. Two lower temperatures were also examined. At 110˚C, final conversion at 72 hours was 49 mol% and acid value was within ASTM standards measured to be 0.46 mg KOH/g sample. Conversion to products at 100˚C is reported to be 19 mol% with an acid value of 0.35 g KOH/g sample. At the new reaction conditions, hydrolysis has been minimized allowing the kinetic model to be applied.

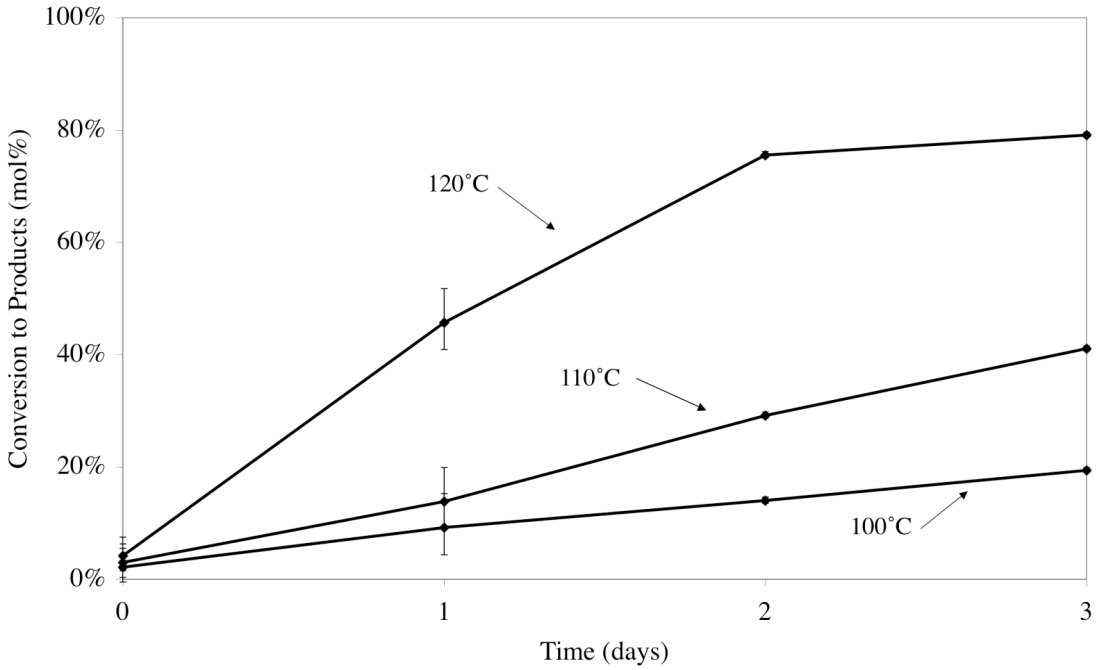

Figure 4-12: Transesterification of canola oil at various temperatures over Amberlyst 15
Conditions: 1:77 oil:methanol, 13 wt% loading, 600 RPM, 50g canola oil

4.7. Kinetics Study of Transesterification Reaction with Amberlyst 15

4.7.1 Kinetic Model Development

A kinetic model was developed to model the three-step transesterification reaction. Triglycerides are converted through two intermediates to methyl esters and glycerol by the reaction listed in Appendix B.1. The rate law for a chemical reaction links the concentrations of reactant species with reaction constants to determine the rate of reaction. Differential equations

derived from the rate law are listed in Appendix B.2. Section 3.5.5 discusses the MATLab model used to fit the kinetic model.

4.7.2 Transesterification Analysis

Kinetics experiments at 100˚C, 110˚C and 120˚C are illustrated in Figure 4-12. A significant increase in methyl ester yield is observed when the temperature was increased from 110˚C to 120˚C. Acid values of the products increase with temperature increase. Acid value for 100˚C, 110˚C and 120˚C are 0.35, 0.46 and 2.1, respectively. This demonstrates that the hydrolysis side reaction has been minimized. The acid value limit of ASTM standards is 0.5 mg KOH/g sample, as listed in Table 3-2. A sample calculation mole balance calculating the glycerol and methanol concentrations is available in Appendix A.5.

4.7.3 Reaction Rate Constants

Kinetic testing data was input into the MATLab model listed in Appendix C. The model was developed to solve for molar concentrations of each component, find reaction constants and Pearson correlation coefficients. The model considers the three reversible reactions using the rate law as derived in Appendix B. Molar concentration data is input to the program over specified time intervals used in the model. Initial guesses for reaction constants are also required. Data input into the model is from HPLC analysis of the kinetics reactions from Figure 4-12. Methanol and glycerol concentrations are calculated by a mole balance shown in Appendix A.5. The data is listed in Appendix C.1. Four values for each variable are listed, one for each sample time at t=0, 24, 48 and 72 hours. Input values for glycerol and methanol are calculated from the measured variables and triolein HPLC measurements. The input data is used as the initial conditions of the model output. The model data is calculated by the program and compared to experimental data in the calculation of Pearson correlation coefficients for error minimization.

Results for the kinetic parameters from the model are tabulated in Table 4-7. An increase in reaction rate constants is demonstrated in each reaction as temperature increases. Reaction rate constants are higher in the forward reactions compared to the reverse reactions. This is expected due to the net formation of products as the reaction continues to completion. The majority of the Pearson correlation coefficients are above 0.98, demonstrating a close approximation to the experimental data. An example of the program output is illustrated in Figure 4-13. As can be seen in the figure, the model demonstrates a close approximation to the experimental data.

Table 4-7: Reaction rate constants for reversible transesterification reactions
Conditions: 100˚C, 110˚C and 120˚C, 1:77 oil:methanol, 13 wt% loading, 600 RPM, 50g canola oil

Reaction	Temperature (˚C)	Rate Constant, k, (L/mol/day)	Pearson Correlation Coeff.
TG ⇒ DG	100	0.011	0.957
	110	0.018	0.990
	120	0.080	0.991
DG ⇒ TG	100	0.001	0.823
	110	0.001	0.991
	120	0.040	0.972
DG ⇒ MG	100	0.090	0.987
	110	0.130	0.905
	120	0.220	0.998
MG ⇒ DG	100	0.030	0.938
	110	0.050	0.992
	120	0.200	0.991
MG ⇒ GL	100	0.980	0.928
	110	2.300	0.992
	120	6.500	0.991
GL ⇒ MG	100	0.250	0.938
	110	4.000	0.992
	120	5.000	0.991

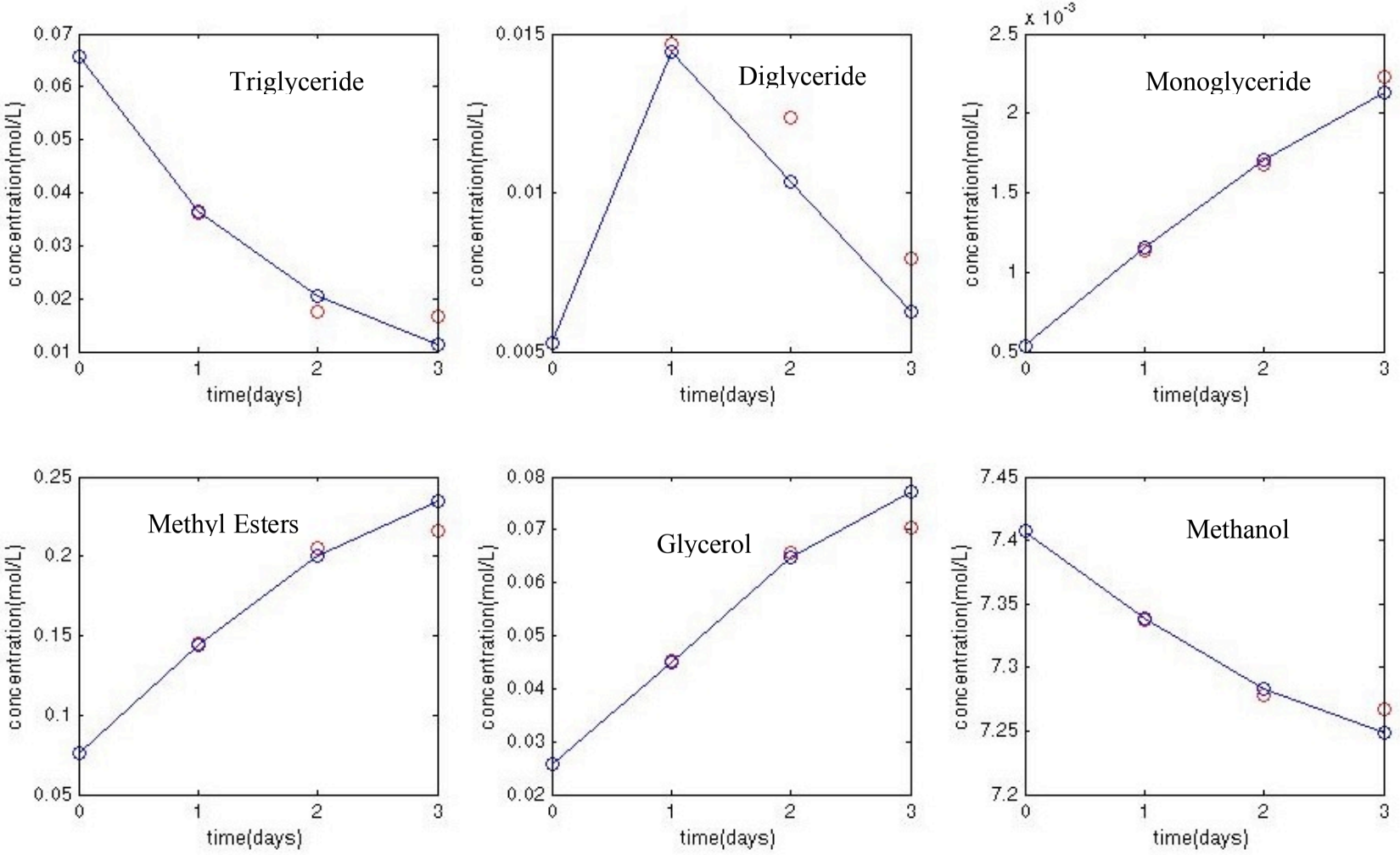

Figure 4-13: Plotgraph function from MATLab model temperature 120˚C

Conditions: 120˚C, 1:77 oil:methanol, 13 wt% loading, 600 RPM, 50g canola oil
Joined lines - model; scatter points - experimental

4.7.4 Reaction Order

The MATLab program was developed based on second order kinetics. Since the simulated results obtained from MATLab fit with the experimental values, it can be concluded that the reaction followed second order kinetics. By the rate law, a second order reaction will produce a straight line when the reaction time is plotted versus the inverse of the reactant concentration. Figure 4-14 confirms second-order reaction kinetics for the triglyceride consumption reaction. This is in agreement with literature, denoting second order kinetics of transesterification (Darnoko, 2000). Figure 4-14 illustrated the second order reaction, which is a reasonable result as the transesterification mechanism is dependent on both glyceride and methanol concentration.

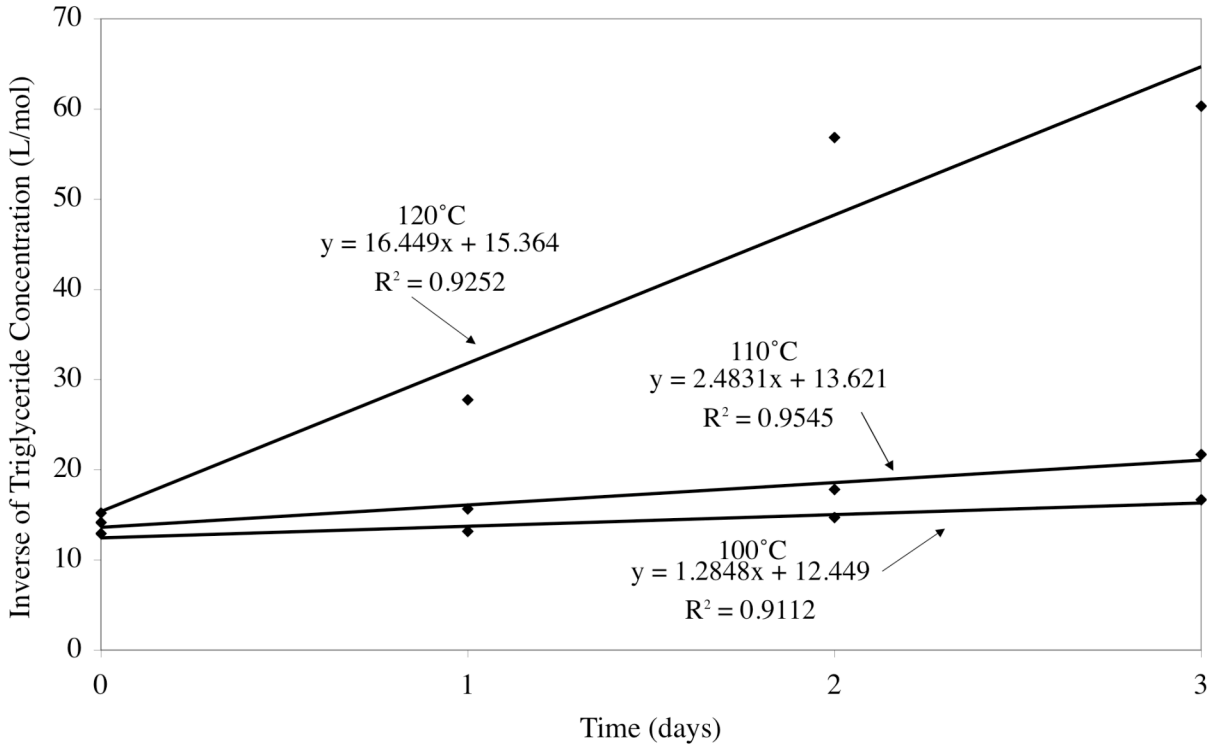

Figure 4-14: Pseudo-second order reaction kinetics for triglyceride consumption over Amberlyst 15
Conditions: 1:77 oil:methanol, 13 wt% loading, 600 RPM, 50g canola oil

4.7.5 Activation Energy

The energy barrier that must be overcome for a chemical reaction to take place is the activation energy. Activation energy is determined from the slope of an Arrhenius plot and equation 3-3. An Arrhenius plot in Figure 4-15 shows the forward reaction rate constants for the three temperatures examined. Linear best fit slopes for each reaction rate constant are natural logarithmic derivations of equation 3-3. From the linear equations the activation energy for the triglyceride to diglyceride reaction was 120 kJ/mol. A sample calculation for activation energy is listed in Appendix A.6. Activation energy for the diglyceride to monoglyceride reaction was 54 kJ/mol and 115 kJ/mol for the monoglyceride to glycerol reaction. These values are comparable to activation energies for similar reactions in literature, see Table 4-8. Literature values for the three reactions using homogeneous acid potassium hydroxide are 61.5, 59.4 and 26.8 kJ/mol, respectively (Darnoko, 2000). In transesterification of triacetin (glycerol triacetate) using Nafion SAC-13, activation energy has previously been reported to be 48.5 kJ/mol (López, 2007). Esterification of acetic acid using Nafion SAC-13 has a reported activation energy of 51.8 kJ/mol at 60˚C (Liu, 2006). Additional work in transesterification of di-esters to tri-esters reports an activation energy of 119 kJ/mol (Hamid, 2010). Published activation energies in similar reactions (organic reactions, both homogeneous and heterogeneous catalysts) are close to values obtained in this work using Amberlyst 15.

4.7.6 Rate Determining Step

The rate limiting step is defined as the reaction step with the highest activation energy. The net chemical reaction can only proceed at the rate of the slowest reaction step. It is this rate determining step that is responsible for the rate equation of an overall reaction. The triglyceride to diglyceride decomposition reaction has the highest activation energy, 120 kJ/mol. This value

is calculated from the slope of the best fit line in Figure 4-15. A sample calculation is in Appendix A.6.

Table 4-8: Comparison of activation energy in current work and literature values

Feedstock	Catalyst	Activation energy (kJ/mol)	Reference
Palm oil	KOH	61.5	Darnoko, 2000
Triacetin	Nafion SAC-13	48.5	López, 2007
Acetic acid	Nafion SAC-13	51.8	Liu, 2006
Di-esters	NaOCH3	119	Hamid, 2010
Soybean oil	No catalyst	92.5	Wang, 2007
Soybean oil	MgO	75.9	Wang, 2007
Canola oil	Amberlyst 15	120	Current work

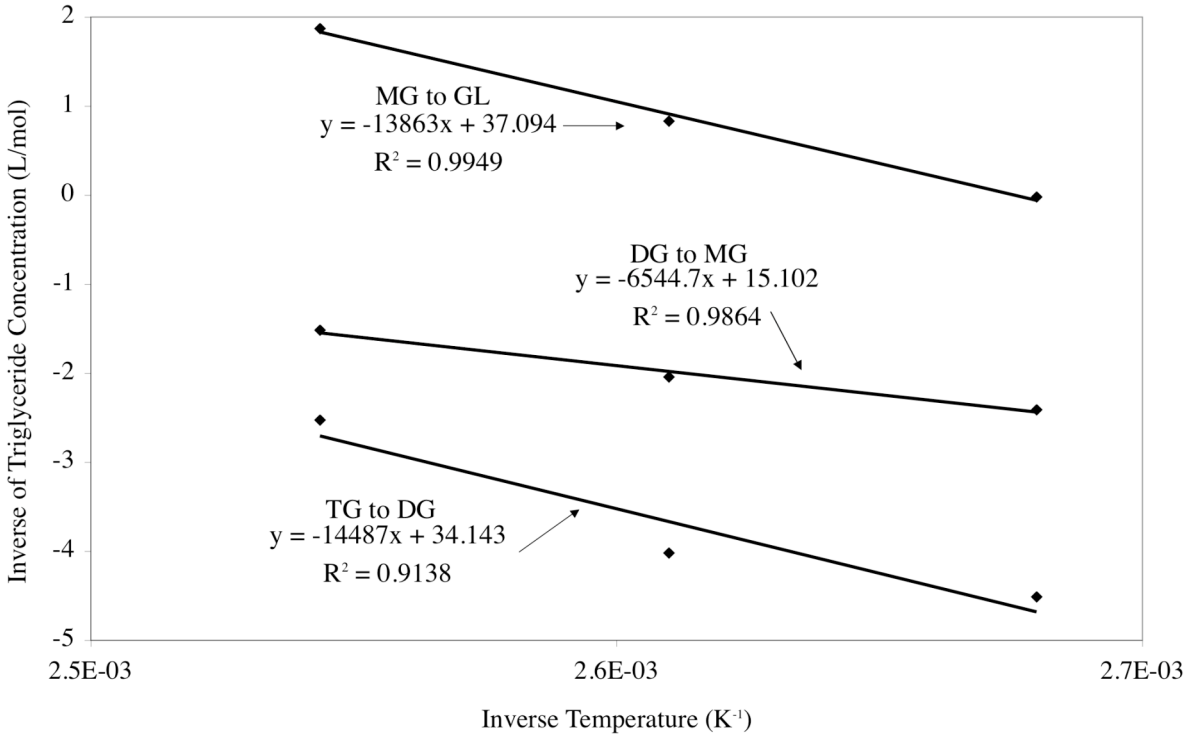

Figure 4-15: Arrhenius plot of tri- di- and monoglyceride consumption during transesterification Conditions: 110˚C, 110˚C and 120˚C, 1:77 oil:methanol, 13 wt% loading, 600 RPM, 50g canola oil

Mass transport limitations can be responsible for the apparent reaction rates. In order to avoid diffusional limitations of the reaction rate in transesterification of triglyceridees, a catalyst must have an interconnected system of large pores (Helwani, 2009). Solid catalysts such as zeolites are often diffusion limited when used in transesterification of oils, due to the small pore sizes of the zeolites and large reactant molecules (Di Serio, 2008; Clark, 2002). The pore diameter of zeolites is up to 14 angstroms (Å), while the pore diameter of Amberlyst 15 is 231 Å (Dacquin, 2012). An experiment was performed with Amberlyst 15 crushed using a mortar and pestle prior to the experiment. This exposes the functional groups, removing any effect of internal mass diffusion. No discernible change in the apparent reaction rate was observed. Previously published work has also found that external mass transfer limitations are negligible when agitation is adequately high and no internal mass transfer limitations are significant using Nafion SAC-13 (López, 2007; Liu, 2006). High activation energy (40 kJ/mol; Bozek-Winkler, 2006) suggests surface controlled rather than diffusion controlled. Diffusional limitations can be assumed negligible in the kinetics study due to the stirring speed of 600 RPM (based on previous work; Kulkarni, 2006a), results from experiments using a crushed catalyst and the large pore diameter of Amberlyst 15.

5. CONCLUSIONS AND RECOMMENDATIONS

5.1. Conclusions

Ion-exchange resins (IER) have been examined at temperatures above the boiling point of methanol. Amberlyst 15 was found to be tolerant to water content and free fatty acids present in low quality feedstock. The optimized catalyst achieved a high conversion to products; however, free fatty acids were formed in a side reaction called hydrolysis. The side reaction prevents the products of reaction from meeting ASTM fuel standards for biodiesel. A mathematical model was developed to represent kinetics of the transesterification reaction at temperatures above the boiling point of methanol.

Various commercial ion exchange resins were screened for catalytic activity. Amberlyst 15 demonstrated the highest catalytic activity of the commercial ion-exchange resins tested in transesterification of triolein during catalyst screening and was selected for statistical optimization of reaction conditions. The central composite design method of statistical optimization was used to plan experiments to optimize reactor conditions: temperature, oil to alcohol molar ratio and catalyst loading. Optimized reaction conditions for conversion of triolein demonstrate high conversion of 97 mol% to products over a reaction time of 2 hours using 13 wt% loading of Amberlyst 15 at 200˚C and 1:24 oil to methanol molar ratio. Oil loading of 100g, stirring speed of 600 RPM and a 4 MPa nitrogen atmosphere were fixed conditions. Acid value of the products at the optimized reaction conditions was reported to be 55 mg KOH/g sample. Addition of water to the reactant mixture did not have an effect on reaction products up to 1 wt% of the feedstock oil. Similarly, addition of the free fatty acid stearic acid did not have an effect on the reaction at a concentration of 15 wt%. Additive testing with water and FFA suggests that esterification and hydrolysis are taking place as side reactions in competition with

transesterification. Greenseed canola oil was tested as a low quality feedstock and at the stated optimized reaction conditions achieved a conversion to products of 97 mol%. The catalyst was not sensitive to the low quality greenseed canola oil feedstock. The catalyst longevity study concluded that Amberlyst 15 was be reused once with no significant decrease in conversion to products. Additional reuses demonstrated decreases in activity.

A study of the kinetics of the transesterification required the reaction conditions be altered in order to circumvent the hydrolysis side reaction. The temperature of the reactor was limited to 120˚C. Conditions for the kinetic study were at temperatures of 100˚C, 110˚C and 120˚C, oil to methanol molar ratio was 1:77, Amberlyst 15 loading was 13 wt%, stirring speed 600 RPM, 2 MPa nitrogen atmosphere, using 50 grams of canola oil. The kinetic study yielded a model with a close fit to experimental data with most Pearson correlation coefficients above 0.98. Reaction rate constants were determined for forward and reverse transesterification reactions. Activation energies for the TG to DG, DG to MG and MG to GL reactions are 120, 54 and 115 kJ/mol, respectively. These values are similar to values reported in literature for similar reactions. Therefore, the triglyceride to diglyceride reaction is the rate limiting step for the transesterification reaction, having the highest activation energy of the three reactions. The rate limiting step was found to be a pseudo-second order reaction.

5.2. Recommendations

1. The conversion to products of triolein at optimized conditions was 97%, however the yield of FFA does not meet ASTM standards. Further work should be done to minimize FFA production and maximize FAME yield.

2. Five commercial IER were examined of the hundreds of commercial varieties currently available. Additional work can be undertaken to develop or locate a more selective and active catalyst compared to Amberlyst 15.
3. Laboratory-synthesized IER have demonstrated promising results in published works. Additional work synthesizing and studying IER properties can be undertaken.
4. Triolein and canola oil are costly feedstocks. Greenseed oil, while less costly is still an expensive feedstock. Additional and less costly feedstocks (such as used cooking oil) can be tested in future work. Third generation feedstocks such as algal oil must also eventually be examined.

LIST OF REFERENCES

Abrams I.M. and L. Benezra, *Ion-Exchange Polymers*, "Encyclopedia of Polymer Science and Technology Volume 7", Interscience Publishers (1967) 692-742.

American Oil Chemists' Society, "Free Fatty Acids", Official Methods and Recommended Practices of the AOCS: Ca 5a-40. (1997).

American Society for Testing and Materials, "Biodiesel Fuel Blend Stock (B100) for Middle Distillate Fuels", ASTM D6751-11a, ASTM International (2011).

Balat, M. and H. Balat, "A Critical Review of Bio-diesel as a Vehicular Fuel", Energy Conversion and Management 49 (2008) 2727-2741.

Banks, S.N.K. "Bill C-33: An Act To Amend The Canadian Environmental Protection Act, 1999", Legislative Summary LS-587E. Library of Parliament. (2008).

Bozek-Winkler, E. and J. Gmehling, "Transesterification of Methyl Acetate and n-Butanol Catalyzed by Amberlyst 15", Industrial & Engineering Chemistry Research 45 (2006) 6648-6654.

Brunauer, S., P.H. Emmett and E. Teller, "Adsorption of Gases in Multimolecular Layers", Journal of the American Chemical Society 60 (1938) 309-319.

Canakci, M. and J. Van Gerpen, "Biodiesel Production via Acid Catalysis", Transactions of the American Society of Agricultural Engineers 42 (1999) 1203-1210.

Canakci, M. and J. Van Gerpen, "Biodiesel Production from Oils and Fats with High Free Fatty Acids", Transactions of the American Society of Agricultural Engineers 44 (2001) 1429-1436.

Canadian Renewable Fuels Association, "Plant Locations", last accessed June (2012), website: http://www.greenfuels.org/en/industry-information/plants.aspx

Chisti, Y, "Biodiesel from Microalgae", Biotechnology Advances 25 (2007) 294-306.

Clark, J.H., "Solid Acids for Green Chemistry", Accounts of Chemical Research 35 (2002) 791-797.

Coutinho, F.M.B., S.M. Rezende and B.G. Soares, "Characterization of Sulfonated Poly(styrene-divinylbenzene) and Poly(divinylbenzene) and its Application as Catalysts in Esterification Reaction", Journal of Applied Science 102 (2006) 3616-3627.

D'Cruz, A., M.G. Kulkarni, L.C. Meher and A.K. Dalai, "Synthesis of Biodiesel from Canola Oil Using Heterogeneous Base Catalyst", Journal of the American Oil Chemists' Society 84 (2007) 937-943.

Dacquin, J.P., A.F. Lee, C. Pirez and K. Wilson, "Pore-Expanded SBA-15 Sulfonic Acid Silicas for Biodiesel Synthesis", Chemical Communications 48 (2012) 212-214.

Darnoko, D. and M. Cheryan, "Kinetics of Palm Oil Transesterification in a Batch Reactor", Journal of the American Oil Chemists' Society 77 (2000) 1263-1267.

de Rezende, S.M., M. de Castro Reis, M.G. Reid, P.L. Silva Jr., F.M.B. Coutinho, R.A. da Silva San Gil and E.R. Lachter, "Transesterification of Vegetable Oils Promoted by Poly(styrene-divinylbenzene) and Poly(divinylbenzene)", Applied Catalysis A: General 349 (2008) 198-203.

Demirbas, A., "Comparison of Transesterification Methods for Production of Biodiesel from Vegetable Oils and Fats", Energy Conversion and Management 49 (2008) 125-130.

Di Serio, M., R. Tesser, L. Pengmei and E. Santacesaria, "Heterogeneous Catalysts for Biodiesel Production", Energy & Fuels 22 (2008) 207-217.

Dmytryshyn, S.L., A.K. Dalai, S.T. Chaudhari, H.K. Mishra and M.J. Reaney. "Synthesis and Characterization of Vegetable Oil Derived Esters: Evaluation for their Diesel Additive Properties", Bioresource Technology 92 (2004) 55-64.

Dorfner, K., "Ion Exchangers Properties and Applications", Ann Arbor Science Publishers Inc. (1972).

dos Reis, S.C.M., E.R. Lachter, R.S.V. Nascimento, J.A. Rodrigues Jr. and M.G. Reid, "Transesterification of Brazilian Vegetable Oils with Methanol over Ion-Exchange Resins", Journal of the American Oil Chemists' Society 82 (2005) 661-665.

Ebiura, T., T. Echizen, A.Ishikawa, K. Murai and T. Baba, "Selective Transesterification of Triolein with Methanol to Methyl Oleate and Glycerol using Alumina Loaded with Alkali Metal Salt as a Solid-Base Catalyst", Applied Catalysis A: General 283 (2005) 111-116.

Encinar, J.M., J.F. Gonzalez, E. Sabio and M.J. Ramiro, "Preparation and Properties of Biodiesel from Cynara cardunculus L. Oil", Industrial & Engineering Chemistry Research 38 (1999) 2927-2931.

Freedman, B., E.H. Pryde and T.L. Mounts, "Variables Affecting the Yields of Fatty Esters from Transesterified Vegetable Oils", Journal of the American Oil Chemists' Society 61 (1984) 1638-1643.

Gelbard, G., "Organic Synthesis by Catalysis with Ion-Exchange Resins", Industrial & Engineering Chemistry Research 44 (2005) 8468-8498.

Hamid, H.A., R. Yunus and T.S.Y. Choong, "Utilization of MATLAB to Simulate Kinetics of Transesterification of Palm Oil-Based Methyl Esters with Trimethylolpropane for Biodegradable Synthetic Lubricant Synthesis", Chemical Product and Process Modeling 5 (2010) 1-17.

Hanh, H.D., N.T. Dong, K. Okitsu, R. Nishimura and Y. Maeda, "Biodiesel Production Through Transesterification of Triolein with Various Alcohols in an Ultrasonic Field", Renewable Energy 34 (2009) 766-768.

Hara, M., "Environmentally Benign Production of Biodiesel Using Heterogeneous Catalysts", ChemSusChem 2 (2009) 129-135.

Hara, M. "Biodiesel Production by Amorphous Carbon Bearing SO_3H, COOH and Phenolic OH Groups, a Solid Bronsted Acid Catalyst", Topics in Catalysis 53 (2010) 805-810.

Harmer, M.A. and Q. Sun, "Solid Acid Catalysis Using Ion-Exchange Resins", Applied Catalysis A: General 221 (2001) 45-62.

Helwani, Z., M.R. Othman, N. Aziz, J. Kim and W.J.N. Fernando, "Solid Heterogeneous Catalysts for Transesterification of Triglycerides with Methanol: A Review", Applied Catalysis A: General 363 (2009) 1-10.

Hou, X., Y. Qi, X. Qiao, G. Wang, Z. Qin and J. Wang, "Lewis Acid-Catalyzed Transesterification and Esterification of High Free Fatty Acid Oil in Subcritical Methanol", Korean Journal of Chemical Engineering 24 (2007) 311-313.

Iso, M., B. Chen, M. Eguchi, T. Kudo and S. Shrestha, "Production o Biodiesel Fuel from Triglycerides and Alcohol using Immobilized Lipase", Journal of Molecular Catalysis B: Enzymatic 16 (2001) 53-58.

Issariyakul, T. and A.K. Dalai, “Biodiesel Production from Greenseed Canola Oil”, Energy Fuels 24 (2010) 4652-4658.

Issariyakul, T., Master’s Thesis “Biodiesel Production from Fryer Grease”, University of Saskatchewan (2006).

Jacobson, K., R. Gopinath, L.C. Meher and A.K. Dalai, “Solid Acid Catalyzed Biodiesel Production From Waste Cooking Oil”, Applied Catalysis B: Environmental 85 (2008) 86-91.

Jothiramalingam, R. and M.K. Wang, “Review of Recent Developments in Solid Acid, Base, and Enzyme Catalysts (Heterogeneous) for Biodiesel Production via Transesterification”, Industrial & Engineering Chemistry Research 48 (2009) 6162-6172.

Kulkarni, M.G., R. Gopinath, L.C. Meher and A.K. Dalai, “Solid Acid Catalyzed Biodiesel Production By Simultaneous Esterification and Transesterification”, Green Chemistry 8 (2006a) 1056-1062.

Kulkarni, M.G., A.K. Dalai and N.N. Bakhshi, “Utilization of Green Seed Canola Oil for Biodiesel Production”, Journal of Chemical Technology and Biotechnology 81 (2006b) 1886-1893.

Liu, Y., E. Lotero and J.G. Goodwin Jr., “A Comparison of the Esterification of Acetic Acid with Methanol using Heterogeneous versus Homogeneous Acid Catalysis”, Journal of Catalysis 242 (2006) 278-286.

López, D.E., J.G. Goodwin Jr., D.A. Bruce and E. Lotero, “Transesterification of Triacetin with Methanol on Solid Acid and Base Catalysts”, Applied Catalysis A: General 295 (2005) 97-105.

López, D.E., J.G. Goodwin Jr. and D.A. Bruce, "Transesterification of Triacetin with Methanol over Nafion Acid Resins", Journal of Catalysis 245 (2007) 381-391.

Lotero, E., Y. Liu, D.E. López, K. Suwannakarn, D.A. Bruce and J.G. Goodwin Jr., "Synthesis of Biodiesel via Acid Catalysis", Industrial & Engineering Chemistry Research 44 (2005) 5353-5363.

Ma, F. and M.A. Hanna, "Biodiesel Production: A Review", Bioresource Technology 70 (1999) 1-15.

Melero, J.A., L.F. Bautista, G. Morales, J. Iglesias and D. Briones, "Biodiesel Production with Heterogeneous Sulfonic Acid-Functionalized Mesostructured Catalysts", Energy & Fuels 23 (2009a) 539-547.

Melero, J.A., J. Iglesias and G. Morales, "Heterogeneous Acid Catalysis for Biodiesel Production: Current Status and Future Challenges", Green Chemistry 11 (2009b) 1285-1308.

Noureddini, H. and D. Zhu, "Kinetics of Transesterification of Soybean Oil", Journal of the American Oil Chemists' Society 74 (1997) 1457-1463.

Peterson, C.L. and T. Hustrulid, "Closed Cycle For Rapeseed Oil Biodiesel Fuels", Biomass and Bioenergy 14 (1998) 91-101.

Peterson, G.R. and W.P. Scarrah, "Rapeseed Oil Transesterification By Heterogeneous Catalysis", Journal of the American Oil Chemists' Society 61 (1984) 1593-1597.

Ramos, M.J., C.M. Fernández, A. Casas, L. Rodríguez and Á. Pérez, "Influence of Fatty Acid Composition of Raw Materials on Biodiesel Properties", Bioresource Technology 100 (2009) 261-268.

Sharma, M.M., “Some Novel Aspects of Cationic Ion-exchange Resins as Catalysts”, Reactive & Functional Polymers 26 (1995) 3-23.

Sharma, Y.C., B. Singh and S.N. Upadhyay, “Advancements in Development and Characterization of Biodiesel: A Review”, Fuel 87 (2008) 2355-2373.

Shibasaki-Kitakawa, N., H. Honda, H. Kuribayashi, T. Toda, T. Fukumura and T. Yonemoto, “Biodiesel Production using Anionic Ion-exchange Resin as Heterogeneous Catalyst”, Bioresource Technology 98 (2005) 416-421.

Sigma-Aldrich Company, “Sigma-Aldrich Homepage”, last accessed on 18 January (2012), website: http://www.sigmaaldrich.com/

Silverstein, R.M., “Spectrometric Identification of Organic Compounds”, John Wiley & Sons (2005).

Singh, A.K. and S.D. Fernando, “Transesterification of Soybean Oil Using Heterogeneous Catalysts”, Energy & Fuels 22 (2008) 2067-2069.

Stiefel, S. and G. Dassori, “Simulation and Biodiesel Production Through Transesterification of Vegetable Oils”, Industrial & Engineering Chemistry Research 48 (2009) 1068-1071.

Yazici, D.T. and C. Bilgiç, “Determining the Surface Acidic Properties of Solid Catalysts by Amine Titration Using Hammett Indicators and FTIR-pyridine Adsorption Methods”, Surface and Interface Analysis 42 (2010) 959-962.

Yu, W., K. Hidajat and A.K. Ray, “Determination of Adsorption and Kinetic Parameters for Methyl Acetate Esterification and Hydrolysis Reaction Catalyzed by Amberlyst 15”, Applied Catalysis A: General 260 (2004) 191-205.

Zabeti, M., W.M.A.W. Daud and M.K. Aroua, "Activity of Solid Catalysts for Biodiesel Production: A Review", Fuel Processing Technology 90 (2009) 770-777.

APPENDICES

A. Sample Calculations

A.1. Error Calculation for Water Content Testing

H_2O content of 1% Aquastar water standard per 1g, 10mg H_2O.

Measured value 1.0129 wt%.

$$error\% = \frac{\left|theoretical - actual\right|}{theoretical} \times 100\%$$

$$error\% = \frac{\left|1.000 - 1.0129\right|}{1.000} \times 100\%$$

$$error\% = 1.29\%$$

A.2. Calculation of Mole Percentage (mol%) from HPLC Results of Triolein Sample

Table A-1: HPLC results of triolein sample and component molecular weights

Component	Amount (wt%)	Molecular weight (g/mol)
Triglyceride	70.99450	885.432
Diglyceride	20.60153	620.998
Monoglyceride	3.98757	356.546
Methyl Esters	-	296.494

$$mol_i\% = \frac{wt_i\% \times \left(mol\ wt_i\right)^{-1}}{\sum_{i=0}^{n} wt_i\% \times \left(mol\ wt_i\right)^{-1}}$$

$$mol_{TG}\% = \frac{70.99450 \times \left(885.432\right)^{-1}}{\left[70.99450 \times \left(885.432\right)^{-1} + 20.60153 \times \left(620.998\right)^{-1} + 3.98757 \times \left(356.546\right)^{-1}\right]}$$

$$mol_{TG}\% = 64.38\ mol\%$$

A.3. Error Calculation from Statistical Experiments

Runs 6, 10, 20

Time = 120 min

Ester percent: 93.52%, 93.75%, 92.95%

Calculation of mean value:

$$Mean = \frac{\sum \%}{n}$$

$$Mean = \frac{93.52 + 93.75 + 92.95}{3}$$

$$Mean = 93.41$$

Calculation of standard deviation:

$$stdev = \sqrt{\frac{\sum (\exp - mean)}{n-1}}$$

$$stdev = \sqrt{\frac{(93.52 - 93.41)^2 + (93.75 - 93.41)^2 + (92.95 - 93.41)^2}{3-1}}$$

$$stdev = \sqrt{\frac{0.0121 + 0.1156 + 0.2116}{2}}$$

$$stdev = \sqrt{0.1697}$$

$$stdev = 0.4119$$

Calculation of 95% confidence interval:

$$95\%\ CI = \frac{stdev}{\sqrt{n}}$$

$$95\%\ CI = \frac{0.4119}{\sqrt{3}}$$

$$95\%\ CI = 0.2378$$

A.4. Statistical Model Quadratic Equation

Table A-2: Factors in statistical model to calculate coded factors

Factor	Code	Value	Average	Range/2	Coded Factor
Temperature	T	200˚C	190	50	0.2
Catalyst Loading	C	13 wt%	10.8	13.2	0.168
Alcohol Molar Excess	A	24:1	16.5	12.6	0.595

Calculation of coded factor:

$$factor = \frac{(actual - average)}{range/2}$$

$$factor = \frac{(200 - 190)}{50}$$

$$factor = 0.2$$

Calculation of predicted conversion:

$$X = 89 + 21.5T + 3.6C + 7.1A - 8.7T^2 - 11.5C^2 + 5.1A^2 + 1.7T \cdot C - 10.7T \cdot A + 6.8C \cdot A$$

$$X = 89 + 21.5(0.2) + 3.6(0.168) + 7.1(0.595) - 8.7(0.2)^2 - 11.5(0.168)^2 + 5.1(0.595)^2 + 1.7(0.2) \cdot (0.168) - 10.7(0.2) \cdot (0.595) + 6.8(0.168) \cdot (0.595)$$

$$X = 89 + 4.3 + 0.60 + 4.2 - 0.35 - 0.32 + 1.8 + 0.06 - 1.3 + 0.68$$

$$X = 98.7\ mol\%$$

A.5. Mole Balance

Calculation of glycerol and methanol concentration:

Table A-3: Feedstock and reactant concentrations in kinetic experiments
Conditions: 120˚C, 1:77 oil:methanol, 13 wt% loading, 600 RPM, 50g canola oil

Component	Feedstock concentration (mol/L)	Initial concentration at t=0 (mol/L)	Net change (mol/L)
Triglyceride (TG)	0.0896	0.0658	-0.0238
Diglyceride (DG)	0.0076	0.0052	-0.0024
Monoglyceride (MG)	0	0.0005	0.0005
Methyl Ester (ME)	0	0.0031	0.0031

Glycerol concentration:

$$GL_{conc} = \frac{ME_{conc}}{3}$$
$$GL_{conc} = \frac{0.0031}{3}$$
$$GL_{conc} = 0.0010\ mol/L$$

Initial methanol concentration:

$$MeOH_{conc,i} = 77 \times \left(TG_{conc} + DG_{conc}\right)$$
$$MeOH_{conc,i} = 77 \times \left(0.0896 + 0.0076\right)$$
$$MeOH_{conc,i} = 7.4844\ mol/L$$

Methanol concentration at t=0:

$$MeOH_{conc} = MeOH_{conc,i} + \Sigma\left(\Delta TG + \Delta DG + \Delta MG\right)$$
$$MeOH_{conc} = 7.4844 + \left(-0.0238 - 0.0024 + 0.0005\right)$$
$$MeOH_{conc} = 7.4844 - 0.0257$$
$$MeOH_{conc} = 7.4587\ mol/L$$

A.6. Calculation of Activation Energy

Linear best fit line equation:

$$y = mx + b$$
$$y = -(14,487)x + 34.143 \qquad from\ fig.4-15$$

From equation 3-3:

$$k = Ae^{\frac{-\Delta E}{RT}}$$
$$R = 8.314\frac{J}{K \cdot mol}$$

Dividing equation 3-3 by itself at an alternate temperature:

$$\frac{k_1}{k_2} = e^{\left[\frac{-\Delta E}{RT_1} - \left(\frac{-\Delta E}{RT_2}\right)\right]}$$
$$\ln\left(\frac{k_1}{k_2}\right) = \frac{-\Delta E}{RT_1} - \left(\frac{-\Delta E}{RT_2}\right)$$
$$\ln\left(\frac{k_1}{k_2}\right) = \frac{-\Delta E}{R}\left(\frac{1}{T_1} - \frac{1}{T_2}\right)$$
$$y = mx + b$$
$$\therefore m = \frac{-\Delta E}{R}$$
$$\Delta E = -14,487\left(8.314\frac{J}{mol}\right)$$
$$\Delta E = 120,445\frac{J}{mol}$$

B. Rate Law Equation

B.1. Transesterification Reaction

$$TG + MeOH \underset{k_2}{\overset{k_1}{\rightleftharpoons}} DG + ME$$

$$DG + MeOH \underset{k_4}{\overset{k_3}{\rightleftharpoons}} MG + ME$$

$$MG + MeOH \underset{k_6}{\overset{k_5}{\rightleftharpoons}} GL + ME$$

Variables $k_{1\text{-}6}$ are reaction constants, TG - triglycerides, DG - diglycerides, MG - monoglycerides, ME - methyl esters, GL - glycerol.

B.2. Differential Rate Law Equations

For an elementary chemical reaction:

$$aA + bB \rightarrow cC$$

The rate equation becomes:

$$r = k[A]^x [B]^y$$

where x and y are the order of the reaction.

From B.1.:

$$\frac{dTG}{dt} = -k_1[TG][MeOH] + k_2[DG][ME]$$

$$\frac{dDG}{dt} = k_1[TG][MeOH] - k_2[DG][ME] - k_3[DG][MeOH] + k_4[MG][ME]$$

$$\frac{dMG}{dt} = k_3[DG][MeOH] - k_4[MG][ME] - k_5[MG][MeOH] + k_6[GL][ME]$$

$$\frac{dME}{dt} = k_1[TG][MeOH] - k_2[DG][ME] + k_3[DG][MeOH] - k_4[MG][ME] + k_5[MG][MeOH] - k_6[GL][ME]$$

$$\frac{dGL}{dt} = k_5[MG][MeOH] - k_6[GL][ME]$$

$$\frac{dMeOH}{dt} = -k_1[TG][MeOH] + k_2[DG][ME] - k_3[DG][MeOH] + k_4[MG][ME] - k_5[MG][MeOH] + k_6[GL][ME]$$

These differential rate law equations are used in Appendix C.2. in the MATLab program.

C. MATLab Program

C.1. Input Values for Time Increments and Concentrations (inputvalue.m)

```
% input values
texp=[0 1 2 3];


%Experimental values
TG=   [0.065          0.036          0.018          0.017];
DG=   [0.005          0.015          0.012          0.008];
MG=   [0.001          0.001          0.002          0.002];
ME=   [0.076          0.145          0.205          0.216];
GL=   [0.026          0.045          0.066          0.071];
MeOH= [7.407          7.338          7.278          7.266];
```

C.2. Ordinary Differential Equations Setup (KinODE.m)

```
function dCdt=KinODE(t,Cinput,K)
global k1 k2 k3 k4 k5 k6;
C1 = Cinput(1); %TG
C2 = Cinput(2); %DG
C3 = Cinput(3); %MG
C4 = Cinput(4); %ME
C5 = Cinput(5); %GL
C6 = Cinput(6); %MeOH


k1 = K(1);
k2 = K(2);
k3 = K(3);
```

```
k4 = K(4);

k5 = K(5);

k6 = K(6);


dCdt = [-k1*C1*C6+k2*C2*C4;...

k1*C1*C6-k2*C2*C4-k3*C2*C6+k4*C3*C4;...

k3*C2*C6-k4*C3*C4-k5*C3*C6+k6*C4*C5;...

k1*C1*C6-k2*C2*C4+k3*C2*C6-k4*C3*C4+k5*C3*C6-k6*C4*C5;...

k5*C3*C6-k6*C4*C5;...

• k1*C1*C6+k2*C2*C4-k3*C2*C6+k4*C3*C4-k5*C3*C6+k6*C4*C5];
```

C.3. Main Program with Initial Guesses for Reaction Rate Constants (main.m)

```
clear

run inputvalue

% Initial guess for k values

KI = [0.08 0.04 0.22 0.2 6.5 5];

[k,fval] = lsqnonlin(@err,KI);

CExp = [TG; DG; MG; ME; GL; MeOH];

Cini = CExp(:,1);

tspan = (0:1:3);

[t,C]=ode45(@KinODE,tspan,Cini,[],k);

TGc=C(:,1)';

DGc=C(:,2)';

MGc=C(:,3)';

MEc=C(:,4)';

GLc=C(:,5)';

MeOHc=C(:,6)';
```

```
TGcal=[TGc(t==0),TGc(t==1),TGc(t==2),TGc(t==3)];
DGcal=[DGc(t==0),DGc(t==1),DGc(t==2),DGc(t==3)];
MGcal=[MGc(t==0),MGc(t==1),MGc(t==2),MGc(t==3)];
MEcal=[MEc(t==0),MEc(t==1),MEc(t==2),MEc(t==3)];
GLcal=[GLc(t==0),GLc(t==1),GLc(t==2),GLc(t==3)];
MeOHcal=[MeOHc(t==0),MeOHc(t==1),MeOHc(t==2),MeOHc(t==3)];
Ccal = [TGcal; DGcal; MGcal; MEcal; GLcal; MeOHcal];

% Pearson correlation coefficient
N = 4; % number of data point for each species
for i = 1:6
r(i) = (N*sum(CExp(i,:).*Ccal(i,:)) - sum(CExp(i,:)) * sum(Ccal(i,:)))
/sqrt((N*sum(CExp(i,:).^2) -  (sum(CExp(i,:)))^2) * (N*sum(Ccal(i,:).^2)-
(sum(Ccal(i,:)))^2));
end
run plotgraph
disp©;
disp('Rate constants: k1, k2, k3, k4, k5, k6');
disp(k);
disp('Pearson correlation coefficient: TG, DG, MG, ME, GL, MeOH');
disp®;
```

C.4. Graphing Function (plotgraph.m)

```
subplot(2,3,1)
plot(texp,CExp(1,:),'ro',texp,TGcal,'bo',t,C(:,1),'b-')
legend('TG experimental values','TG simulated values')
```

```
xlabel('time(days)')
ylabel('concentration(mol/L)');

subplot(2,3,2)
plot(texp,CExp(2,:),'ro',texp,DGcal,'bo',t,C(:,2),'b-')
legend('DG experimental values','DG simulated values')
xlabel('time(days)')
ylabel('concentration(mol/L)');

subplot(2,3,3)
plot(texp,CExp(3,:),'ro',texp,MGcal,'bo',t,C(:,3),'b-')
legend('MG experimental values','MG simulated values')
xlabel('time(days)')
ylabel('concentration(mol/L)');

subplot(2,3,4)
plot(texp,CExp(4,:),'ro',texp,MEcal,'bo',t,C(:,4),'b-')
legend('ME experimental values','ME simulated values')
xlabel('time(days)')
ylabel('concentration(mol/L)');

subplot(2,3,5)
plot(texp,CExp(5,:),'ro',texp,GLcal,'bo',t,C(:,5),'b-')
legend('GL experimental values','GL simulated values')
xlabel('time(days)')
ylabel('concentration(mol/L)');

subplot(2,3,6)
plot(texp,CExp(6,:),'ro',texp,MeOHcal,'bo',t,C(:,6),'b-')
```

```
legend('MeOH experimental values','MeOH simulated values')
xlabel('time(days)')
ylabel('concentration(mol/L)');
```

C.5. Error Calculation Function (err.m)

```
function error=err(KI)
run inputvalue
CExp = [TG; DG; MG; ME; GL; MeOH];
Cini = CExp(:,1);
tspan = (0:1:3);
[t,C] = ode45(@KinODE,tspan,Cini,[],KI);
disp©;
disp(KI);
TGc=C(:,1)';
DGc=C(:,2)';
MGc=C(:,3)';
MEc=C(:,4)';
GLc=C(:,5)';
MeOHc=C(:,6)';
TGcal=[TGc(t==0),TGc(t==1),TGc(t==2),TGc(t==3)];
DGcal=[DGc(t==0),DGc(t==1),DGc(t==2),DGc(t==3)];
MGcal=[MGc(t==0),MGc(t==1),MGc(t==2),MGc(t==3)];
MEcal=[MEc(t==0),MEc(t==1),MEc(t==2),MEc(t==3)];
GLcal=[GLc(t==0),GLc(t==1),GLc(t==2),GLc(t==3)];
MeOHcal=[MeOHc(t==0),MeOHc(t==1),MeOHc(t==2),MeOHc(t==3)];
Ccal = [TGcal; DGcal; MGcal; MEcal; GLcal; MeOHcal];
CError = Ccal-CExp;
```

```
abs(CError);

n=1;

error = sum(sum(CError))/n;

disp(error);
```

.

D. Example HPLC Chromatograms

D.1. Chromatogram of Triolein Oil

```
Injection Date  : 9/9/2010 11:47:05 AM                Inj :   1
                                                  Inj Volume : 5.0 µl
Acq. Method     : C:\CHEM32\1\DATA\GREG\GREG 2010-09-09 11-13-17\CHINMOYMAYCAL2.M
Analysis Method : C:\CHEM32\1\METHODS\CHINMOYMAYCAL2.M
```

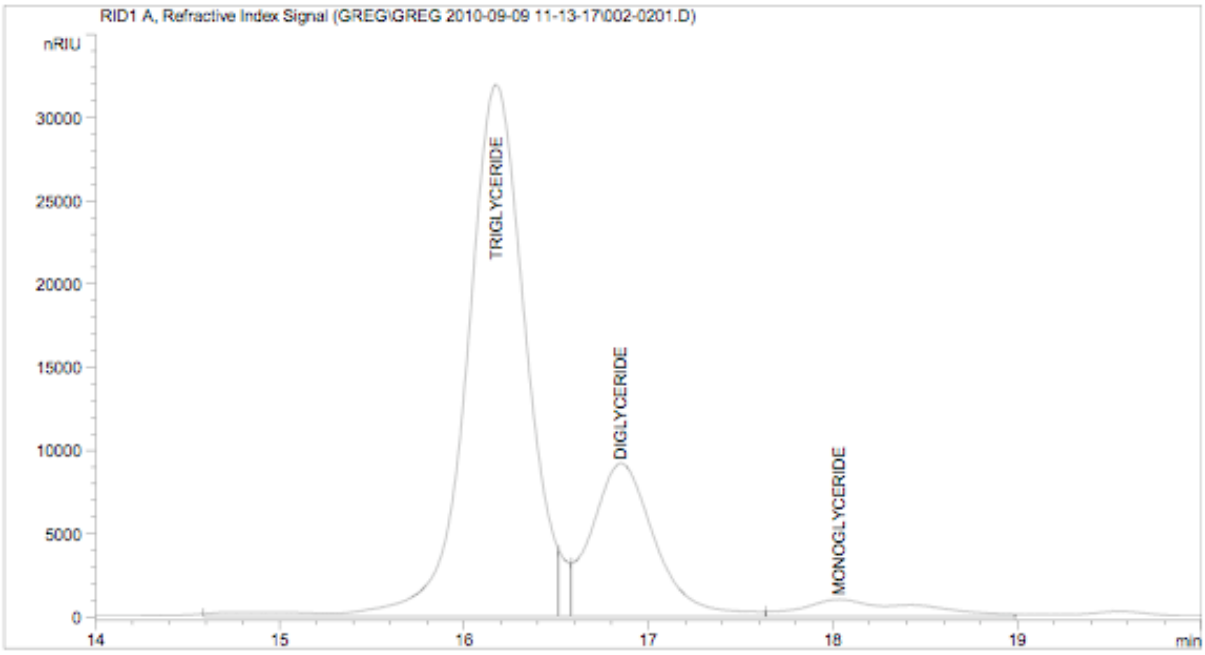


```
=====================================================================
                    External Standard Report
=====================================================================

Sorted By             :      Retention Time
Calib. Data Modified  :      11/23/2011 11:02:56 AM
Multiplier:                   :     20.0000
Dilution:                     :      1.0000
Use Multiplier & Dilution Factor with ISTDs

Signal 1: RID1 A, Refractive Index Signal

RetTime Sig Type     Area      Amt/Area    Amount   Grp   Name
 [min]             [nRIU*s]               [percent]
-------|--|------|----------|----------|----------|--|---------------
 16.173  1 BF     7.02891e5  5.04662e-6   70.94450    TRIGLYCERIDE
 16.849  1 VB     2.18689e5  4.71023e-6   20.60153    DIGLYCERIDE
 18.033  1 BB     4.26810e4  4.67136e-6    3.98757    MONOGLYCERIDE
 18.600  1            -          -           -        PRODUCTS

Totals :                                   95.53361
```

D.2. Chromatogram of Canola Oil

```
Data File C:\CHEM32\1\DATA\GREG\GREG 2010-09-09 11-13-17\003-0301.D
Sample Name: CANOLA

======================================================================
Acq. Operator    : Greg                          Seq. Line :   3
Acq. Instrument : 1100                           Location : Vial 3
Injection Date   : 9/9/2010 12:19:04 PM              Inj :   1
                                                Inj Volume : 5.0 µl
Acq. Method      : C:\CHEM32\1\DATA\GREG\GREG 2010-09-09 11-13-17\CHINMOYMAYCAL2.M
Analysis Method : C:\CHEM32\1\METHODS\CHINMOYMAYCAL2.M
```

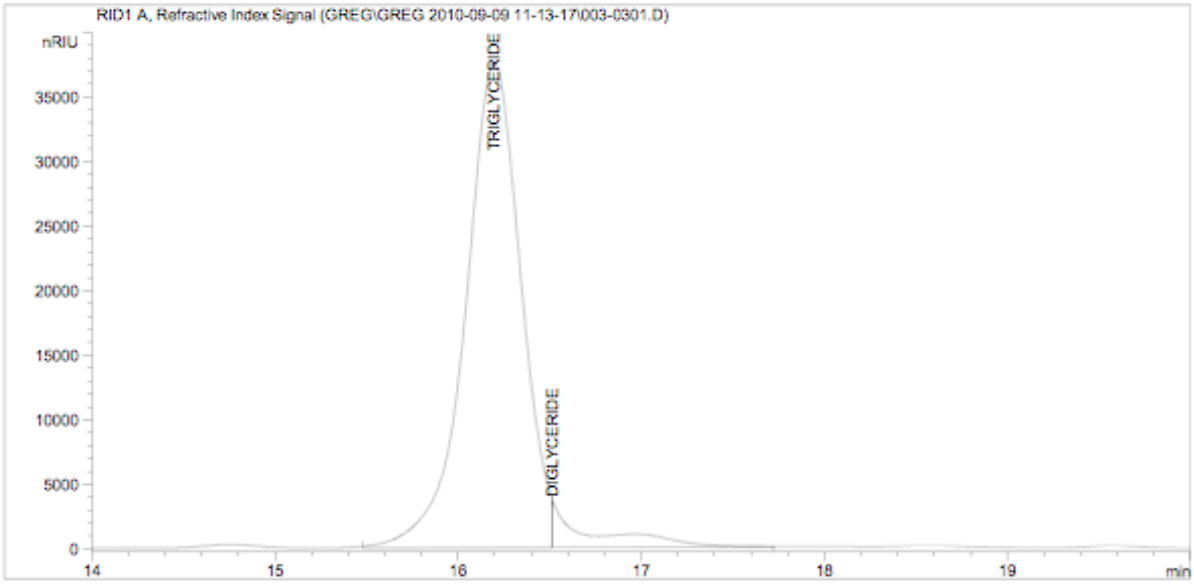


```
======================================================================
                      External Standard Report
======================================================================

Sorted By             :      Retention Time
Calib. Data Modified  :      3/7/2012 3:20:12 PM
Multiplier:                   :     20.0000
Dilution:                     :      1.0000
Use Multiplier & Dilution Factor with ISTDs

Signal 1: RID1 A, Refractive Index Signal

RetTime Sig Type     Area      Amt/Area    Amount   Grp   Name
 [min]             [nRIU*s]               [percent]
-------|--|------|----------|----------|----------|--|---------------
 16.195  1 BF     7.86048e5  5.04716e-6   79.34613    TRIGLYCERIDE
 16.513  1 VB     5.01839e4  4.68288e-6    4.70010    DIGLYCERIDE
 17.992  1            -          -           -        MONOGLYCERIDE
 18.236  1            -          -           -        PRODUCTS
```

D.3. Chromatogram of Greenseed Canola Oil

```
Data File C:\CHEM32\1\DATA\GREG\GREG 2011-04-08 11-07-54\091-0101.D
Sample Name: GS Canola

======================================================================
Acq. Operator    : Greg                          Seq. Line :   1
Acq. Instrument : 1100                           Location : Vial 91
Injection Date   : 4/8/2011 11:09:46 AM               Inj :   1
                                                Inj Volume : 5.0 µl
Acq. Method      : C:\CHEM32\1\DATA\GREG\GREG 2011-04-08 11-07-54\CHINMOYMAYCAL2.M
Analysis Method : C:\CHEM32\1\METHODS\CHINMOYMAYCAL2.M
```

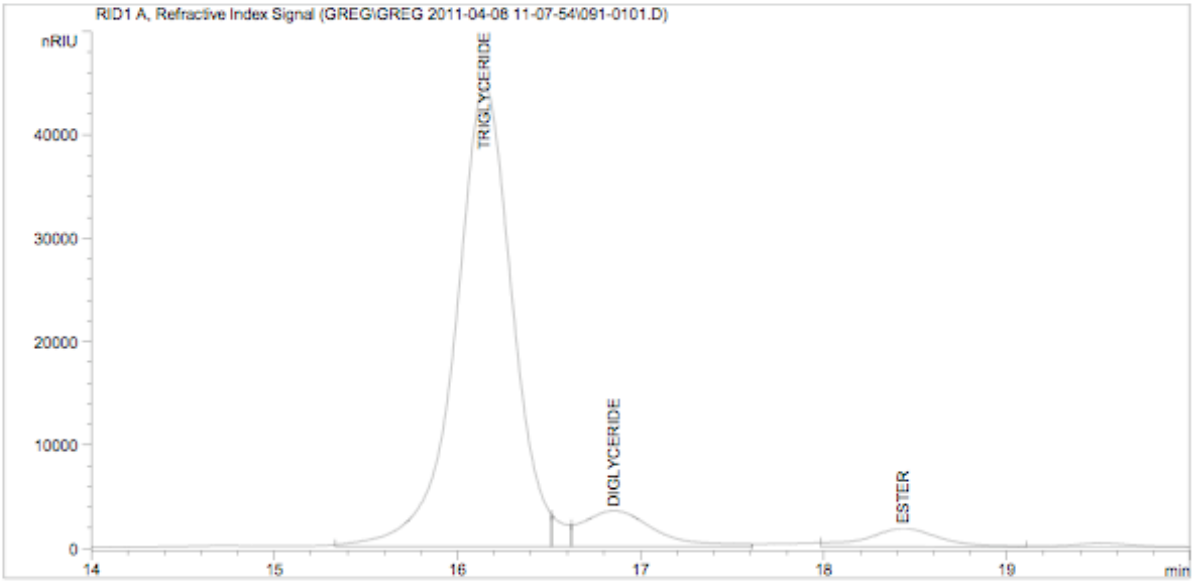


```
======================================================================
                      External Standard Report
======================================================================

Sorted By             :      Retention Time
Calib. Data Modified  :      3/7/2012 3:20:12 PM
Multiplier:                   :     20.0000
Dilution:                     :      1.0000
Use Multiplier & Dilution Factor with ISTDs

Signal 1: RID1 A, Refractive Index Signal

RetTime Sig Type     Area     Amt/Area    Amount   Grp   Name
 [min]            [nRIU*s]               [percent]
-------|--|------|---------|----------|----------|--|---------------
 16.147  1 BF     9.52008e5  5.04794e-6   96.11359     TRIGLYCERIDE
 16.851  1 VB     9.44108e4  4.69950e-6    8.87368     DIGLYCERIDE
 17.992  1            -          -           -         MONOGLYCERIDE
 18.433  1 BB     4.92370e4  6.47308e-6    6.37430     PRODUCTS
```

D.4. Chromatogram of Experiment at t=0 Minutes at Optimized Conditions

```
Injection Date  : 5/21/2010 2:17:47 PM                Inj :   1
                                                  Inj Volume : 5.0 µl
Acq. Method     : C:\CHEM32\1\DATA\GREG\GREG 2010-05-21 11-36-27\CHINMOYMAYCAL2.M
Analysis Method : C:\CHEM32\1\METHODS\CHINMOYMAYCAL2.M
```

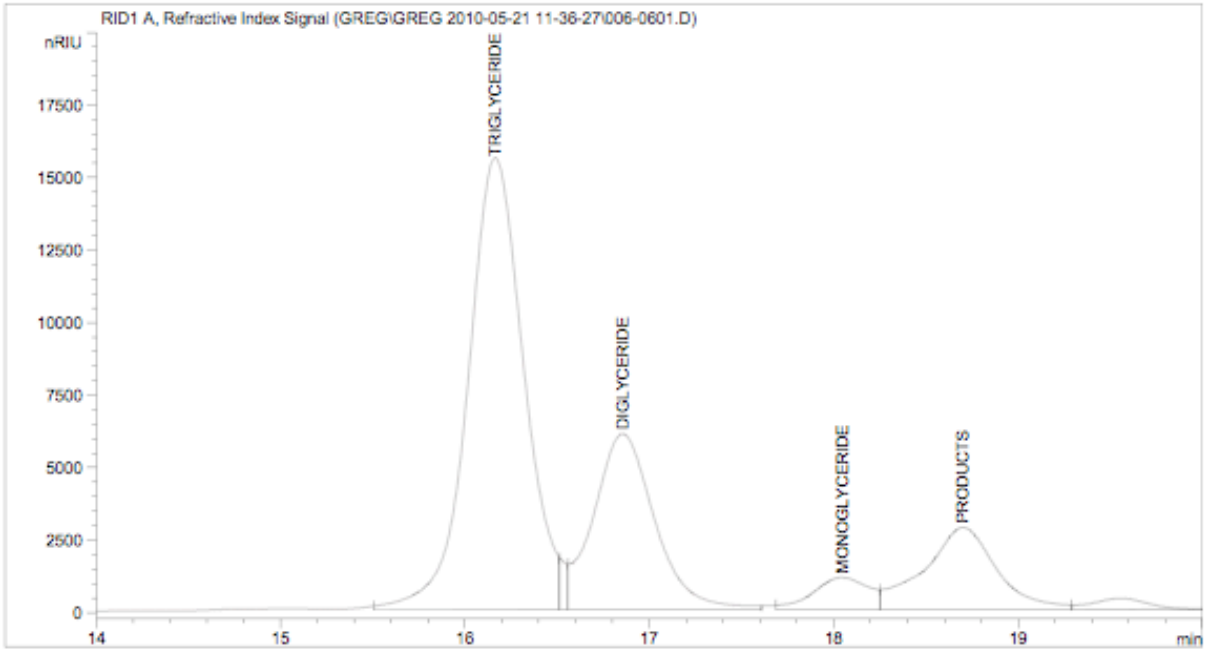


```
=====================================================================
                      External Standard Report
=====================================================================

Sorted By             :      Retention Time
Calib. Data Modified  :      11/23/2011 11:02:56 AM
Multiplier:                   :     20.0000
Dilution:                     :      1.0000
Use Multiplier & Dilution Factor with ISTDs

Signal 1: RID1 A, Refractive Index Signal

RetTime Sig Type     Area      Amt/Area    Amount   Grp   Name
 [min]             [nRIU*s]               [percent]
-------|--|------|----------|----------|----------|--|---------------
 16.163  1 BF     3.27375e5  5.04086e-6   33.00499    TRIGLYCERIDE
 16.853  1 VB     1.39812e5  4.70563e-6   13.15803    DIGLYCERIDE
 18.045  1 BV     2.33745e4  4.63538e-6    2.16699    MONOGLYCERIDE
 18.698  1 VV     7.72938e4  6.48881e-6   10.03090    PRODUCTS

Totals :                                  58.36091
```

D.5. Chromatogram of Experiment at t=120 Minutes at Optimized Conditions

```
Injection Date  : 5/21/2010 4:25:56 PM                Inj :   1
                                                  Inj Volume : 5.0 µl
Acq. Method     : C:\CHEM32\1\DATA\GREG\GREG 2010-05-21 11-36-27\CHINMOYMAYCAL2.M
Analysis Method : C:\CHEM32\1\METHODS\CHINMOYMAYCAL2.M
```

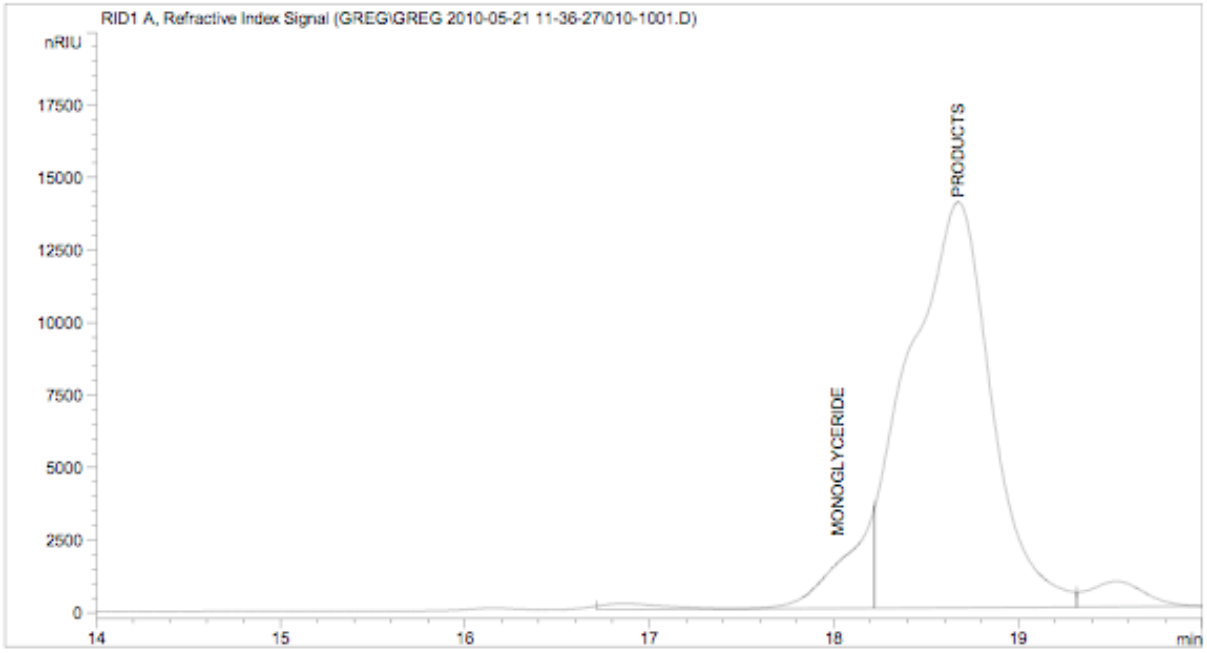


```
=====================================================================
                      External Standard Report
=====================================================================

Sorted By             :      Retention Time
Calib. Data Modified  :      11/23/2011 11:02:56 AM
Multiplier:                   :     20.0000
Dilution:                     :      1.0000
Use Multiplier & Dilution Factor with ISTDs

Signal 1: RID1 A, Refractive Index Signal

RetTime Sig Type     Area      Amt/Area    Amount   Grp   Name
 [min]            [nRIU*s]              [percent]
-------|--|------|----------|----------|----------|--|---------------
 16.123  1            -          -          -         TRIGLYCERIDE
 16.791  1            -          -          -         DIGLYCERIDE
 18.216  1 MF     4.53269e4  4.67391e-6    4.23707    MONOGLYCERIDE
 18.672  1 FM     4.31602e5  6.51147e-6   56.20734    PRODUCTS

Totals :                                  60.44441
```